

**PETROGRAPHY, GEOCHEMISTRY AND MECHANICAL PROPERTIES
OF IGNEOUS ROCKS FROM THE UTLA AREA OF GADOON,
NW PAKISTAN**



Muhammad Sajid

Thesis Submitted to the National Center of Excellence in Geology,
University of Peshawar for Partial Fulfillment of Requirements for the Degree of
M.Phil in Geology

**NATIONAL CENTER OF EXCELLENCE IN GEOLOGY,
UNIVERSITY OF PESHAWAR**

DEDICATION

To my beloved father
for the understanding and encouragement
provided throughout my life
&
To my respected supervisor
for teaching me that I should never surrender

ACKNOWLEDGMENTS

I meekly thank Allah Almighty, the Merciful and the Beneficent, who gave me health, thoughts and co-operative people to enable me achieve this goal.

Deepest appreciation goes to Prof. Dr. Mohammad Arif, supervisor of my thesis, without whose consistent help, completion this project would not have been possible. His generosity, demonstrative guiding, compassionate attitude and encouraging nature will always be appreciated.

I am also highly obliged to Prof. Dr. M. Tahir Shah, my co-supervisor, for his useful suggestions and assistance regarding the geochemical studies of rocks.

Heartfelt thanks are also extended to Dr. Muhammad Ashraf, Department of Civil engineering, Khyber Pukhtoonkhwa, University of Engineering and Techology, for his help in arrangements for mechanical tests of studied rocks.

Dr. Teheenullah Khan, Bahria University is also highly acknowledged for his comprehensive comments on the thesis.

I am also grateful to Prof. Dr. M. Asif Khan, Director, National Center of Excellence in Geology for his cooperation in arrangements of geological fieldwork and geochemical analysis.

Mr. Saeed Afridi is also thanked for his company and help during the geological fieldwork. Mr. Hammad Ghani and Mr. Mustafa are also thanked for their support and encouragement.

All members of the clerical and technical staff of the National Center of Excellence in Geology and Department of Geology are accredited, especially Mr. Tariq and Mr. Rasheed Masih, for being supportive during geochemical analysis and thin section preparation.

My family members, especially my mother, also deserve deepest regards and special thanks for their moral and financial support throughout my educational carrier, without which I might not have been able to achieve my goals. May Allah sanctify them all.

Muhammad Sajid

LIST OF FIGURES

Chapter One Introduction

- Fig. 1.1 Geological map of the study area.....5
Fig. 1.2 Map showing location of studies samples.....6

Chapter Two Regional Geology

- Fig. 2.1 Geological map of the area south of the Main Mantle Thrust.....11
Fig. 2.2 Generalized geological map showing the major alkaline complexes.....12

Chapter Three Petrography

- Fig. 3.1 (A) The mega-porphyritic Utla granite.....18
(B) A small patch of fine-grained granite within the mega-porphyritic granite...18
(C) A fine to medium-grained dyke of granitic composition.....18
(D) A quartz rich vein cutting the Utla granite.....18
- Fig. 3.2 IUGS classification diagram for the studied granitic rocks.....19
- Fig. 3.3 Photomicrographs:
(A) Undulose extinction in quartz grain.....20
(B) Clusters of unstrained quartz grains around a strained quartz phenocryst....20
(C) Cross-hatched twinning in microcline.....20
(D) Perthitic alkali feldspar.....20
- Fig. 3.4 Photomicrographs:
(A) Blebs of zoned plagioclase in a phenocryst of perthitic microcline.....21
(B) Graphic texture.....21
(C) A phenocryst of zoned plagioclase.....21
(D) Color zoning in tourmaline.....21
- Fig. 3.5 (A) A thin tourmaline-rich vein cutting across the Utla granite.....22
(B) Micas wrapping the alkali feldspar megacryst (photomicrograph).....22
(C, D) Topotaxial growth of muscovite about biotite (photomicrographs).....22
- Fig. 3.6 Photomicrographs:
(A, B) Alteration of andalusite to muscovite.....23
(C) A thin border of sphene around an opaque ore mineral grain.23
(D) Garnet grains.....23
- Fig. 3.7 Photomicrograph showing Fibrolitic sillimanite.....24
- Fig. 3.8 (A) A basic dyke cutting across the Utla granite.....26
(B) Ophitic texture (photomicrograph).....26
(C) Clinopyroxene alteration to chlorite and amphibole (photomicrograph).....26
(D) Sphene around an opaque ore mineral grain (photomicrograph).....26
- Fig. 3.9 Photomicrographs:
(A) Preferred orientation in basic dyke.....27
(B) Relics of clinopyroxene (Cpx) in green amphibole.....27

Chapter Four Geochemistry

- Fig. 4.1 Major elements versus SiO₂ variation diagrams of Utla granites.....32
Fig. 4.2 SiO₂ versus FeO^t+MgO+TiO₂ diagram.....33
Fig. 4.3 Classification diagram: Al₂O₃/CaO + Na₂O +K₂O versus Al₂O₃/Na₂O+K₂O....33

Fig. 4.4	SiO ₂ versus K ₂ O diagram.....	34
Fig. 4.5	AFM plot.....	34
Fig. 4.6	FeO ^l /MgO versus SiO ₂ plot.....	35
Fig. 4.7	FeO ^l /MgO versus Zr+Nb+Ce+Y plot.....	35
Fig. 4.8	(a) Al ₂ O ₃ /TiO ₂ versus CaO/Na ₂ O.....	36
	(b) Rb/Ba versus Rb/Sr diagram.....	36
Fig. 4.9	Trace elements versus silica and Zr-Th variation diagrams (Utla granites).....	39
Fig. 4.10	Variation of La, Th and Ce with P ₂ O ₅ (Utla granites).....	40
Fig. 4.11	Trace elements spidergrams for the Utla granites:	
	a) Ocean ridge granite-normalized plot.....	41
	b) Chondrite-normalized plot.....	41
Fig. 4.12	Nb vs SiO ₂ discriminant diagram	42
Fig. 4.13	Variation of Y, Rb and Nb with SiO ₂ (Utla granites).....	43
Fig. 4.14	The Rb-Y+Nb and Nb-Y relations (Utla granites).....	44
Fig. 4.15	Major element oxides versus SiO ₂ variation diagrams (Utla dykes).....	47
Fig. 4.16	Trace elements versus silica variation diagrams (Utla dykes).....	48
Fig. 4.17	Selected trace elements versus P ₂ O ₅ variation diagrams (Utla dykes).....	49
Fig. 4.18	FeO ^l /MgO versus SiO ₂ plot (Utla dykes).....	49
Fig. 4.19	TiO ₂ -Zr discriminant diagram (Utla dykes).....	50
Fig. 4.20	Zr/Y-Zr discriminant diagram (Utla dykes).....	50
Fig. 4.21	Nb*2-Zr/4-Y discriminant diagram (Utla dykes).....	51
Fig. 4.22	Ti/100-Zr-Y*3 discriminant diagram (Utla dykes).....	51
Fig. 4.23	Hf/3-Th-Ta discriminant diagram (Utla dykes).....	52

Chapter Five Mechanical Properties

Fig. 5.1	Core samples of the different textures varieties of the Utla granite.....	55
Fig. 5.2	Relationship between UCS and quartz to feldspar ratio.....	61
Fig. 5.3	Relationship between UTS and quartz to feldspar ratio.....	62
Fig. 5.4	Relationship between porosity and quartz to feldspar ratio.....	63
Fig. 5.5	Relationship between UCS and porosity.....	64
Fig. 5.6	Relationship between UCS and water absorption.....	65
Fig. 5.7	Relationship between UCS and UTS.....	66
Fig. 5.8	Relationship between UCS and Mica Content.....	67

Chapter Six Discussion

Fig. 6.1	Rb-Ba-Sr discriminant diagram.....	71
Fig. 6.2	Comparison of Utla granites with Ambela granite and Singo granite.....	73

LIST OF TABLES

Chapter Three Petrography

Table 3.1	Modal mineralogical composition of granitic rocks from Utlá area.....	17
-----------	---	----

Chapter Four Geochemistry

Table 4.1	Representative chemical analysis of Utlá granite.....	31
Table 4.2	Whole-rock chemical analyses of representative dyke samples.....	46

Chapter Five Mechanical Properties

Table 5.1	Modal composition of mega-crystic granite.....	56
Table 5.2	Modal composition of foliated mega-crystic granite.....	56
Table 5.3	Modal composition of fine grained homogeneous granite.....	56
Table 5.4	Details and results of the UCS testing.....	57
Table 5.5	Details and results of the UTS testing.....	58
Table 5.6	Details and results of water absorption, specific gravity and porosity.....	59

Chapter Six Discussion

Table 6.1	Grades of unconfined compressive strength.....	74
Table 6.2	Average values of UCS, UTS, porosity, water absorption and specific gravity..	75

**Petrography, Geochemistry and Mechanical Properties of Igneous Rocks
from the Utla Area of Gadoon,
North-West Pakistan**

TABLE OF CONTENTS

Abstract.....	i
Acknowledgements.....	ii
List of Figures.....	iii
List of Tables.....	v
Chapter One	Introduction
1.1. General Statement.....	1
1.2. Location of the Study Area.....	2
1.3. Previous Work.....	2
1.4. The Present Investigation.....	3
1.4.1. Scope.....	3
1.4.2. Aims and Objectives.....	3
1.5. Methodology.....	4
Chapter Two	Regional Geology
2.1. Geology and Tectonics of Northern Pakistan.....	7
2.2. Geology of Indian Plate Rocks.....	7
Chapter Three	Petrography
3.1. General Statement.....	13
3.2. Samples and Methods.....	13
3.3. Petrography.....	13
3.3.1. Granites.....	13
3.3.2. Basic Dykes.....	24
Chapter Four	Geochemistry
4.1. General Statement.....	28
4.2. Methodology.....	28
4.3. Granites.....	29
4.3.1. Major elements geochemistry.....	29
4.3.2. Minor and Trace Element Geochemistry.....	37
4.3.3. Tectonic setting.....	37
4.4. Basic Dykes.....	45
4.4.1. Major Element Geochemistry.....	45
4.4.2. Minor and trace element geochemistry.....	45
4.4.3. Tectonic Setting.....	45
Chapter Five	Mechanical Properties
5.1. General Statement.....	53
5.2. Methodology.....	54
5.3. Petrographic descriptions.....	54

5.4. Physical and Mechanical Properties.....	55
5.4.1. Strength Tests.....	57
5.4.2. Water Absorption.....	58
5.4.3. Specific Gravity.....	58
5.4.4. Porosity.....	59
5.5. Relationship among Petrographic, Physical and Mechanical Properties.....	60

Chapter Six Discussion

6.1. General Statement.....	68
6.2. Petrographic and Geochemical Characteristics.....	68
6.3. Comparison with Ambela Granitic Complex and Mansehra Granite.....	70
6.4. Mechanical Properties.....	72

Chapter Seven Conclusions and Recommendations

7.1. Conclusions.....	76
7.2. Recommendations for Future Studies.....	77

References.....	78
------------------------	-----------

Abstract

The igneous rocks around the Utla area (Gadoon), NW Pakistan are studied in terms of their petrographic features, geochemical characteristics and mechanical properties. Field relationships and petrographic studies lead to a distinction of the Utla rocks into (i) granite and (ii) basic dykes. Although predominantly mega-porphyritic, some of the Utla granites are massive and display fine-grained equi-granular texture. Some of the mega-porphyritic varieties exhibit foliation and seem to be restricted to shear zones. In addition to being distributed largely as phenocrysts, all the essential minerals (plagioclase, perthitic alkali feldspar and quartz) also constitute the groundmass. The studied samples of Utla granites also contain minor to accessory amounts of tourmaline, muscovite and biotite and accessory to trace amounts of apatite, andalusite, garnet, zircon, monazite, epidote and sphene.

A detailed geochemical investigation reveals a calc-alkaline and per-aluminous character of the Utla granites. The per-aluminous character and total lack of hornblende indicate their formation as S-type granites in a volcanic arc or syn-collisional tectonic setting. Further examination shows that the melt parental to the Utla granite was derived from a plagioclase-poor, clay-rich rock, i.e. pelite.

The petrogenetically significant petrographic and geochemical characteristics of the Utla granite show greater resemblance to the Mansehra than the Ambela granites. These include (i) predominantly mega-porphyritic texture, (ii) presence of andalusite and tourmaline, (iii) the calc-alkaline geochemical signature and (iv) indication of similar melt source rock characteristics.

On the basis of textural characteristics and modal composition, the Utla dykes are sub-divided into (i) dolerite and (ii) altered/metamorphosed basic types. Their petrographic and geochemical characteristics are broadly similar to those exposed in Malka, Ambela and elsewhere in the region. Hence the studied Utla dykes might be related genetically with group-III rocks of the Ambela granitic complex.

Some of the physico-mechanical properties including unconfined compressive strength (UCS), unconfined tensile strength (UTS), water absorption, specific gravity and porosity of samples representing different textural varieties of the Utla granites were also determined. Compared to the foliated mega-crystic and fine-grained equi-granular types, the non-foliated mega-crystic variety of the Utla granites is very strong. An attempt to investigate a possible relationship between the physico-mechanical properties and petrographic characteristics through statistical analysis reveals that higher strength of the non-foliated mega-crystic samples is most probably because of the greater variation in grain size, non-alignment of micaceous minerals and subordinate values of water absorption and porosity.

INTRODUCTION

1.1. General Statement

Granites are widely distributed throughout the continental crust and constitute the most abundant basement rocks that underlie relatively thin sedimentary veneer of continents. The rocks of granitic composition occur also in a number of localities in north Pakistan. In addition to batholithic dimensions, these rocks also occur in the form of numerous small stocks (Calkins, 1975; Tahirkheli and Jan, 1979). A plethora earlier workers has described these granitic plutons in a range of geological aspects including their geochemical characteristics, genesis of associated mineralization and tectonic settings. Shams (1983a) gave a detailed comparative note on various granitic complexes of NW Pakistan. He compared these complexes in terms of their field features and petrography and found that there is a close relationship between the granitic bodies and the associated metamorphic formations.

Butt (1983) described a prominent example of Pb-Zn-Mo and Uranium mineralization associated with a granitic complex of NW Himalaya in Pakistan, the significance of which is notable for application elsewhere in the region. The granitic rocks have inherent potential for the Uranium mineralization. In this regard, the granitic complexes from the Himalayas are used for the tectonic modeling by Shams (1983b) on the basis of their nature of origin and mode of emplacement.

Granitic rocks and the associated pegmatites also serve as host rock for a variety of gemstones. A wide range of gems has been reported from the pegmatites and associated quartz-feldspar (hydrothermal) veins in various localities of northern Pakistan. These include tourmaline, aquamarine (sea blue to inky blue), topaz (colorless, brown, honey color), zoisite-epidote (pink, green), Mn-rich garnet, clear to colored quartz (including amethyst), fluorite, moonstone, sphene, rutile, apatite, zircon, axinite, and many others (Jan and Kazmi, 2005).

Furthermore, granitic rocks are widely used as dimension stone and construction material. However, the suitability of rocks for use in construction depends on their mechanical properties. The latter are in turn generally controlled by the petrographic characteristics including grain size, shape of grains, fabric (arrangement of mineral grains and degree of interlocking), type of contacts, mineralogical composition and the degree of weathering (Irfan, 1996). The parameters that may be used in a description of the mechanical aspects of a rock therefore include mineral

composition, texture, lithological characteristics, degree of weathering or alteration, density, porosity, strength, hardness, primary permeability, seismic velocity and modulus of elasticity.

1.2. Location of the Study Area

A large body of granitic rocks is well exposed in and around the Utla area of Gadoon, NW Pakistan. The Utla village ($34^{\circ}15'20.6''$ N, $72^{\circ}40'20.2''$ E) is located in the northern portion of Swabi district, along the western side of Indus River (Fig. 1.1). This area is well accessible through Peshawar-Swabi-Topi road. Geologically, the study area is a part of the Peshawar basin constituting the south-eastern portion of the lower Swat-Buner schistose group.

1.3. Previous Work

The stratigraphy of lower Swat area was initially established by Martin et al. (1962) and King (1964). The base of this sequence is intruded by augen and tourmaline granitic gneisses which they called as Swat granites and granitic gneisses. The Swat granitic gneisses are believed to be late Cambrian to early Ordovician in age (Le Fort et al., 1980; Jan et al., 1981a).

Le Fort et al., (1980) obtained a whole rock Rb-Sr age of 516 ± 16 for the Mansehra granite in Hazara area. This granite was later considered to be contemporaneous with the granitic gneisses in lower Swat (Jan et al., 1981a; Le Fort et al., 1983). The dominant characteristics of these rocks are their strongly gneissose fabric and generally porphyritic texture with feldspar megacrysts up to 15 cm long. However, these granites are non-foliated in the southern portion, the effects of deformation start appearing along a line passing just north of Mansehra (Shams, 1969; Coward et al. 1982). The Swat granitic gneisses, according to Martin et al. (1962), also are non-foliated at the base.

The existence of Peshawar Plain Alkaline Igneous Province (PPAIP) was first reported by Kempe and Jan (1970), which extends from Tarbela in the east to Pak-Afghan border in the west (Kempe and Jan, 1980). Ambela granitic complex (AGC) constitutes the major portion of PPAIP (Rafiq and Jan, 1988). Khan and Hammad (1978) noted petrographic similarities between the Utla granites and the granitoids from AGC.

The mafic dykes intrude rocks of the PPAIP and constitute an important lithological component of PPAIP. The petrography, mineral chemistry and rock chemistry of such basic dykes from Malka area, lower Swat are studied in detail by Majid et al. (1991). They accomplished the

association of these dykes with the rifting in northern portion of Indian plate on the basis of their composition.

The Utla granites appear to be in spatial continuity with and thus most probably representing an eastward extension of the Ambela granitic complex (Rafiq and Jan, 1988). Jan et al. (1981a) have, however, noted that a slice of calc-alkaline granitoid, i.e. the Chingalai granodiorite, separates the Utla rocks from those of the Ambela complex. Some of the workers, however, mapped the rocks of Utla area with the granitic rocks of Swat and Mansehra (Le Fort et al., 1980; DiPietro et al., 1998; Hussain et al., 2004; Sajid and Arif, 2010).

1.4. The Present Investigation

1.4.1. Scope

The Utla area contains well exposed and easily accessible exposures of granitic rocks. Most of the other rocks in the region, particularly those representing the PPAIP, have been studied in reasonable detail in the past. In contrast, the Utla rocks despite their petrologic significance and important tectonic setting have received very little attention, if at all. The present research work was planned to furnish field, petrographic and geochemical details of the igneous rocks of Utla so that the existing discrepancies and confusion regarding their geochemical affinity and tectonic setting could properly be addressed. Similarly, details regarding the mechanical aspects of other granitic rocks in the region have been explored by earlier workers, however, such details regarding the Utla rocks are currently lacking and hence need to be investigated.

1.4.2. Aims and Objectives

The main objectives of the present studies are outlined below:

1. A detailed petrographic examination of the Utla granites and associated dykes to determine their modal mineralogy and discuss their genesis on the basis of these petrographic details.
2. Geochemical characterization of the petrographically investigated rocks in terms of their major, minor and trace elements concentrations.
3. A comparison of the Utla granite with other granitic rocks in the region, especially the Ambela and Mansehra granites, in terms of their petrographic details and geochemical characteristics.
4. Utilization of the trace element data for the purpose of petrogenetic modeling and determination of tectonic setting of the rocks.

5. The determination of mechanical properties of the Utlā granitoids to assess their suitability for use as construction material and dimension stones and to establish a possible relationship between their petrographic details and mechanical properties.

1.5. Methodology

A total of 37 samples were collected for petrographic and geochemical observations. The proper geographic coordinates of each sample were recorded (Fig. 1.2). The petrogenetically important field features were also noted and photographed. Thirty one of the collected samples were cut into thin sections for detailed petrographic studies in the Rock Cutting laboratory, National Center of Excellence in Geology, University of Peshawar. These thin sections were studied in the Petrography laboratory, Department of Geology, University of Peshawar.

Twenty four representative samples were ground to powder for whole-rock geochemical analysis in the National Center of Excellence in Geology, University of Peshawar. The components determined include major, minor and trace elements. The analyses were performed using X-ray fluorescence (XRF) and Ultra-Violet (UV) spectrometric techniques. The details regarding sample preparation and their processing are discussed in the respective chapters.

For the purpose of studying mechanical properties of the Utlā granites, three bulk samples representing different textural varieties were collected. Seven cores were obtained from each bulk samples for the determination of mechanical properties. The details of sample preparation and testing instruments are presented in the concerned chapter.

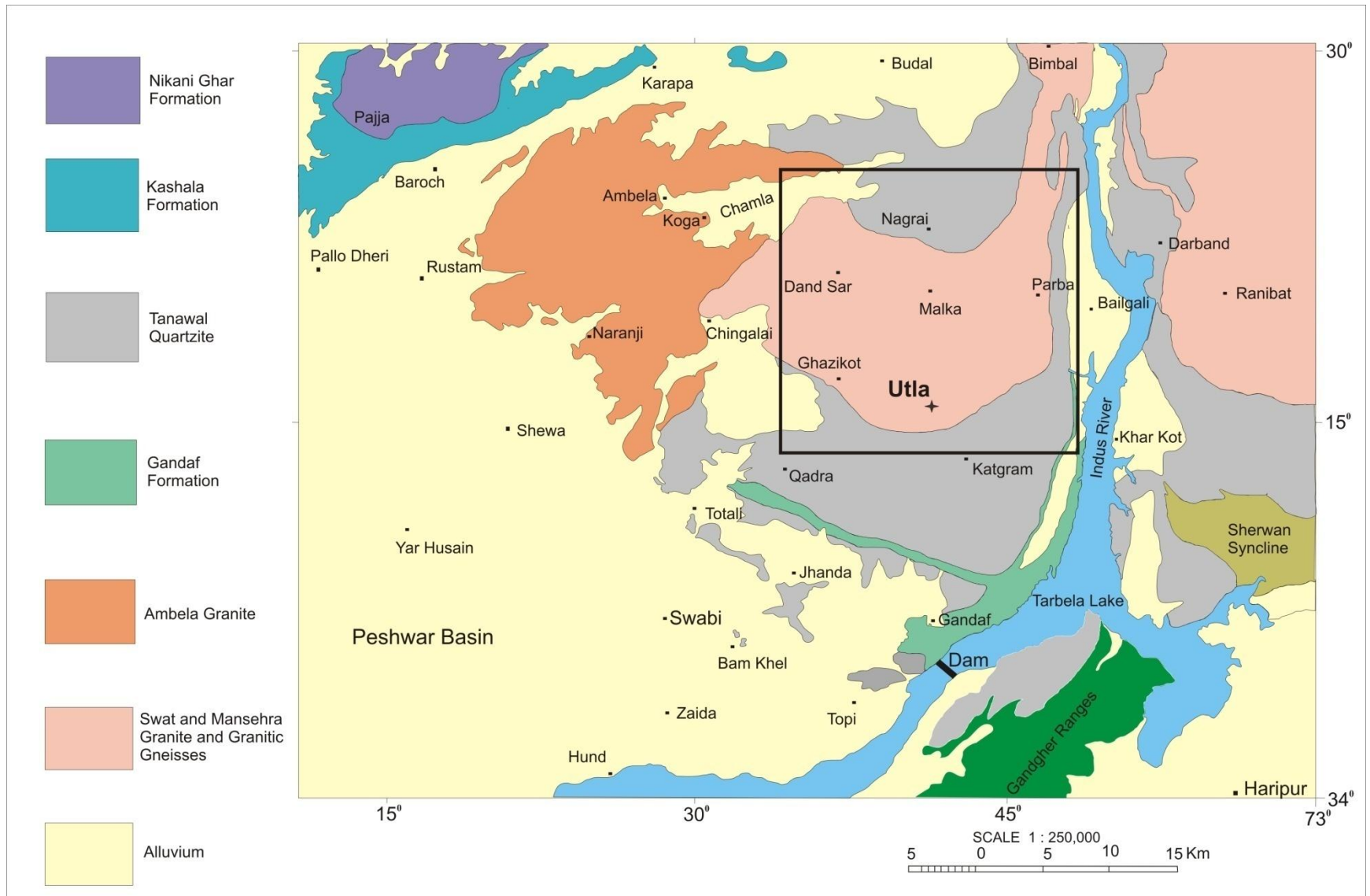


Fig. 1.1. Geological map of the study area (after Hussain et al., 2004). Box encloses the location of figure 1.2.

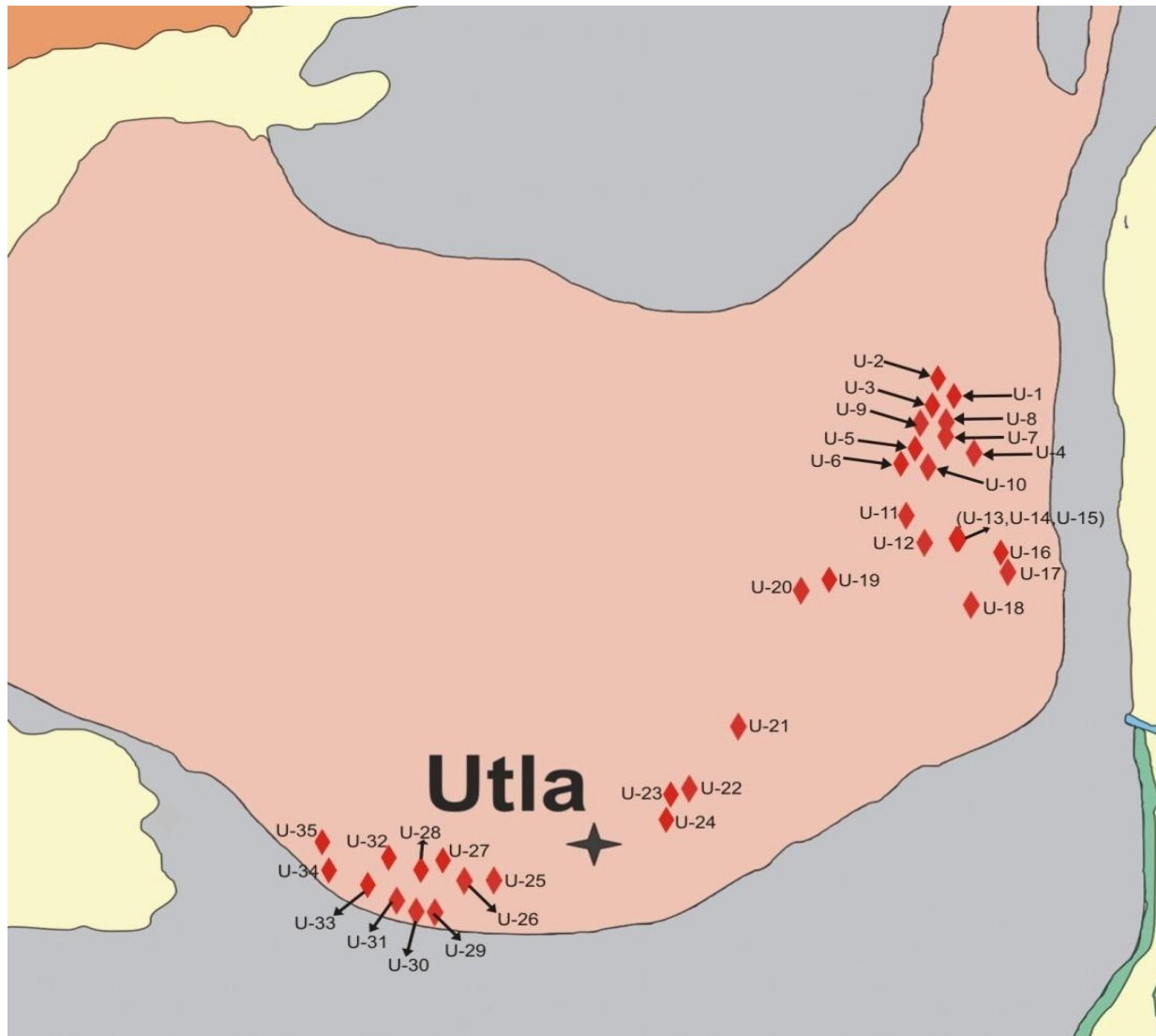


Fig.1.2. Map showing location of studies samples.

REGIONAL GEOLOGY

2.1. Geology and Tectonics of Northern Pakistan

Three distinct tectonic domains are present in the northern Pakistan i.e. Eurasian plate, Kohistan island arc (KIA) and Indian plate. The Kohistan island arc is an intra-oceanic arc within Tethys which first collided with Eurasian plate along the Main Karakoram Thrust (MKT) or Shyok suture during the latest Cretaceous (Searle et al., 1999; Shaltegger et al., 2002). The suture formed by early to mid Eocene collision of KIA with Indian plate is known as the Main Mantle Thrust (MMT) (Coward et al., 1986; Searle et al., 1999). The obduction of KIA on to the Indian plate rocks is the result of this collision. The MMT was described as extending eastward from Afghanistan through Swat to Babusar and then northward around Nanga Parbat-Haramosh massif to Ladakh where it is connected with Indus suture zone (DiPietro et al., 2000). The KIA consists of late Cretaceous and Eocene plutonic belts, gabbro-norites/pyroxene granulites, calc-alkaline volcanics, amphibolites and minor meta-sediments (Coward et al., 1986; Jan, 1988). From south to north, the KIA consists of the six units including (i) Jijal Complex, (ii) Kamila amphibolites, (iii) Chilas complex, (iv) Kohistan batholith and Gilgit gneisses, (v) Chalt volcanics and (vi) Yasin group metasediments. The ultramafic-mafic Jijal Complex represents the upper mantle to lower crust transition (Jan and Howie, 1981; Ringuette et al., 1999; Dhuime et al., 2007). The Kamila amphibolite belt is dominated by amphibolite-facies metaplutonic and metavolcanic rocks (Khan et al., 1997) representing multiple mantle sources (Shaltegger et al., 2002). On the basis of petrological data, Jagoutz et al. (2010) propose a genetic model of combined flux and decompression melting in the back-arc for the ultramafic-mafic rocks of the Chilas Complex.

2.2. Geology of Indian Plate Rocks

The Indian plate is divided into two zones by Hissartang Fault (Coward et al., 1988). The northern zone between Hissartang Fault and MMT is called internal metamorphosed zone while southern zone is called external unmetamorphosed or low-grade metamorphic zone (Treloar et al., 1989). Farther to the south, the Main Boundary Thrust (MBT) separates these rocks from Tertiary fore land basin deposits.

Treloar et al. (1989) divide the internal zone of the Indian plate into six stratigraphically distinct crustal nappes (Fig. 2.1). These nappes include Besham, Swat, Hazara, Banna, Lower Kaghan and Upper Kaghan nappes.

The Swat nappe is constituted by Pre-Cambrian Manglaur crystalline schist, intruded by the porphyritic Swat granitic gneisses (closely resemble the granitic rocks from Mansehra) (Kazmi et al., 1984). The Manglaur Formation is a probable correlative to the Pre Cambrian-Cambrian (?) Tanawal Formation which forms the base of the Paleozoic section in Peshawar basin (Kazmi et al., 1984; Lawrence et al., 1989). This basement is unconformably overlain by late Paleozoic to early Mesozoic calcareous schists, marble and amphibolites of the Alpurai group (Lawrence et al., 1989; DiPietro, 1990; DiPietro et al., 1993). Previously this meta-sedimentary cover was termed as lower Swat-Buner schistose group by Martin et al. (1962).

Swabi-Chamla sedimentary group is present at the southern portion of lower Swat-Buner schistose group (Siddique et al., 1968) consisting of rocks ranging from Paleozoic to Mesozoic in age (Pogue et al., 1992a). Earlier workers, including Martin et al. (1962) and Stauffer et al. (1968), described the stratigraphy of rocks from this group which is revised by Pogue and Hussain (1986) and Pogue et al. (1992a). These rocks include Tanawal Formation, Ambar Formation, Misri Banda Quartzite, Panjpir Formation, Nowshera Formation, Jafar Kando Formation, Karapa Greenschist, Kashala Formation and Nikanai Ghar Formation (Pogue and Hussain, 1986; Pogue et al., 1992a). Tanawal Formation is intruded by Mansehra granite which yielded a whole rock Rb/Sr age of 516 ± 16 m.y. (Le Fort et al., 1980).

Lower Swat-Buner schistose group and Swabi-Chamla sedimentary group serve as country rocks for the alkaline magmatism i.e. Peshawar Plain Alkaline Igneous Province (PPAIP), in this region (Fig. 2.2). Kempe and Jan (1970) first reported the existence of the alkaline province in northern Pakistan. PPAIP extends from Tarbela in the east to Pak-Afghan border in the west (Kempe, 1973). The component rocks of PPAIP include carbonatites and silicate rocks. The latter category consists of alkali granites, porphyritic granites, quartz syenites, syenites, nepheline syenites and ijolites. Whereas the carbonatites occur in the Loe Shilman, Sillai Patti, Jawar and Jambil areas, major

exposures of the alkaline silicate rocks are located in Warsak, Shewa-Shahbazghari, Ambela, Tarbela and Malakand (Kempe, 1973; Kempe and Jan, 1980).

Two ideas about the origin of the carbonatite complexes and their associated alkaline rocks of PPAIP are suggested. Le Bas et al. (1987) proposed that these were formed as a result of at least two magmatic episodes; one during the Carboniferous and the other in Tertiary (Oligocene). These authors further suggested that the PPAIP was not related to the Himalayan collision, and that there was no evidence for rift-related emplacement at least in the case of the Loe-Shilman and Sillai Patti carbonatite complexes. According to them, whereas the Koga carbonatite was emplaced during Carboniferous, emplacement of the Loe-Shilman and Sillai Patti carbonatites took place during the Tertiary (Oligocene) magmatic episode. The results of relatively recent studies by Khattak et al. (2005 & 2008) also support the occurrence of Tertiary alkaline magmatic episode in the region.

Butt et al. (1989) noticed the presence of epidote in the Sillai Patti carbonatites and correlated them with the Koga carbonatite (Carboniferous) and concluded that all the carbonatite complexes and associated alkaline rocks of the alkaline belt of the northern Pakistan were emplaced during Permo-Carboniferous tensional rifting and break-up of Gondwanaland. He further postulated that the Sillai Patti carbonatite and associated country rocks were metamorphosed under greenschist or epidote–amphibolite facies conditions. Jan and Karim (1990) noted the total absence of carbonatites and associated alkaline rocks from the post-Paleozoic sequences and hence proposed that all the components of the PPAIP were emplaced during the Permo-Carboniferous tensional rifting.

Ambela granitic complex is the principal member of PPAIP and covers over 900km² area. Rafiq and Jan (1988) distinguished and grouped the rocks of the Ambela area into three: (i) granites, alkali granites and microporphyrites, (ii) quartz syenites, alkali quartz syenites, syenites, feldspathoidal syenites, ijolite, lamprophyre and associated pegmatites and fenites, and (iii) basic dykes. The last mentioned, which constitute about 5 % of the Ambela complex, intrude the rocks belonging to both (i) and (ii) and hence represent the last magmatic episode. According to these authors, group (i) appears to represent the earliest magmatic episode in the Ambela area.

Basic intrusions are widespread in Pre-Permian sections between Khairabad thrust and MMT but have not been observed in Mesozoic or younger rocks (Pogue et al., 1992b). Petrographic observation and chemical analysis of such basic intrusions from the Malka area, lower Swat, led Majid et al. (1991) to conclude that these intrusions are associated with Permian rifting of the northern portion of the Indian plate. These dykes are also reported from the Shewa-Shahbaz Garhi complex (Ahmed, 1986), Ambela granitic complex (Rafiq and Jan, 1988), Tarbela alkaline complex (Jan et al., 1981b), southern Hazara (Calkins et al., 1975). Similar intrusions are also reported from the Paleozoic formations of the Attock-Cherat ranges (Yeats and Hussain, 1987) and Khyber agency (Shah et al., 1980). Mafic dykes intruding Mansehra granite in Hazara region yielded $^{39}\text{Ar}/^{40}\text{Ar}$ plateau dates of 284 ± 4 and 262 ± 1 Ma confirming a Permian age for the basaltic magmatism (Baig, 1990).

The Uvla area, Gadoon is located at the south-eastern extremity of the lower Swat-Buner schistose group. The rocks of the Uvla area are mainly granitic in composition intruded by dykes of basic and intermediate composition. These granitoids probably represent the eastward extension of the Ambela granitic complex (Rafiq and Jan, 1988), however, some of the recent workers have mapped these rocks with the granitic rocks of Swat and Mansehra (Sajid and Arif, 2010; Hussain et al., 2004; DiPietro et al., 1998).

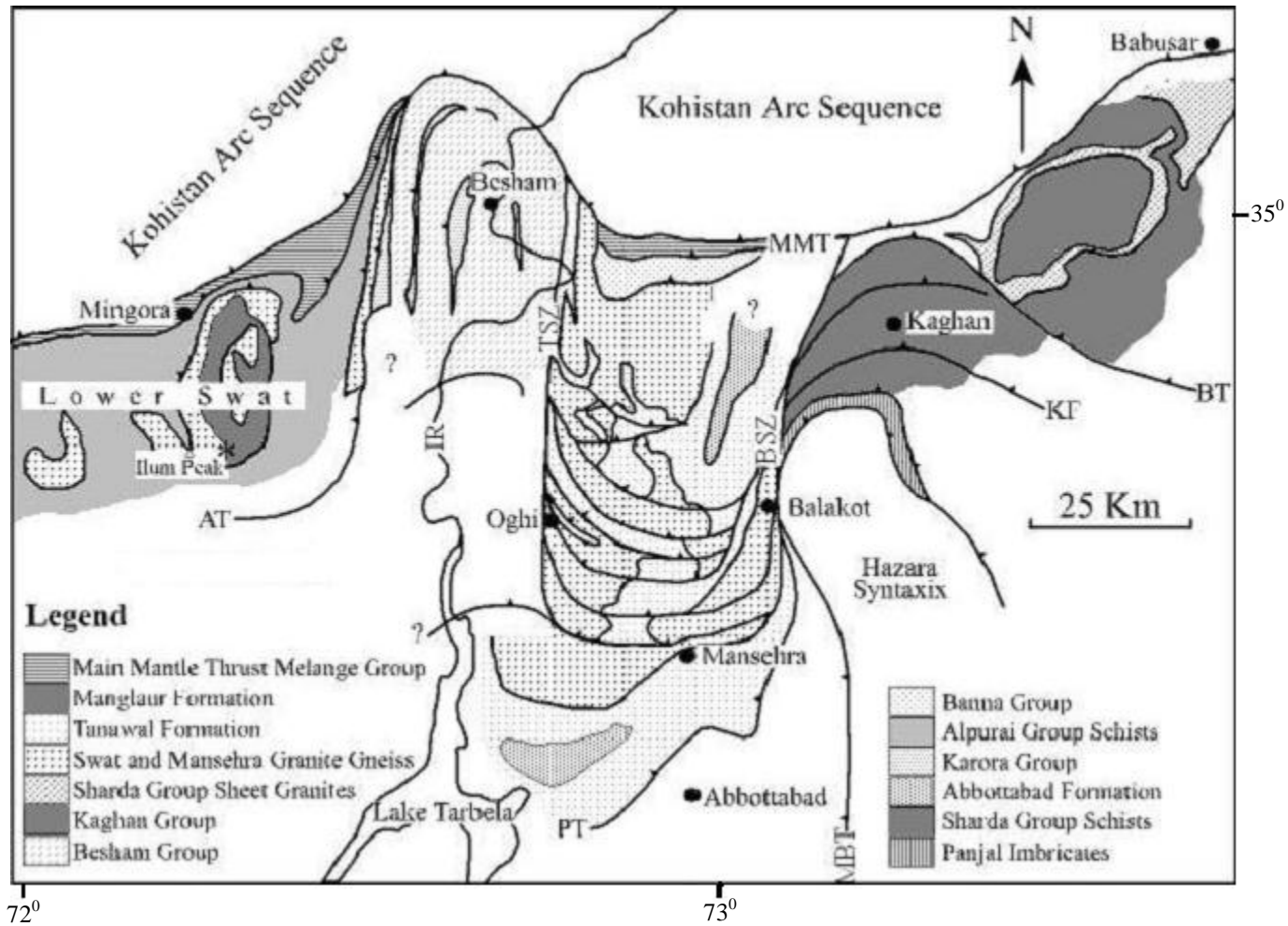


Fig. 2.1. Geological map of the area south of the Main Mantle Thrust between the Swat and Kaghan valleys (redrawn from Treloar and Rex, 1990). Abbreviations: AT = Alpurai Thrust; BSZ = Balakot Shear Zone; BT = Batal Thrust; IR = Indus River; KF = Khannian Fault; MBT = Main Boundary Thrust; MMT = Main Mantle Thrust; PJ = Panjal Thrust; TSZ = Thakot Shear Zone.

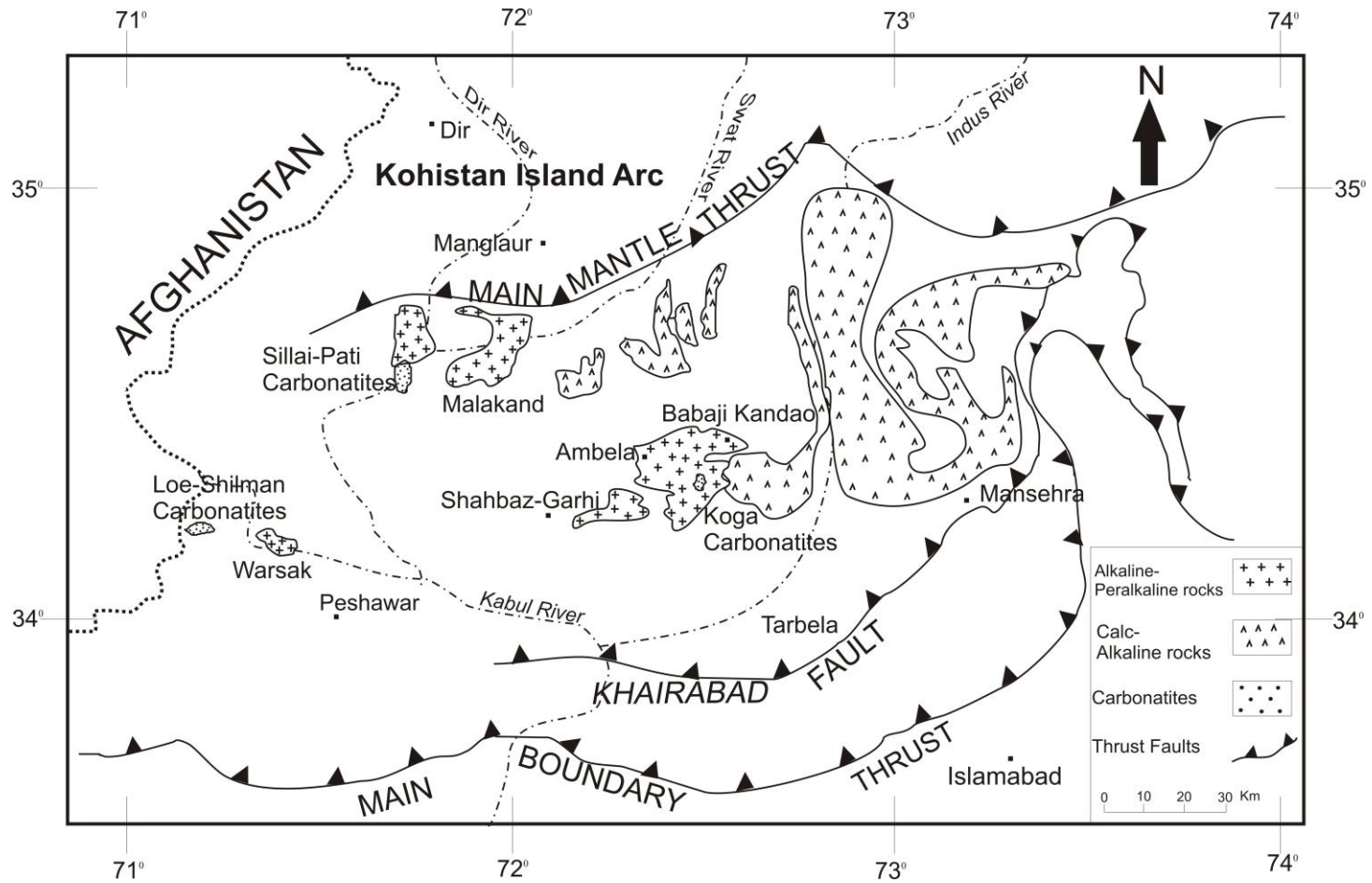


Fig. 2.2. Generalized geological map showing the major alkaline complexes in Northern Pakistan (Redrawn from Khattak et al., 2005)

PETROGRAPHY

3.1. General Statement

The modal mineralogy and the textural relationships within a rock are best described with the help of petrographic studies. These include observation of important field features as well as detailed microscopic examination of rocks. Detailed analyses of minerals and their textural relationship by microscopic study of thin sections are critical to understanding the origin of rock. The igneous rocks of the Utla area, NW Pakistan, exposed to the southeast of the lower Swat-Buner schistose group, are believed to be a part of the Peshawar Plain Alkaline Igneous Province (PPAIP). In contrast to the rocks of Utla area, the petrographic and mineralogical details of most of the other rocks in the region have been studied in reasonable detail. A detailed petrographic account of the Utla rocks is presented in this chapter.

3.2. Samples and Methods

During the fieldwork, 37 rock samples were collected. These samples predominantly consist of granitic rocks, including both massive and foliated textural varieties, and the intruding dark colored dykes. Thirty one samples were cut into thin sections for detailed petrographic studies.

3.3. Petrography

On the basis of detailed field and petrographic observations, igneous rocks of the Utla area can be grouped into two broad categories:

1. Granitic rocks
2. Dykes of basic composition cutting across these granites

The petrographic details of the two rock groups are separately described below.

3.3.1. Granites

Texturally, the granitic rocks of the Utla area are mega-porphyritic (Fig. 3.1a). At places, however, massive fine-grained and foliated varieties also occur, particularly along shear zones. Furthermore, the equigranular fine-grained varieties also occur as small patches within the mega-porphyritic granite (Fig. 3.1b). Texturally homogenous, fine to medium grained granitic dykes also cut across these mega-porphyritic granitic rocks at places (Fig. 3.1c).

The frequently large size (5-6cm) of the phenocrysts present in these rocks makes them visible even from some distance. These phenocrysts consist of zoned and saussuritized plagioclase, perthitic alkali feldspar, including both the orthoclase and microcline varieties, and quartz. The groundmass predominantly consists of alkali feldspar and quartz, minor to accessory amounts of tourmaline, biotite and muscovite and accessory to trace amounts of apatite, andalusite, zircon, monazite, sphene and garnet. The modal abundance of these minerals is presented in Table 3.1 and plotted on the relevant IUGS classification triangle (Fig. 3.2). Most of the compositional spots spread over the field of granite due to wide range in the concentration of essential minerals, however, two of the samples deviate from the granite field.

Quartz is the most abundant mineral occurring in most of these rocks and shows a wide range of modal proportion (15-69 %). At places quartz rich veins (Fig. 3.1d), containing more than 90% quartz (Table 3.1) and accessory feldspars, cut across the megaporphyritic granites. Almost all the quartz grains display undulose extinction (Fig. 3.3a). However, some of the studied samples display mortar or flaser texture whereby clustering of unstrained fine-grained quartz separate large strained grains (porphyroclasts) of alkali feldspar, plagioclase and quartz (Fig. 3.3b). It reflects the strain-induced syntectonic recrystallization and is the evidence of shearing and deformation in these rocks.

Alkali feldspar, including both orthoclase and microcline (Fig. 3.3c), is the next most abundant mineral in these rocks and its modal abundance ranges from 16 to 60 %. Exsolution is commonly observed in most of the alkali feldspar grains (Fig. 3.3d), however, samples representing northern part of the area also contain grains of homogenous alkali feldspar. The gradual increase in the modal abundance of homogenous feldspar and corresponding decrease in the perthitic grains suggests that the amount of exsolution decreases from south to north. The extent of albite exsolution in the samples from the southern part is also variable most probably because of difference in the composition of the original homogeneous alkali feldspar grains and/ or degree and rate of their undercooling below the crystallization temperature. Blebs of zoned plagioclase (Fig. 3.4a) are also observed in some microcline grains. Some of the studied samples display the intergrowth of alkali feldspar and quartz in the form of graphic texture (Fig. 3.4b).

The amount of plagioclase ranges from 13 to 32 % and constitutes the third most abundant mineral in these rocks. It occurs as phenocryst as well as medium sized grains

in groundmass. Most of the plagioclase grains have cloudy appearance because of partial alteration. The alteration products include clay minerals, sericite, muscovite and epidote; hence, the processes of alteration are largely sericitization and saussuritization. Some of the plagioclase phenocrysts are zoned (Fig. 3.4c) with a saussuritized/ sericitized core and fresh margin thereby indicating 'normal' zoning, i.e. the margins of the grains are more sodic and hence less susceptible to alteration than their respective cores.

Tourmaline is the most common and abundant mafic mineral occurring in the rocks under discussion. The presence of appreciable amounts (0.33-11.08%) of tourmaline makes the Utla rocks resemble the granitic rocks of Mansehra. Most of the tourmaline grains display irregular color zoning (Fig. 3.4d) and variable degree of alteration. The modal abundance of tourmaline seems to be gradually increasing in moving from south (Utla proper) to north across the granitoid body. At places, thin veins of blue-green tourmaline cutting across the mega-porphyrific granites also occur (Fig. 3.5a). These are most probably formed by the injection of residual boron-rich magmatic fluids along fractures in the already crystallized granite.

The flakes of biotite and muscovite mostly occur in close association. Their modal abundance is relatively high in the foliated varieties where they may wrap around the megacrystic feldspar (Fig. 3.5b). Some of the muscovite grains have diffused margins with associated biotite grains which suggest that these muscovite grains might have formed at the expense of biotite. Such a relationship also suggests topotaxial growth of muscovite over biotite (Fig. 3.5c-d). Topotaxial growth is the conversion of a single crystal into one or more products which have a definite crystallographic orientation with respect to the original crystal, with the added requirements that the conversion occur throughout the entire crystal and that there be three-dimensional accord between the initial and final structures (Shannon and Rossi, 1964).

Trace amounts of andalusite also occur in the Utla granites. Optically it is distinguished from apatite by its pleochroism and biaxial interference figure. Most of the andalusite grains show variable degree of alteration to muscovite (Fig. 3.6a-b). The presence of andalusite, like that of tourmaline, suggests that the rocks of Utla area could be a continuation of the granitic rocks of Mansehra rather than those of the Ambela complex as andalusite is not reported from the latter.

Trace amounts of sphene occur in some of the studied samples. It is mostly associated with biotite and ore mineral(s). It occurs as small discrete grains as well as thin rims or broader zones around small grains of an opaque ore mineral (Fig. 3.6c). In some of the studied samples small grains of monazite are also associated with sphene and ore mineral grains.

Fine to medium sized grains of epidote and clinozoisite mostly associated with sericite are also observed in some of the studied samples. Some epidote grains are distinctly zoned. The zoning is indicated by a marked difference in interference color within individual grains. Such zoned grains have bluish interference color along the margins and yellowish/pinkish interference color in the core, indicating low (-medium) grade prograde metamorphism of these granitic rocks.

Relatively larger, colorless grains of garnet also occur in some of the studied samples (Fig. 3.6d). These grains may be magmatic in origin. Although mostly found in pegmatites and aplitic dykes, magmatic garnet is also reported to occur in felsic to very felsic per-aluminous granitoids (e.g. du Bray, 1988; Kebede et al., 2001). Dahlquist et al. (2007) used such a magmatic garnet as a geothermobarometer.

Medium sized discrete grains of apatite also occur in some of the studied samples. In addition, sillimanite with typical fibrous habit has also been observed in few of the samples (Fig. 3.7). It is distinguished from andalusite by having positive elongation, higher birefringence and fibrous form. The occurrence of fibrolitic sillimanite is also reported from Ambela granitic complex (Rafiq and Jan, 1988) and Mansehra granite (Le Fort et al., 1983).

Table 3.1. Modal mineralogical composition of granitic rocks from Utlá area

	Qtz	Alkf	Plg	Bt	Mus	Tour	Clay	Rut	Sph	Zir	Apt	Ore	Grt	Flrt	And	Mzt	Epdt	Srct
U-3	37.08	27.92	14.58	--	7.42	11.08	1.17	0.75	--	--	--	--	--	--	--	--	--	--
U-5	40.63	20.63	18.38	9.38	6.88	0.38	--	0.63	2.13	1.00	--	--	--	--	--	--	--	--
U-7	45.38	18.23	23.46	6.92	3.69	0.85	--	--	0.31	--	0.92	0.23	--	--	--	--	--	--
U-9	41.33	23.00	18.80	4.27	6.67	2.07	--	--	1.47	--	1.27	--	0.67	0.47	--	--	--	--
U-10	26.25	38.75	19.42	6.17	6.92	--	--	0.17	1.08	0.25	0.75	0.25	--	--	--	--	--	--
U-12	35.00	18.80	27.00	7.60	3.90	4.90	--	--	--	0.60	1.70	--	--	--	0.50	--	--	--
U-13	31.00	34.33	15.00	3.80	8.87	5.27	--	--	0.67	--	0.47	0.07	--	--	0.53	--	--	--
U-15	35.12	28.24	13.26	9.75	7.2	4.3	--	0.73	--	--	0.2	1.2	--	--	--	--	--	--
U-16	30.83	25.00	25.83	4.67	6.67	6.17	--	0.83	--	--	--	--	--	--	--	--	--	--
U-17	21.00	31.54	23.31	9.00	4.69	5.54	--	--	1.08	0.38	1.62	0.85	--	--	1.00	--	--	--
U-18	33.13	39.38	13.75	7.88	3.63	1.75	--	--	--	--	0.38	0.13	--	--	--	--	--	--
U-19	23.46	27.31	30.77	4.15	4.23	2.54	--	--	2.31	--	1.08	1.00	1.15	--	--	0.23	1.77	--
U-22	37.00	25.50	31.00	--	--	--	--	--	--	--	--	--	--	--	--	--	--	6.50
U-23	36.25	25.42	20.42	8.58	4.33	0.33	--	--	1.58	0.33	1.08	1.08	--	--	--	0.58	--	--
U-24	36.16	20.24	13.29	8.24	9.2	11.25	0.84	--	--	--	--	--	--	--	0.32	0.61	--	--
U-26	17.50	63.79	10.36	1.14	3.21	0.43	--	--	--	--	--	0.14	--	--	--	--	3.43	--
U-27	15.64	49.55	32.27	--	--	--	--	--	--	--	--	--	--	--	--	--	0.73	1.82
U-29	18.31	63.85	13.31	1.54	3.00	--	--	--	--	--	--	--	--	--	--	--	--	--
U-30	37.15	30.23	14.24	6.74	8.35	--	1.29	--	1.24	--	0.36	0.48	--	--	--	--	--	--
U-31	30.45	49.55	13.18	0.91	0.64	--	--	--	0.18	--	--	0.27	--	--	--	--	--	4.82
U-32	69.67	20.00	3.67	1.33	1.67	--	--	1.00	--	--	1.33	--	1.33	--	--	--	--	--
U-33	32.50	41.67	16.08	1.92	3.33	0.67	--	--	--	--	--	--	--	--	--	--	--	3.83
U-35*	95.75	4.25	--	--	--	--	--	--	--	--	--	--	--	--	--	--	--	--

* = Quartz rich vein

Qtz= Quartz, Alkf=Alkalifeldspar including orthoclase and microcline, Plg= Plagioclase, Bt= Biotite, Mus= Muscovite, Tour= Tourmaline, Rut= Rutile, Sph= Sphene, Zir= Zircon, Apt= Apatite, Grt= Garnet, Flrt= Flourite, And= Andalusite, Mzt= Monazite, Epdt= Epidote, Srct= Sericite,

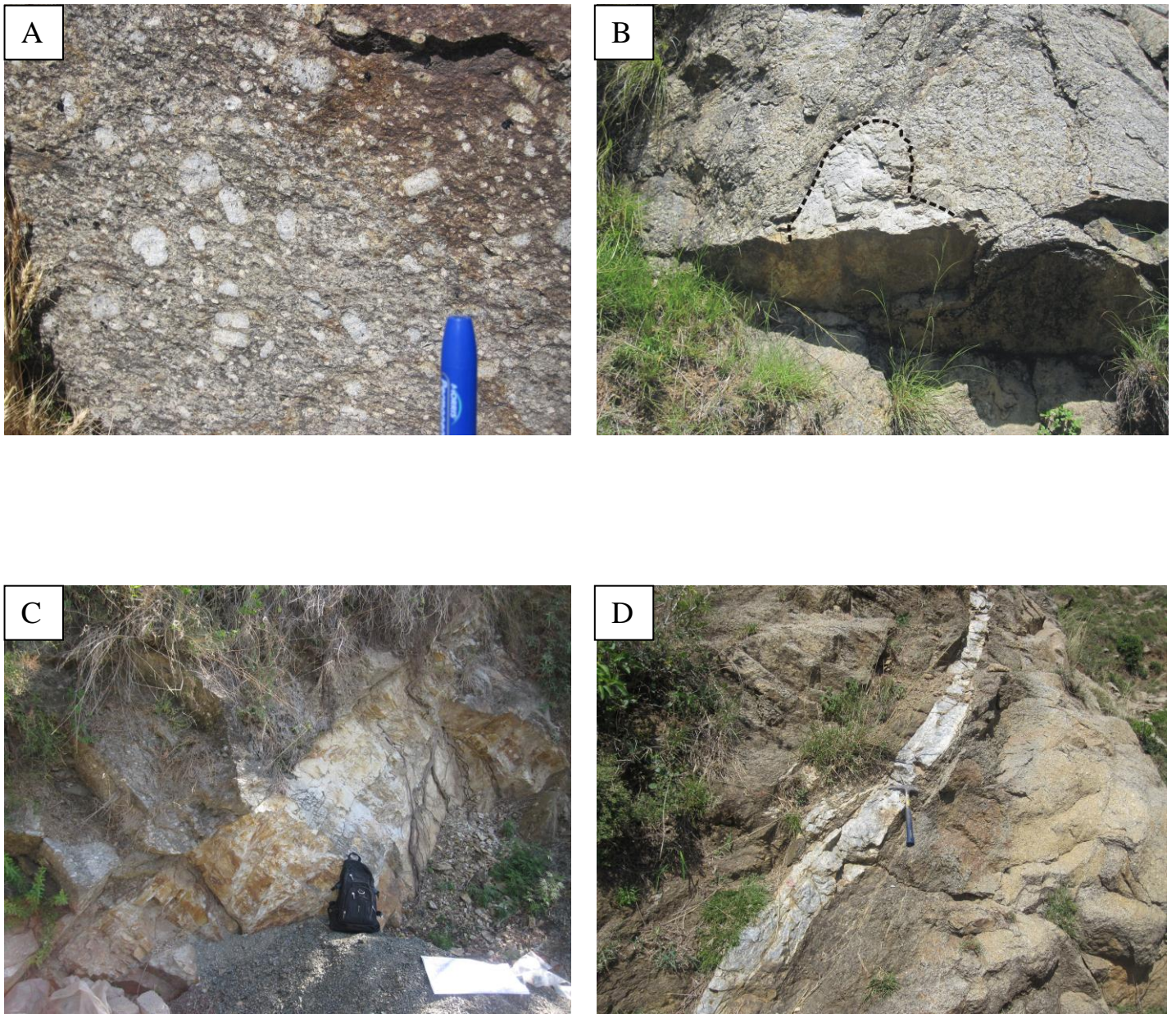


Fig. 3.1. Field photographs: (A) The mega-porphyritic Utlá granite; (B) A small patch of fine-grained granite within the mega-porphyritic granite; (C) A fine to medium-grained dyke of granitic composition, (D) A quartz rich vein cutting the Utlá granite.

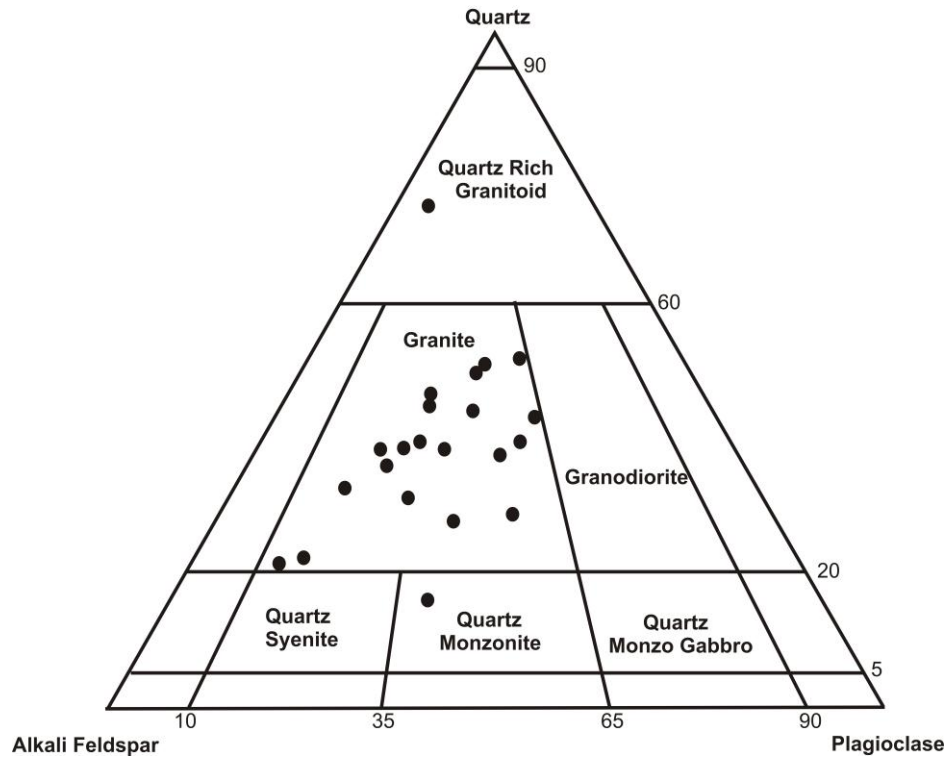


Fig. 3.2. Modal composition of the studied granitic rocks plotted on the IUGS classification diagram (from Le Maitre, 2002)

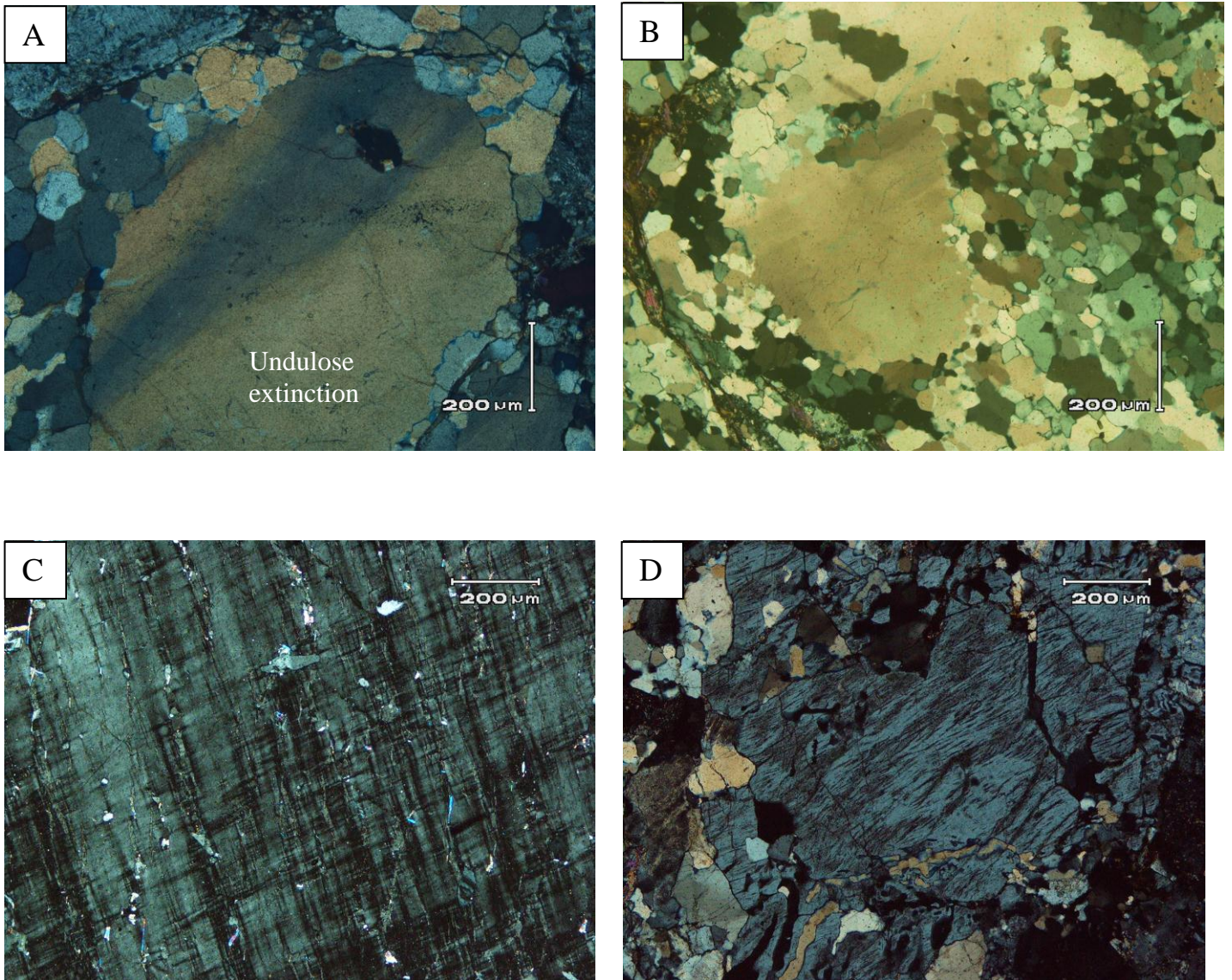


Fig. 3.3. Photomicrographs (XPL): (A) Undulose extinction in quartz grain, (B) Clusters of unstrained fine-grained quartz grains around a strained quartz phenocryst, (C) Cross-hatched twinning in microcline, (D) Perthitic alkali feldspar.

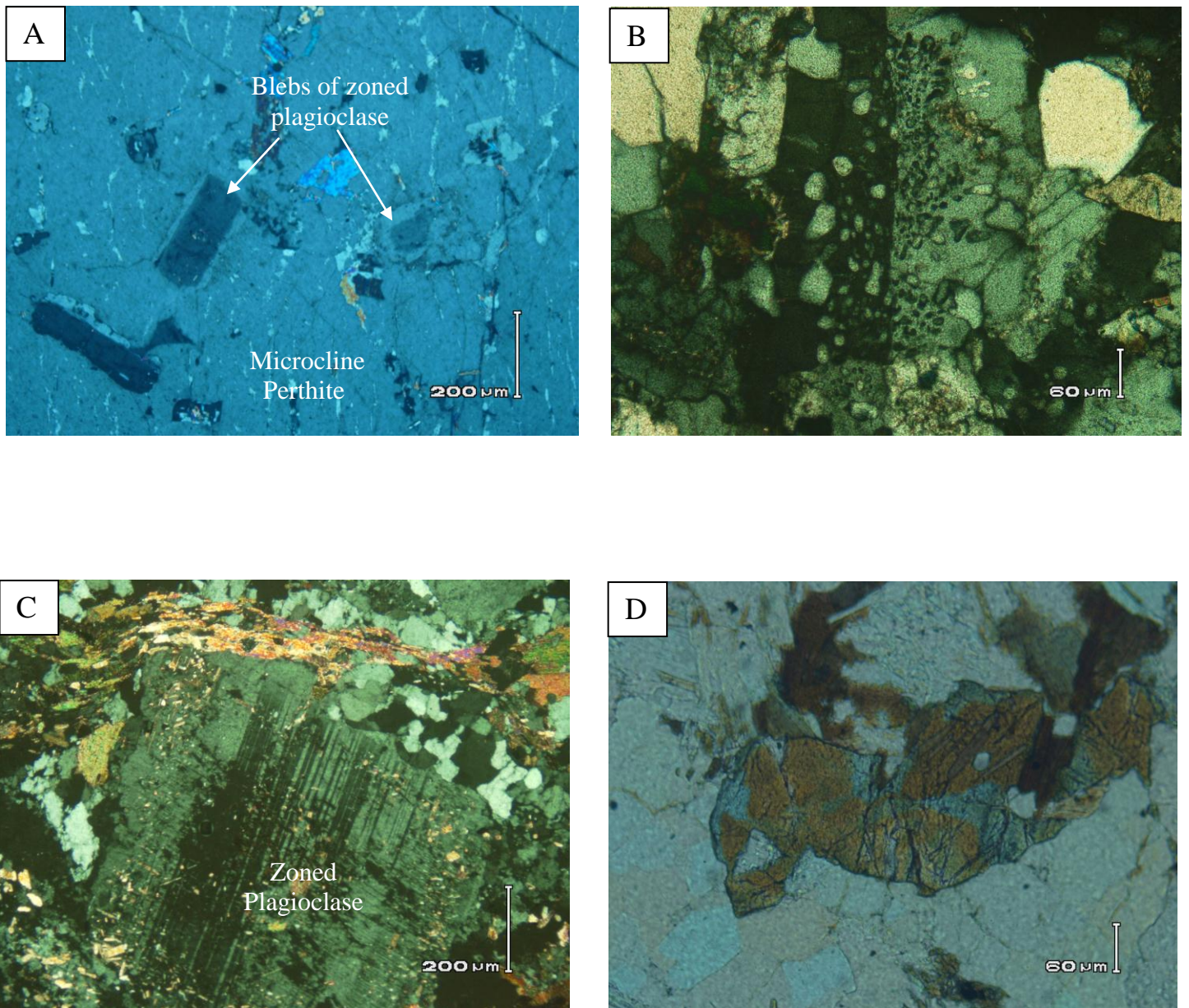


Fig. 3.4. Photomicrographs (XPL): (A) Blebs of zoned plagioclase in a phenocryst of perthitic microcline, (B) Graphic texture, (C) A phenocryst of zoned plagioclase, (D, PPL) Color zoning in tourmaline

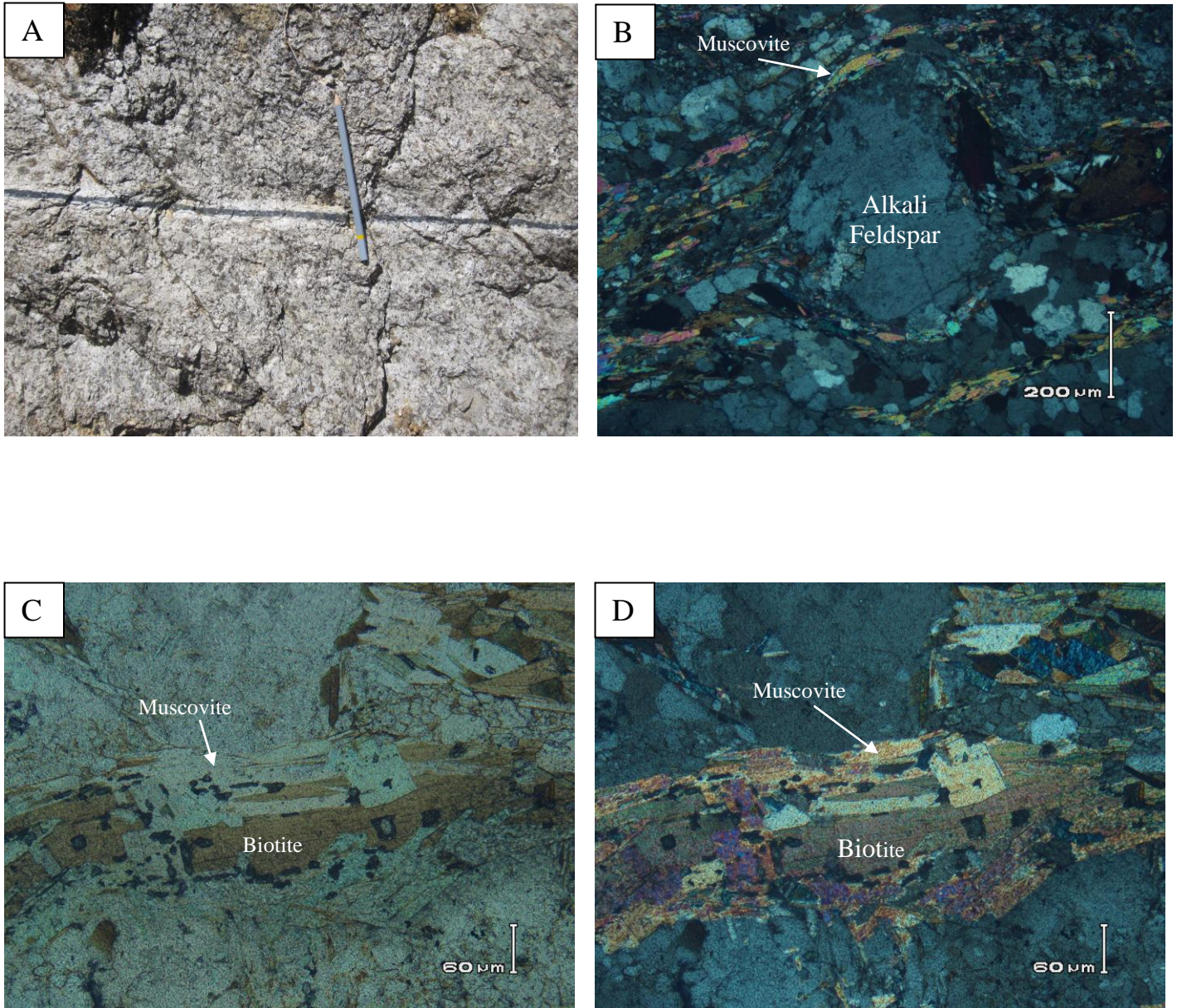


Fig. 3.5: (A) A thin tourmaline-rich vein cutting across the Utlå granite, (B) A photomicrograph showing muscovite and biotite wrapped around a megacryst of alkali feldspar (XPL), (C, PPL; D, XPL) Photomicrographs showing topotaxial growth of muscovite about biotite.

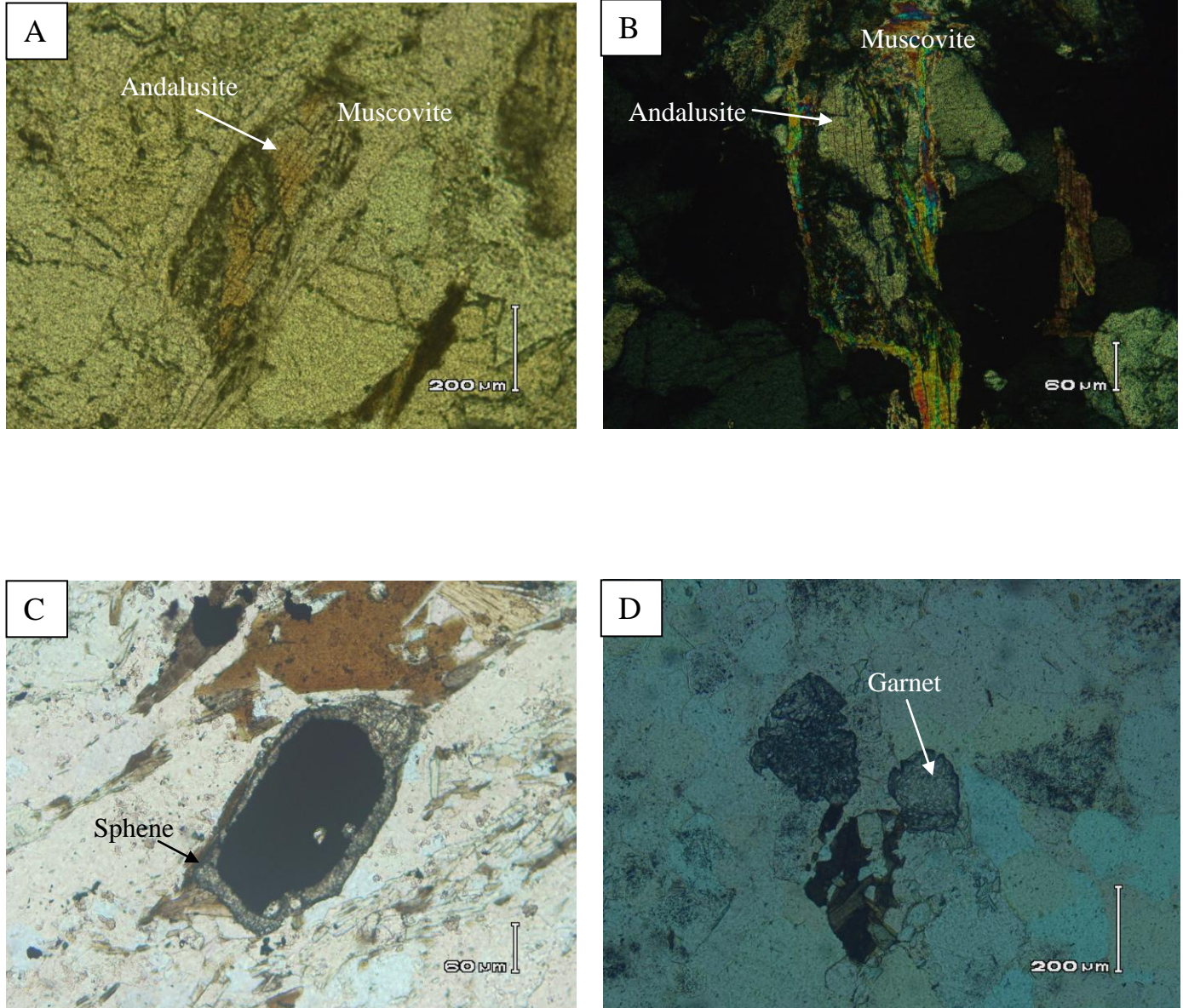


Fig. 3.6. Photomicrographs: (A, PPL; B, XPL) Alteration of andalusite to muscovite, (C) A thin border of sphene around an opaque ore mineral grain (PPL), (D) Garnet grains (PPL).

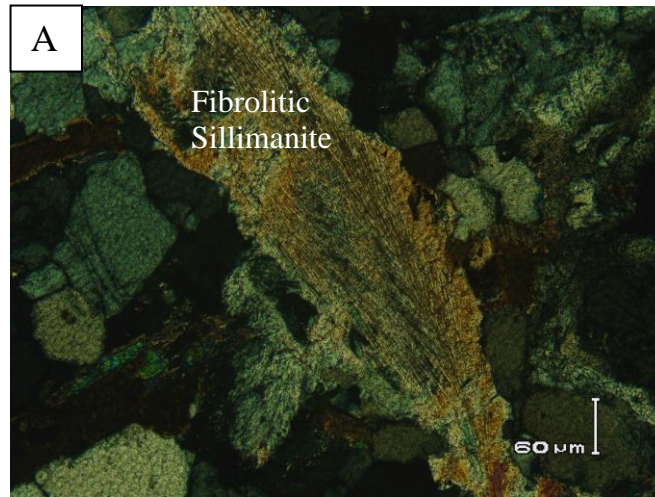


Fig. 3.7. Photomicrograph showing Fibrolitic sillimanite

3.3.2. Basic Dykes

At places, variably thick (1-4m), dark color dykes cut across the Uta granites (Fig. 3.8a). Almost all the dykes are fine to medium grained and foliated especially along their margins. The modal mineralogy confirms the basic nature of these dykes. On the basis of their textural and mineralogical characteristics, these dykes are further divided into the following two types:

a. Dolerite Dykes

These dykes essentially consist of plagioclase and clinopyroxene and display ophitic texture (Fig. 3.8b) and, thus, appear to be dolerite. Plagioclase is mostly subhedral to anhedral and medium to fine grained and displays a variable degree of alteration to clay mineral (s). The clinopyroxene is anhedral to subhedral and fine to medium grained. The clinopyroxene grains are pink/violet in plane light (Fig. 3.8c) and, hence, may contain significant amounts of titanium. In other words, the clinopyroxene may be titaniferous augite. It is important to mention that dykes of more or less similar mineralogical and textural characteristics are also reported from the adjoining areas (Majid et al. 1991). The grains of clinopyroxene show variable degree of alteration to chlorite and amphibole (Fig. 3.8c). Besides, brownish hornblende also occurs as discrete grains in some of these dolerite dykes.

These rocks also contain accessory amounts of other minerals including biotite, sphene, epidote, apatite, ilmenite and rutile. Like that in the host granite, sphene in the dolerite

dykes occurs both as discrete grains and thin rims or zones around opaque ore grains forming corona texture (Fig. 3.8d).

b. Altered/ metamorphosed Basic Dykes

Most of the dykes from this subgroup display a certain degree of preferred orientation (Fig. 3.9a) and largely consist of plagioclase and hornblende. They contain only traces of clinopyroxene either as relics enclosed within or totally pseudomorphed by green amphibole and chlorite (Fig. 3.9b).

Most of the plagioclase grains are altered and occur as relics within the products of its alteration, however, euhedral to subhedral, fresh grains also occur in some of the studied samples. The alteration products include epidote, zoisite, biotite, sericite and clay mineral (s).

Subhedral to anhedral amphibole occurs as fine to medium sized discrete grains displaying brown color in plane light and partial alteration to chlorite and biotite. This brown color of amphibole may be due to the presence of significant amount of Ti (Lamoen, 1980). Amphibole with similar optical character has also been reported from dykes of Malka area (Majid et al., 1991).

Appreciable amounts of epidote and clinozoisite also occur in these rocks. Both these minerals occur as subhedral to anhedral discrete grains as well as fine aggregates. The mode of occurrence and association suggest that epidote formed by the alteration of amphibole and plagioclase. This feature and formation of amphibole and chlorite at the expense of clinopyroxene suggest metamorphism of the dykes under green schist to epidote-amphibolite facies conditions.

The more or less commonly occurring accessory phases in these rocks include sphene, rutile, ilmenite, calcite and apatite. As also observed in dolerite dykes, described above, corona texture consisting of sphene around an opaque ore mineral is a common feature noticed in these rocks.

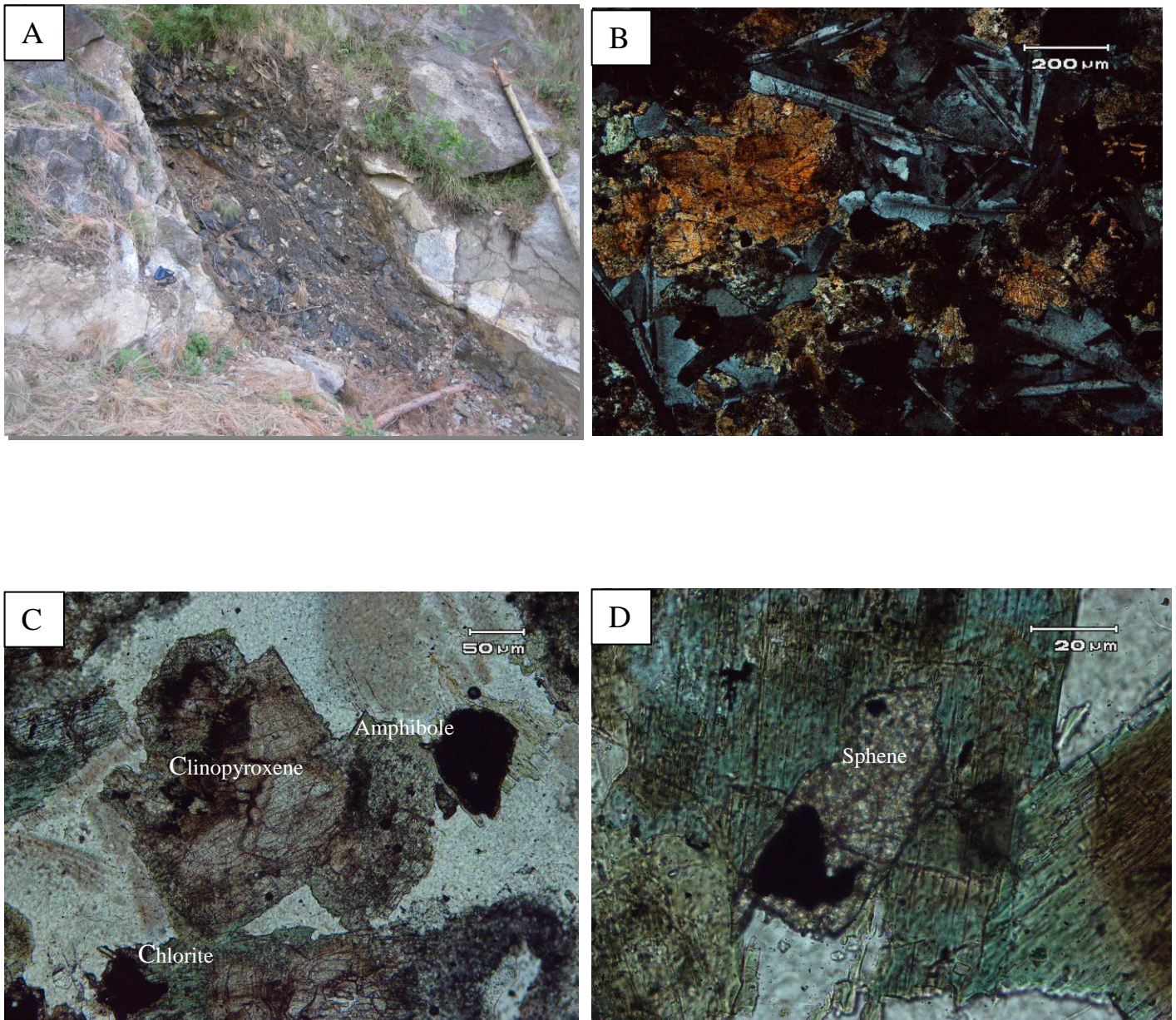


Fig. 3.8. (A) A basic dyke cutting across the Utlå granite; (B, C and D, Photomicrographs): Ophitic texture (B, XPL), a pinkish clinopyroxene grain showing alteration to chlorite and amphibole (C, PPL), and a rim of sphenes around an opaque ore mineral grain (D, PPL).

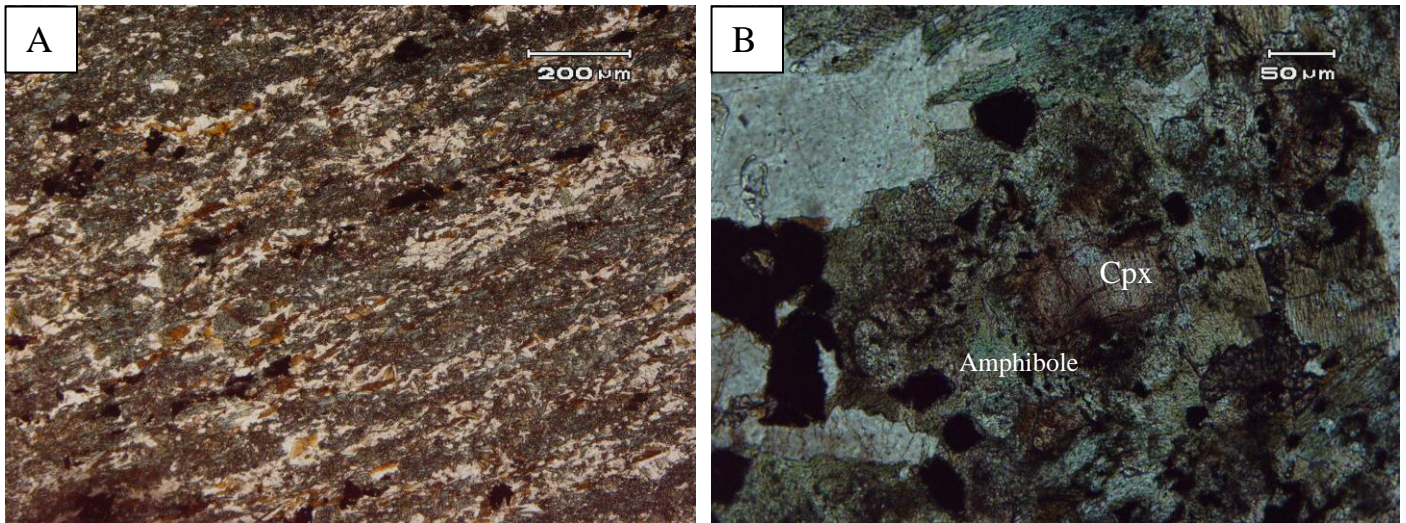


Fig. 3.9. Photomicrographs (PPL): (A) preferred orientation in basic dyke and (B) relics of pinkish clinopyroxene (Cpx) in green amphibole.

GEOCHEMISTRY

4.1. General Statement

The petrographically investigated rocks of the Utrla area belong to two broad categories i.e. granites and dykes. Selected samples representing both these rock groups were analyzed chemically. The main objectives of the chemical analysis are outlined below:

- a) Determination and detailed investigation of major, minor and trace element contents of rocks for their geochemical characterization.
- b) Determination of petrogenetic affinity and geotectonic settings through discriminant diagrams using trace elements as they can serve as important indicators of the magmatic processes.

4.2. Methodology

A total of 24 samples, sixteen from granitoids and eight from dykes, was pulverized for the whole-rock chemical analysis in the National Center of Excellence in Geology, University of Peshawar. Except for silica, the contents of the major, minor and trace elements were determined through X-ray fluorescence spectrometry. The silica concentration was determined by UV spectrophotometer. The XRF analyses were carried out on fused disks called as glass beads. A small amount of each sample (~ 4-5gm) was dried overnight at 110°C to remove the absorbed moisture, if any. After cooling in desiccators, 0.7 gm of each of the samples was mixed with 7 gm of flux (mixture of lithium metaborate and lithium tetraborate). Two-three drops of releasing agent (lithium iodide) was added to the mixture. The resulting sample-flux mixture was fused in platinum (95%)-gold (5%) crucible at 1100°C for 10-15 minutes. During this period the crucible was periodically swirled over a burner to eliminate the gas bubbles and ensure the thorough mixing and homogeneity of the melt. The melt was cast in platinum mold having a diameter of 30 mm. Each bead was analyzed for TiO₂, Al₂O₃, Fe₂O₃, MnO, MgO, CaO, Na₂O, K₂O and P₂O₅. The analyses were performed through a PANalytical PW4400/24 spectrometer equipped with a rhodium anode X-ray tube. International standards, namely WROXI-1, WROXI-2, WROXI-3, DT-N, SDC-1, PG-1, G-2 were alternately run with each batch of five samples to monitor the precision and accuracy of the machine. The minimum detection limits for major elements are as follows: TiO₂ (0.003%), Al₂O₃ (0.0039%), Fe₂O₃ (0.0085%), MnO (0.016%), MgO (0.0055%), CaO (0.0042%), Na₂O (0.0039%), K₂O (0.0038%) and P₂O₅ (0.0013%).

The minor and trace element analyses of the samples were performed on powdered pellets. An approximately 12 gm of powdered dried samples was mixed with 3 gm of wax with the help of a small glass rod. This mixture was then placed in steel cups and pressed into the shape of pellets by applying pressure. The powdered pellets were run through PANalytical PW4400/24 XRF spectrometer for the analyses of the following set of elements: Sc, V, Cu, Cr, Ni, Zn, Ga, As, Br, Rb, Sr, Y, Zr, Nb, Mo, Ag, Cd, Sn, Ba, La, Ce, Hf, Pb, Bi, Th. A set of standards was run with each batch of five samples to monitor the accuracy and precision of the machine. The concentrations of major elements are given in weight percent (wt %) of oxides and trace elements are reported in parts per million (ppm).

4.3. Granites

4.3.1. Major elements geochemistry

The major, minor and trace element composition of sixteen representative samples from Utlá granitoids are listed in table 4.1. The chemical analyses reveal that these granitoids display a broad spectrum of SiO₂ content (67.45-78.79 wt. %). The other major element oxides are plotted against SiO₂ in order to portray the pattern of fractionation (Fig. 4.1). The observed gap between the silica percentages probably reflects missing of some representative samples. Alternatively, it might represent some sort of contamination. The TiO₂ (0.05 to 0.62 wt. %), Fe₂O₃ (0.12-1.38 wt. %) and MgO (0.08-0.99 wt. %) contents display a poorly defined negative relation with SiO₂. A fairly significant negative correlation with SiO₂ content is shown by CaO (0.02-1.57 wt %) and P₂O₅ (0.07-0.39 wt %). Strongly negative trends with SiO₂ are observed for Al₂O₃ (11.73-20.34 wt %), Na₂O (1.29-5.44 wt %) and K₂O (0.73-9.09 wt %). The negative correlation of K₂O, Al₂O₃, MgO and Fe₂O₃ with SiO₂ probably indicates the fractionation of biotite during the process of crystallization. A positive correlation between CaO and TiO₂ and their negative correlation with SiO₂ most probably reflects the fractionation of sphene (CaTiSiO₅). There has also been fractionation of apatite as indicated by the positive relation between CaO and P₂O₅ and their negative correlation with SiO₂.

The low values of FeO^t+MgO+TiO₂ (0.25-2.99) (Fig. 4.2) and low color index (0.35-5.34) (Table 4.1) reflect the leuco-granitic nature of the Utlá granitoids. The mostly high alumina saturation index (ASI) (0.75-2.23; averaging 1.22; Table 4.1) and the appearance of normative corundum (1.71-8.52 wt %; Table 4.1) indicate a per-aluminous character for most of the granitoids. Only three of the samples have their ASI falling below 1 and they therefore plot in the

field of per-alkaline rocks (Fig. 4.3). The high potash and calc-alkaline nature of these rocks is reflected by the $\text{SiO}_2\text{-K}_2\text{O}$ relation (Fig. 4.4), AFM plot (Fig. 4.5) and FeO^t/MgO versus SiO_2 diagram (Fig. 4.6).

The FeO^t/MgO vs Zr+Nb+Ce+Y plot points to the 'normal' S-type or I-type character of the Utlá granites (Fig. 4.7). The $\text{Al}_2\text{O}_3/\text{TiO}_2$ and $\text{CaO}/\text{Na}_2\text{O}$ ratios in granitic rocks depend on the melt's source composition, temperature, pressure and the effect of added water (Holtz and Johannes, 1991; Patino Douce and Beard, 1995; Skjerlie and Johnston, 1996). According to Chappell and White (1992), variation in the abundances of CaO and Na_2O in strongly per-aluminous granites reflects different amounts of clay in their protolith. Plagioclase to clay ratio of the source rock, particularly, has the dominant control on $\text{CaO}/\text{Na}_2\text{O}$ ratio of the per-aluminous granites (Sylvester, 1998). According to the melting experiments on plagioclase-poor natural pelites by Patino Douce and Johnston, (1991), Na_2O dissolves in the melt and CaO is stabilized as garnet until garnet is consumed at high temperature, thus the melt has low $\text{CaO}/\text{Na}_2\text{O}$ ratio. In contrast, psammites contain larger proportion of plagioclase and, according to the melting experiments of Skjerlie and Johnston (1996), the concentration of both CaO and Na_2O in the initial melt is lower but increases steadily as plagioclase is consumed further, thus $\text{CaO}/\text{Na}_2\text{O}$ ratio will remain broadly constant with increasing temperature. As a result, the pelite-derived melts have lower $\text{CaO}/\text{Na}_2\text{O}$ (<0.3) ratio than the psammite-derived per-aluminous granitic melt (Sylvester, 1998). These observations led Sylvester (1998) to suggest that $\text{Al}_2\text{O}_3/\text{TiO}_2$ versus $\text{CaO}/\text{Na}_2\text{O}$ diagram and Rb/Ba versus Rb/Sr plot may be used for identifying the composition of source for melts parental to per-aluminous granites. Plots of data on these diagrams suggest a clay-rich, plagioclase-poor (i.e. pelitic) source for the melt that gave rise to the formation of the Utlá granitoids (Fig. 4.8).

Table 4.1. Representative chemical analysis of Utla granite

Sample	U-3	U-7	U-9	U-12	U-13	U-15	U-17	U-18	U-19	U-23	U-24	U-26	U-27	U-29	U-30	U-31
SiO ₂	75.76	77.35	75.34	68.12	73.23	67.45	72.89	73.78	75.67	74.21	78.79	71.68	77.86	71.25	74.89	76.89
TiO ₂	0.1	0.41	0.33	0.62	0.39	0.47	0.29	0.26	0.11	0.35	0.31	0.09	0.05	0.23	0.19	0.55
Al ₂ O ₃	15.61	11.73	15.76	15.23	16.12	20.34	16.13	16.34	15.1	16.12	14.78	16.23	14.35	15.78	15.42	14.14
Fe ₂ O ₃	0.14	0.7	0.77	0.99	0.53	0.59	0.34	0.34	0.19	0.54	0.41	0.09	0.08	0.55	0.21	0.71
MnO	0.08	0.07	0.10	0.13	0.12	0.04	0.08	0.07	0.09	0.06	0.03	0.02	0.08	0.05	0.04	0.04
MgO	0.21	0.56	0.57	1.38	0.82	1.01	0.51	0.46	0.21	0.79	0.99	0.17	0.12	0.26	0.22	0.96
CaO	0.53	0.57	0.02	1.44	1.02	1.16	0.9	0.86	0.59	1.35	0.32	0.49	0.28	0.57	0.42	1.57
Na ₂ O	4.35	1.29	3.34	4.8	2.71	5.44	3.61	3.46	3.5	3.22	3.2	4.58	2.62	3.26	3.14	2.82
K ₂ O	4.75	5.35	5.31	9.01	5.97	4.65	6.95	5.86	5.6	5.47	0.73	8.2	4.74	9.09	7.04	4.63
P ₂ O ₅	0.22	0.07	0.21	0.39	0.23	0.28	0.3	0.32	0.15	0.15	0.15	0.14	0.08	0.17	0.13	0.14
L.I.O	0.02	0.02	0.02	0.02	0.04	0.03	0.02	0.02	0.02	0.03	0.02	0.02	0.02	0.01	0.03	0.01
Total	101.66	98.02	101.67	102.06	101.05	101.42	101.96	101.67	101.14	102.23	99.7	101.62	100.2	101.18	101.69	102.42
Norm C	2.82	3.00	4.44	0.00	3.85	4.84	1.71	3.44	2.53	2.74	8.52	0.00	4.58	0.00	2.14	1.92
ASI	1.18	1.31	1.40	0.75	1.26	1.26	1.07	1.20	1.17	1.18	2.23	0.94	1.44	0.97	1.14	1.13
C.I	0.62	2.10	2.15	5.34	2.53	3.05	1.59	1.43	0.70	2.45	2.87	0.35	0.38	1.19	0.74	3.02
Minor and Trace elements (ppm)																
Sc	7	4	5	8	5	3	8	4	2	2	4	0	8	2	3	3
V	54	44	32	53	46	0	41	26	8	43	50	7	0	41	20	27
Cu	114	126	98	204	170	128	117	81	116	108	66	216	276	115	182	125
Zn	35	23	43	44	46	14	29	28	-2	19	23	0	41	8	8	0
Ga	34	30	38	33	33	33	37	34	33	35	32	27	35	32	33	31
As	13	7	20	6	5	5	5	6	2	7	1	6	11	8	3	3
Br	2	2	4	4	3	3	3	4	2	3	2	3	4	3	4	3
Rb	182	179	295	270	268	198	179	291	237	218	42	182	210	272	253	244
Sr	70	61	41	51	50	134	47	46	20	60	22	45	93	40	29	24
Y	22	40	26	28	26	26	32	23	18	31	23	10	33	34	38	33
Zr	145	215	91	94	98	105	104	81	19	109	130	7	166	62	54	60
Nb	11	9	13	12	14	15	15	15	11	9	8	4	13	8	12	9
Mo	2	3	1	1	1	1	1	1	0	1	1	0	2	0	0	1
Ag	20	22	20	12	17	21	20	20	16	21	18	14	24	14	15	16
Cd	12	13	12	10	10	13	12	14	12	11	9	11	15	7	11	11
Sn	31	30	41	34	32	33	35	36	33	32	64	28	32	29	34	32
Ba	372	399	204	269	256	2844	231	295	87	309	62	155	2524	184	118	196
La	48	47	32	39	49	48	41	41	28	39	28	22	38	25	41	27
Ce	118	120	118	0	0	183	168	85	114	121	127	93	155	105	117	126
Hf	28	21	37	17	27	20	38	27	41	18	26	23	32	28	26	34
Pb	19	29	28	22	21	11	22	17	25	20	0	22	26	19	16	11
Bi	22	21	21	23	23	24	19	18	19	22	17	20	24	18	22	20
Th	46	43	43	42	48	46	46	44	38	46	46	34	49	38	41	41

*Norm C= Normative Corundum, ASI= Alumina saturation index, C.I= Color index

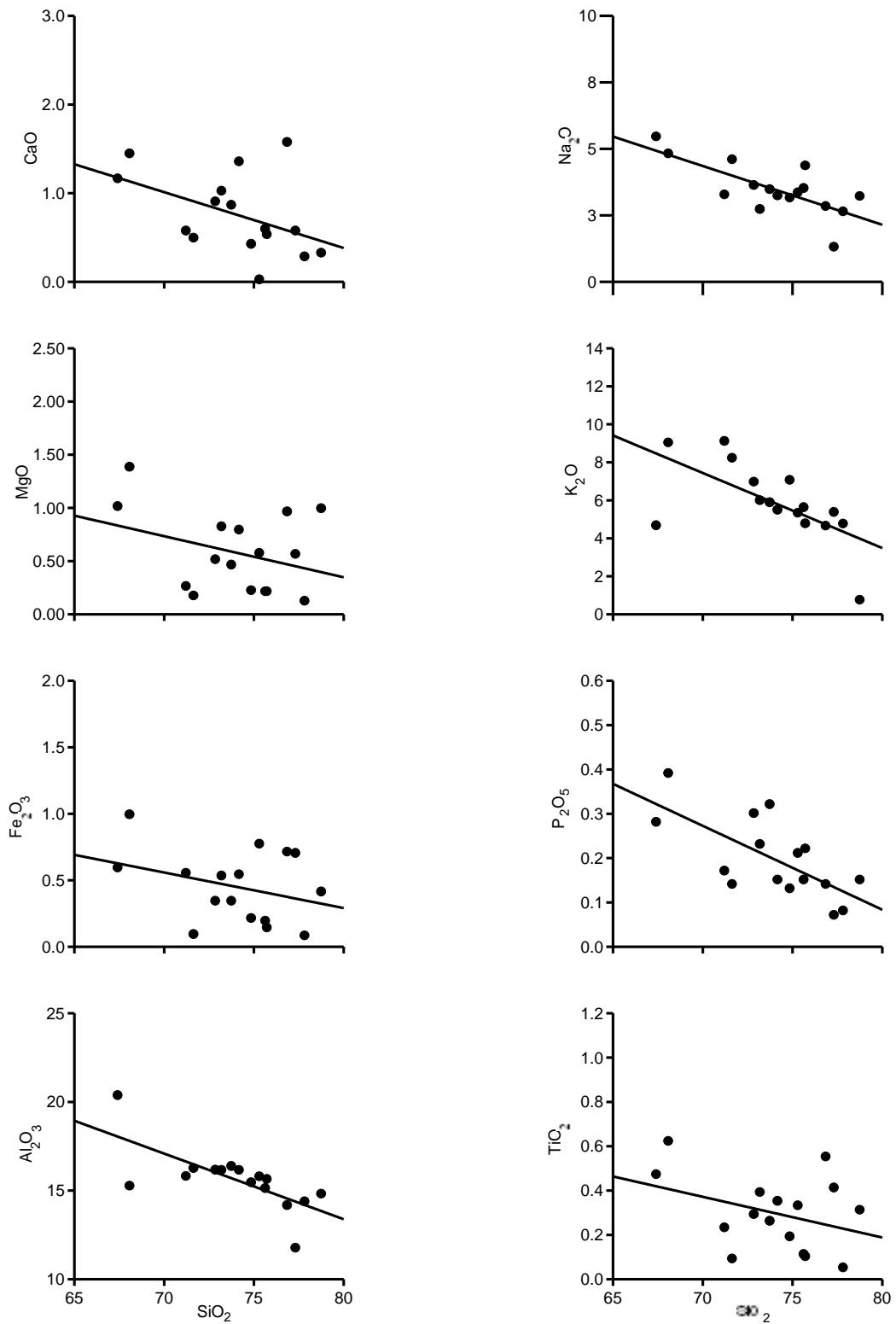


Fig. 4.1. Major elements versus SiO_2 variation diagrams of Utlá granites

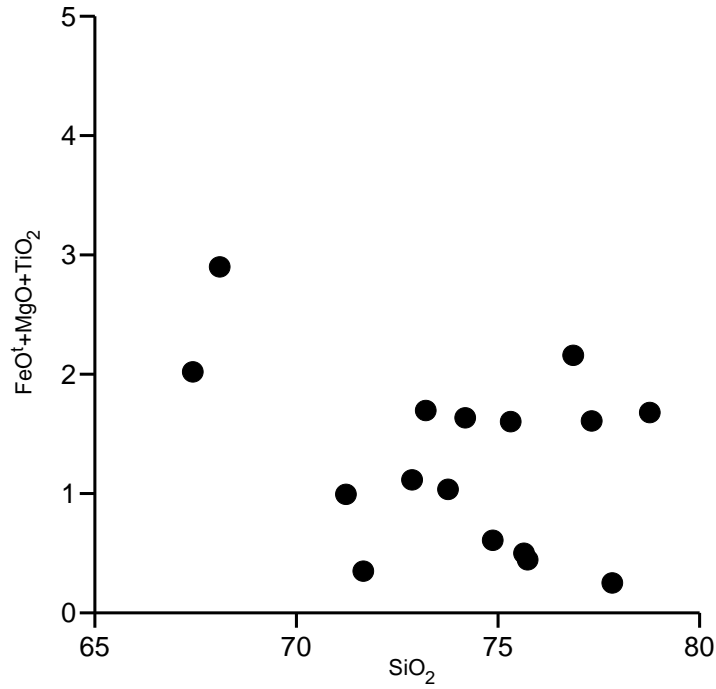


Fig. 4.2. SiO₂ versus FeO^t+MgO+TiO₂ diagram.

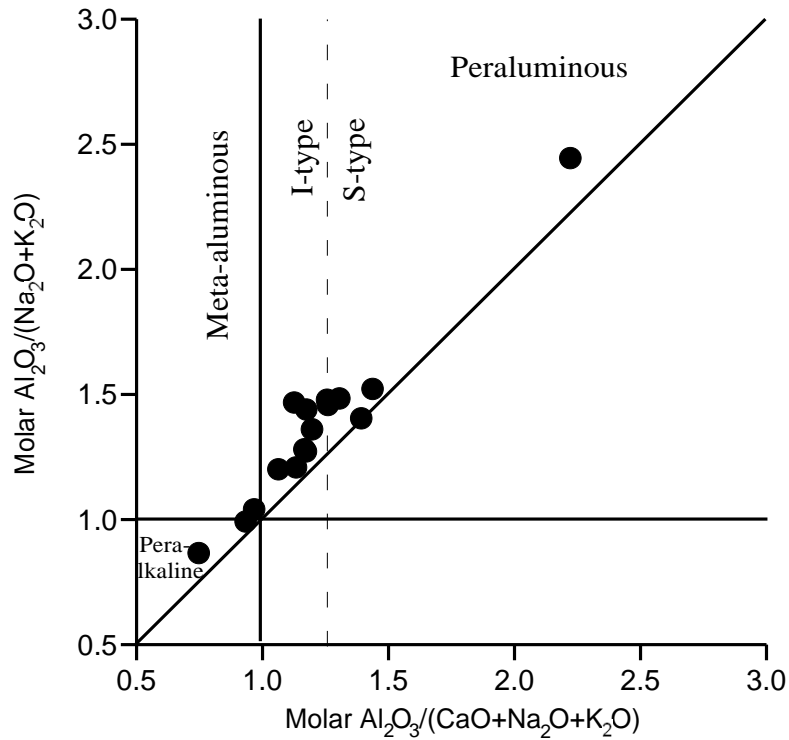


Fig. 4.3. Classification diagram: Al₂O₃/CaO + Na₂O + K₂O versus Al₂O₃/Na₂O+K₂O (from Maniar and Piccoli, 1989). (Molar ratio= concentration of oxide/molecular weight of oxide)

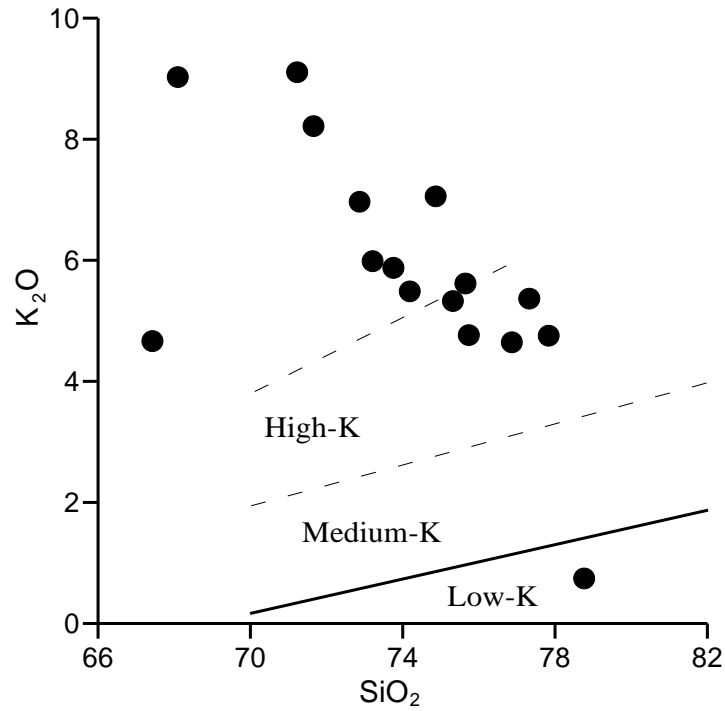
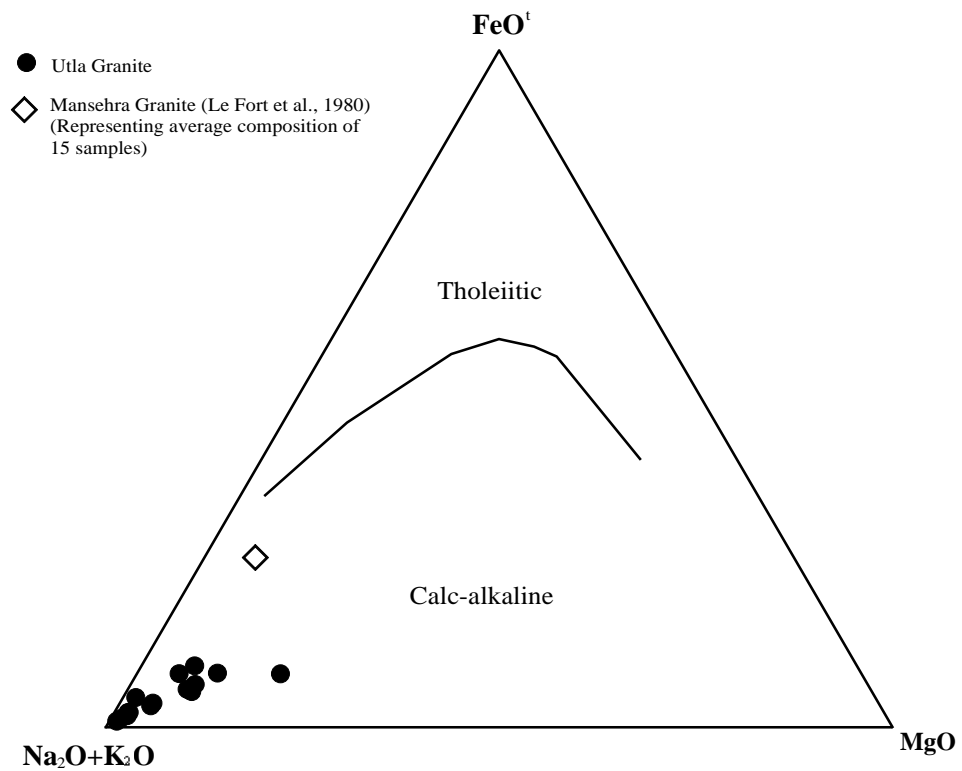
Fig. 4.4. SiO₂ versus K₂O diagram

Fig. 4.5. AFM plot (fields after Irvine and Baragar, 1971). The average composition of the Manshira granite is also shown for the purpose of comparison.

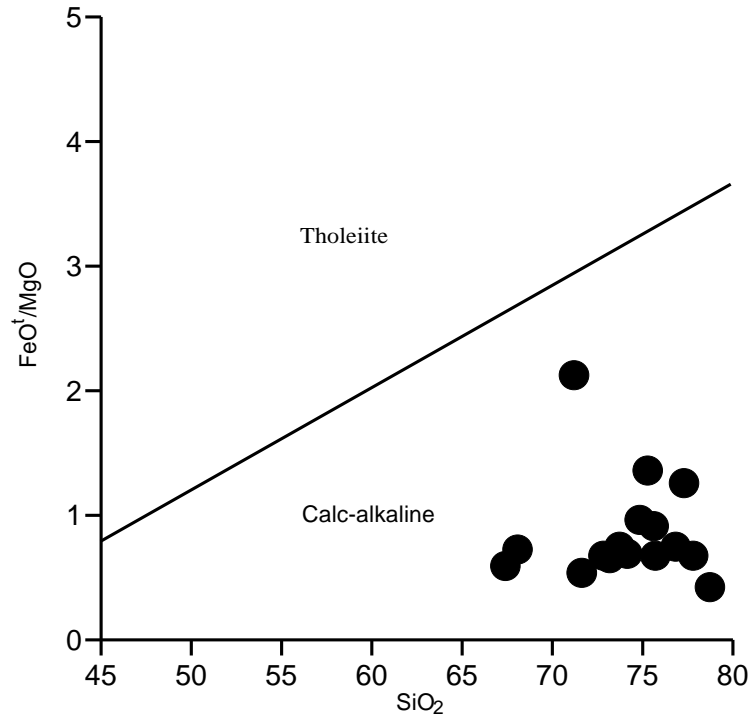


Fig. 4.6. FeO^I/MgO versus SiO_2 plot (fields after Miyashiro, 1973)

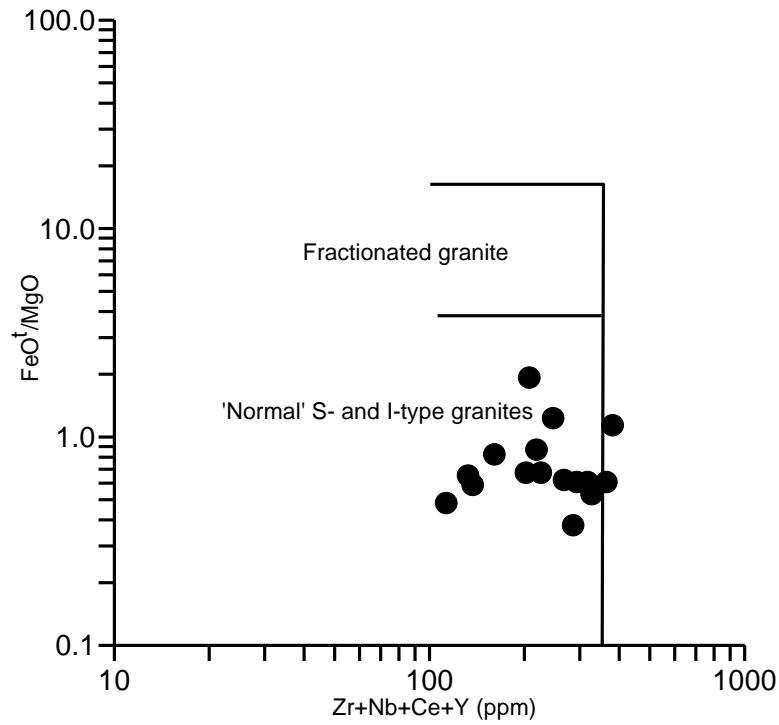


Fig. 4.7. FeO^I/MgO versus Zr+Nb+Ce+Y plot.

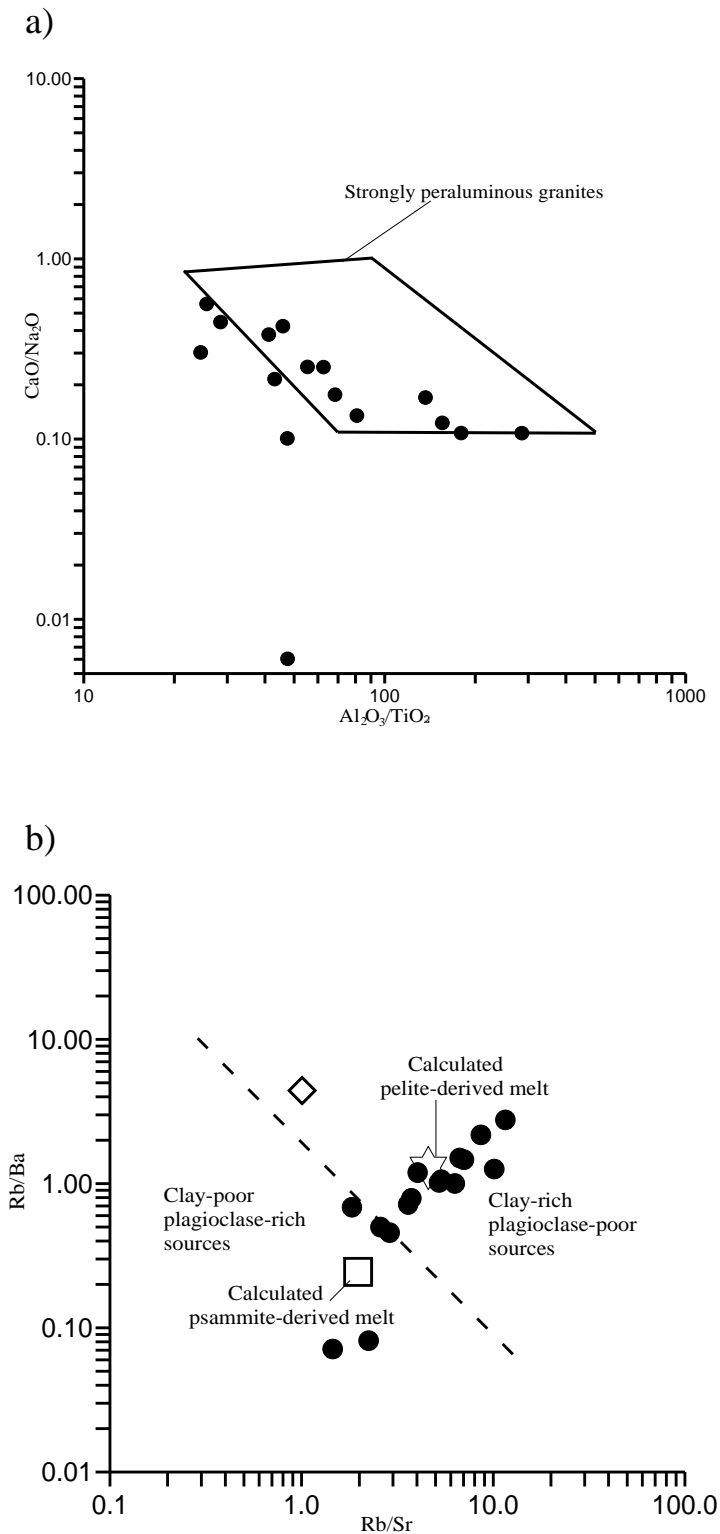


Fig. 4.8. (a) $\text{Al}_2\text{O}_3/\text{TiO}_2$ versus $\text{CaO}/\text{Na}_2\text{O}$ and (b) Rb/Ba versus Rb/Sr diagram (Sylvester, 1998). The average composition of the Mansehra granite is also shown for the purpose of comparison. The symbols are as in figure 4.5.

4.3.2. Minor and Trace Element Geochemistry

The variation diagrams of selected trace elements against silica are presented in figure 4.9. The concentrations of Zr (7-215 ppm), Y (10 ppm-40 ppm) and Th (34.4-49.1 ppm) all display slightly positive trends with increasing silica (Fig. 4.9). The positive relationship between Zr and Th indicates fractional crystallization of zircon (Fig. 4.9). Similar results were also presented by Koh and Yun (2003) for the Yuksipreong two-mica leuco-granites. The concentration of Rb ranges from 42 to 295 ppm and that of Sr from 20 to 134 ppm. Both the Rb and Ba show a poorly defined negative relation with silica (Fig. 4.9). The Uta granites show a strong positive correlation between the Rb/Sr as Rb/Ba ratios and provide useful information regarding their source rock (Fig 4.8). Rubidium, Sr and Ba may set significant limitations on the conditions that prevailed during melting (Miller, 1985; Harris and Inger, 1992). The concentrations of Ba, Pb and Nb in the studied samples range from 62 to 2844 ppm, 0 to 29 ppm and 4 to 15 ppm, respectively. A moderately positive correlation of each of Ce (85-183 ppm), La (22-49 ppm) and Th (34.4-49.1 ppm) with P_2O_5 (Fig. 4.10) points to a probable fractionation/ crystallization of monazite. Likewise, the sympathetic relationship observed between Y and P_2O_5 suggests fractionation of xenotime (YPO_4).

The ocean ridge granite (ORG)-normalized and chondrite-normalized spider-grams for Uta granites are shown in figure 4.11. Normalization values of Pearce et al., 1984 (for ORG) and Taylor and McLennan, 1985 (for chondrite) were used. Relative to both the ORG and chondrite, the Uta granites show enrichment in K, Ba, Rb and Th. The fractionation of zircon and xenotime is indicated by the evidently negative Zr and Y anomaly in ORG normalized pattern (Fig 4.11a). The chondrite-normalized pattern of the Uta granites exhibit negative Nb and Sr anomalies (Fig. 4.11b). The concentration of Ce is higher than those of Nb, Zr and Y (Fig 4.11a). Such a Ce enrichment is commonly noticed and hence seems to be a typical geochemical feature of the volcanic-arc and syn-collisional granites (Pearce et al., 1984).

4.3.3. Tectonic setting

The large ion lithophile elements (LILE) and high field strength elements (HFSE) are the two groups of incompatible elements that can be used as indicators of the magmatic processes and tectonic settings of granitic rocks. The former group includes elements having large ionic radius e.g. K, Rb, Sr, Ba and Cs, while the latter contains elements with higher valencies including Zr, Th, U, Ta, REE etc. A variety of discriminant diagrams based on LILE and HFSE is used for the determination of tectonic settings of granitic rocks (Pearce et. al., 1984). Niobium is one of the

HFS elements and its abundance can be used to differentiate between the tectonic setting of magmas responsible for the formation of volcanic-arc granites and within-plate granites (Pearce and Gale, 1979). The Nb abundance in volcanic-arc granites is markedly lower (<14 ppm) than that in within-plate granites (with Nb content exceeding 100 ppm) across the entire range of SiO₂. On this basis, all the studied granitoid samples from Utlá show volcanic arc magmatic setting (Fig. 4.12).

The Y versus SiO₂, Rb versus SiO₂ and Nb versus SiO₂ (Fig. 4.13), Rb versus Y+Nb, Nb versus Y (Fig. 4.14) discriminant diagrams are employed here to investigate a probable tectonic setting of the Utlá granites. On the basis of these diagrams, the studied samples show transitional character between volcanic arc and syn-collisional settings. None of the samples falls in the field of within-plate granites.

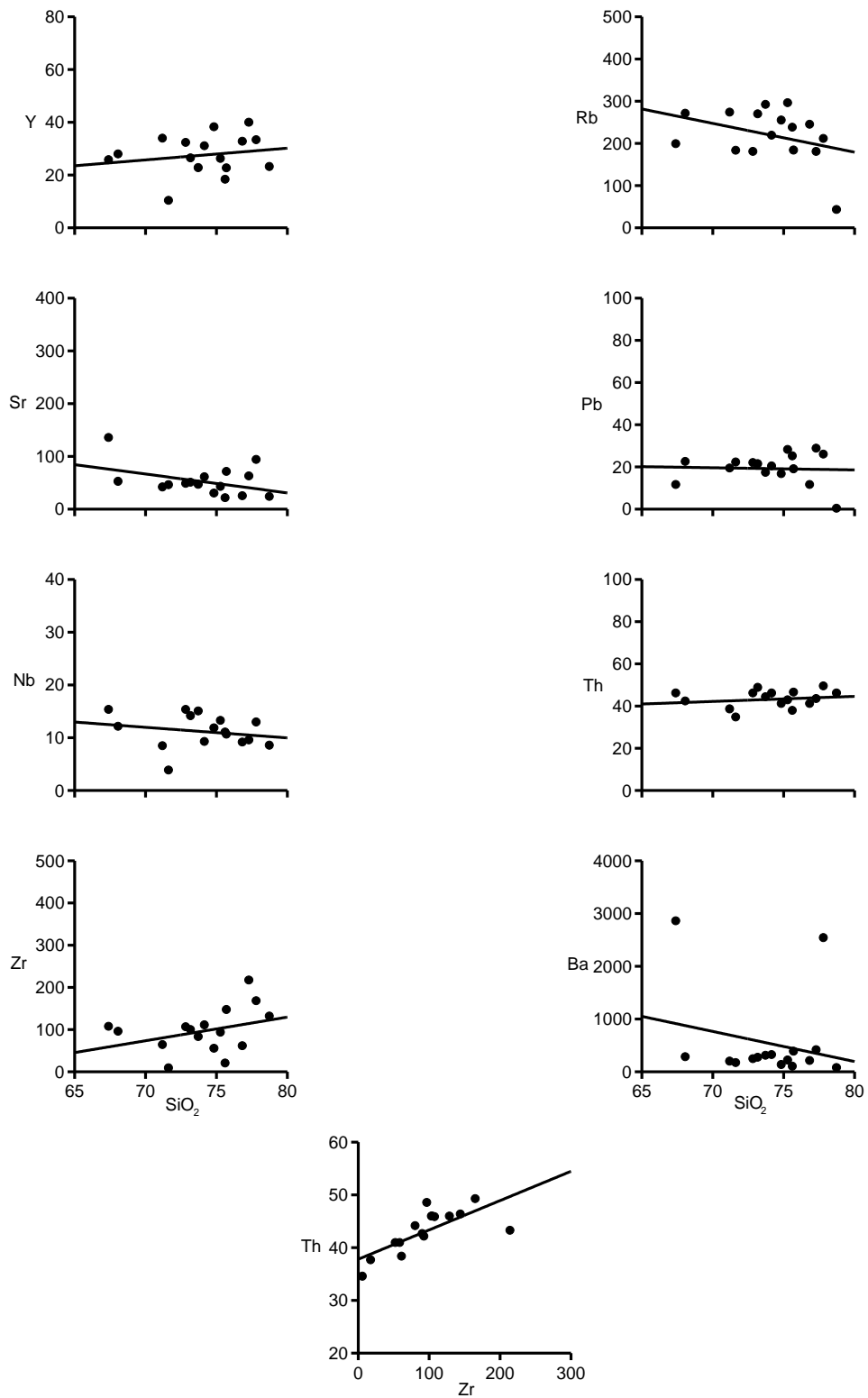


Fig. 4.9. Trace elements versus silica and Zr-Th variation diagrams of the Utlá granites

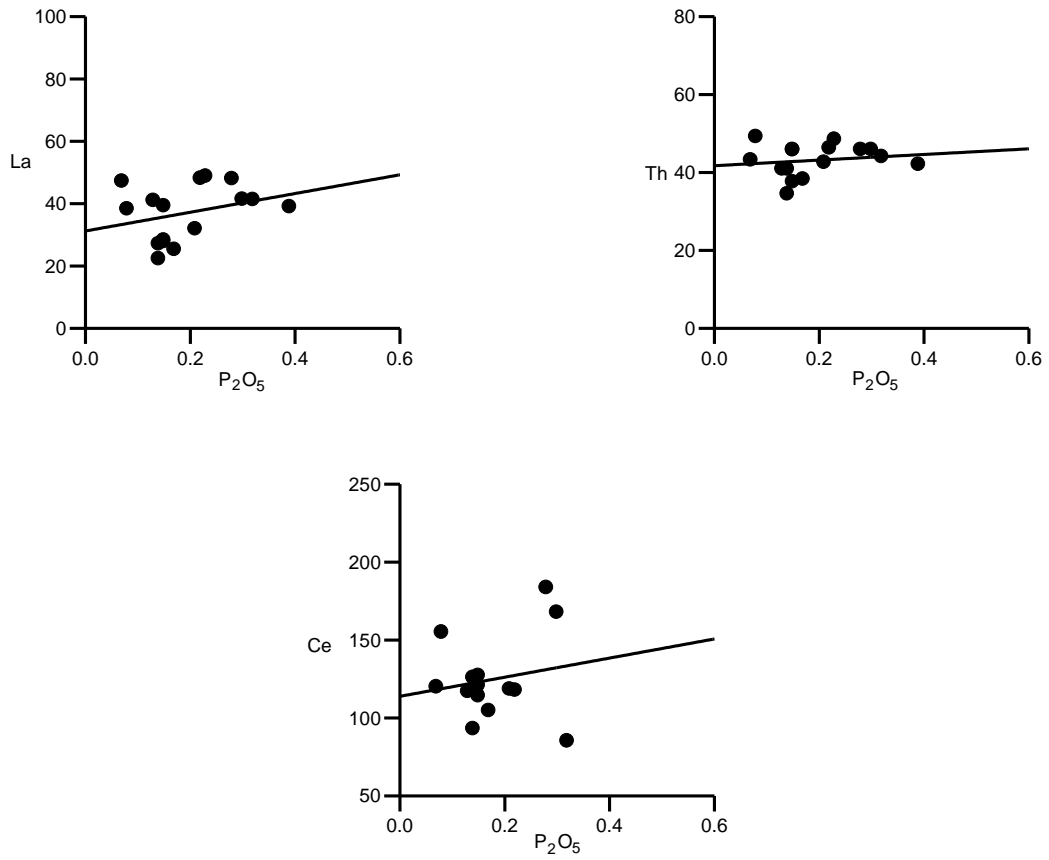


Fig. 4.10. Variation of La, Th and Ce with P₂O₅ in the Utlá granites.

a)

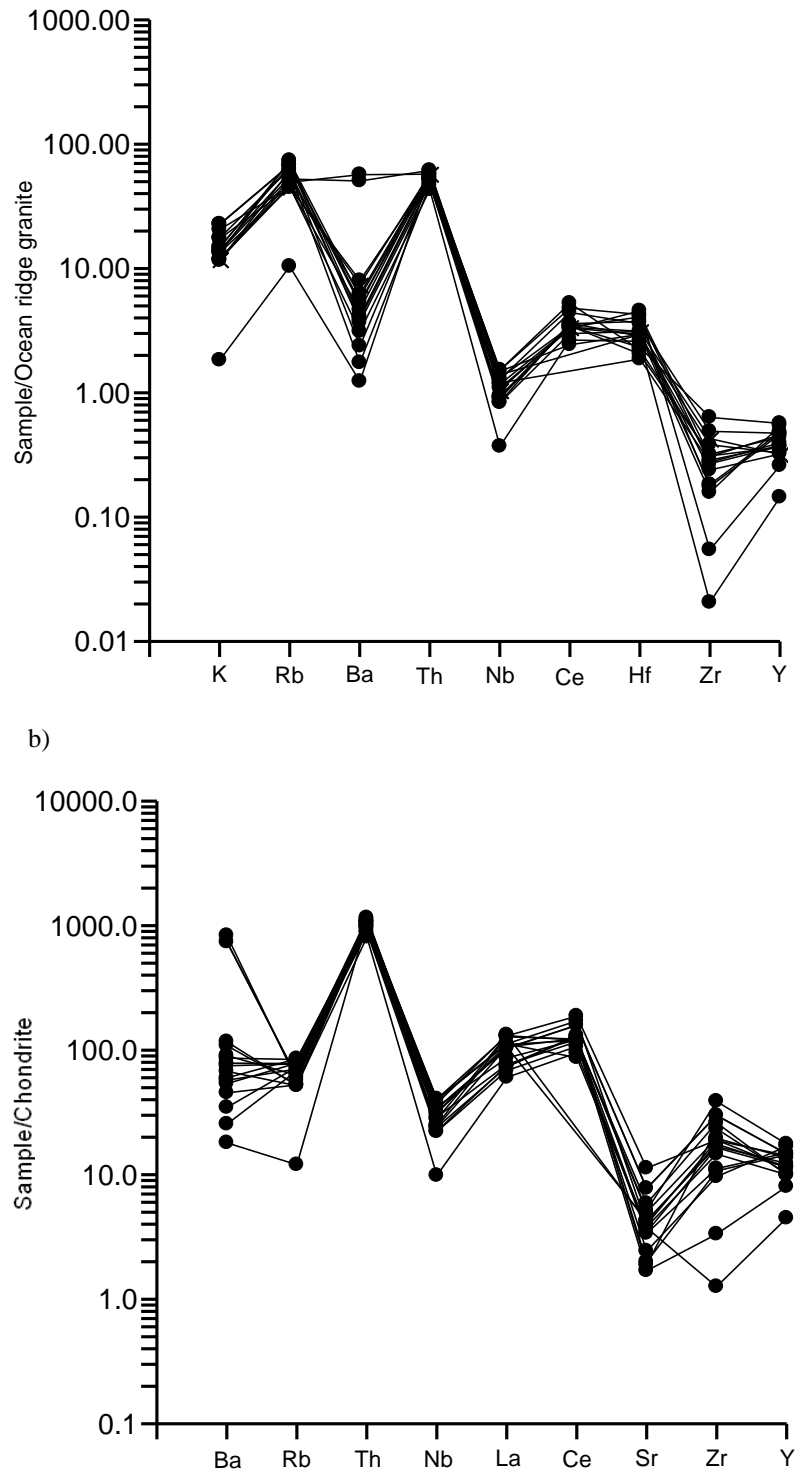


Fig. 4.11. Trace elements spidergrams for the Utlá granites: a) Ocean ridge granite (ORG)-normalized plot (normalization value after Pearce et al., 1984), b) Chondrite-normalized plot (normalization value after Taylor and McLennan, 1985)

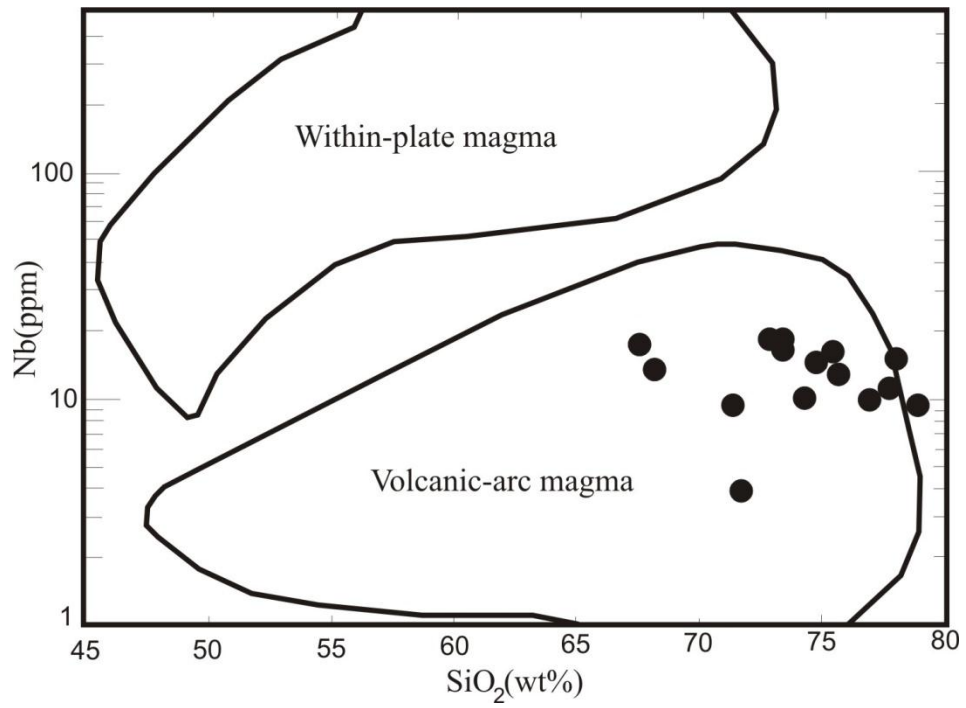


Fig. 4.12. Nb vs SiO₂ discriminant diagram (after Pearce and Gale, 1979)

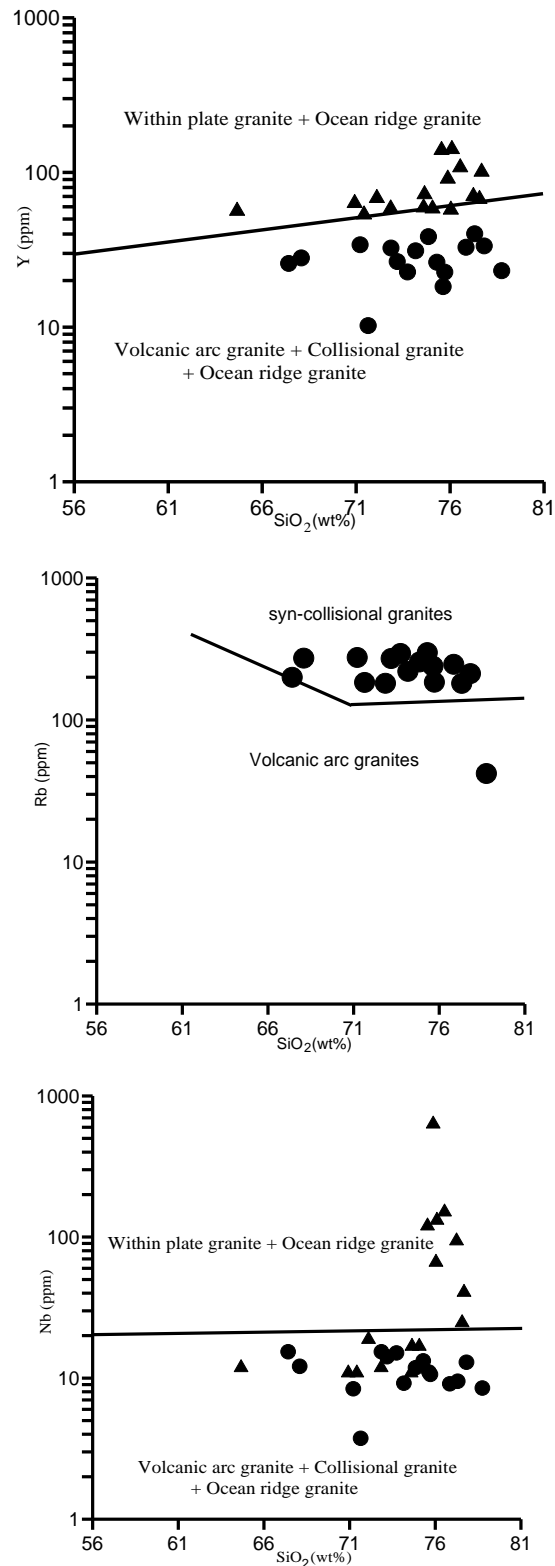


Fig. 4.13. Variation of Y, Rb and Nb with SiO₂ in the Utlá granites: The compositional fields are from Pearce et al. (1984). The corresponding data for the Ambela are also plotted for the purpose of comparison (Rafiq and Jan, 1989). ●=Utlá Granite, ▲=Ambela Granite (Rafiq and Jan, 1989)

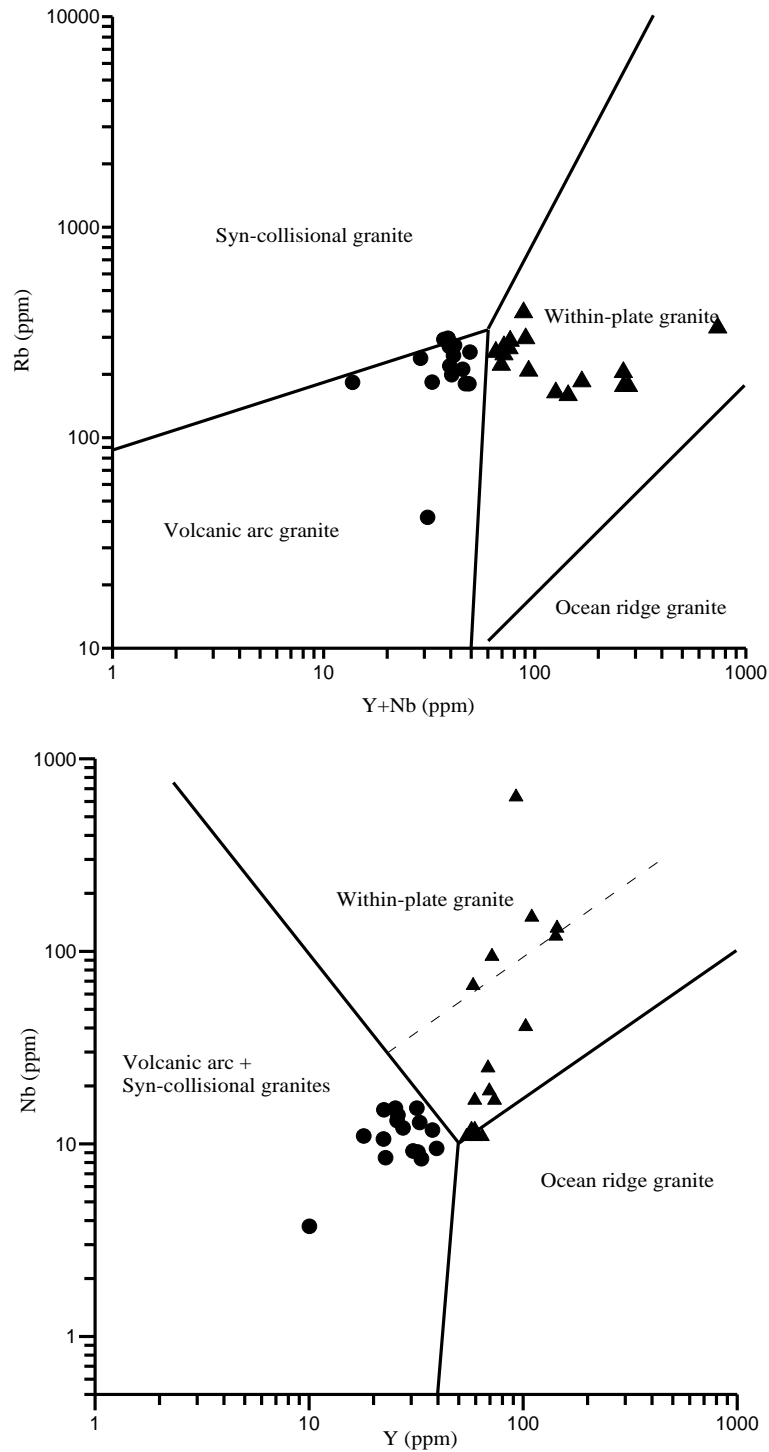


Fig. 4.14. The Rb-Y+Nb and Nb-Y relations in the Utla granites. The compositional fields are from Pearce et al. (1984). The corresponding data for the Ambela granites are also plotted for the purpose of comparison (Rafiq and Jan, 1989). The symbols are as in fig. 4.13.

4.4. Basic Dykes

4.4.1. Major Element Geochemistry

The major, minor and trace element compositions of representative samples from the Utla dykes are presented in table 4.2. The concentration of SiO_2 in these dykes ranges from 48.32 to 54.78 wt %. The other major element oxides are plotted against SiO_2 in order to depict the pattern of fractionation (Fig. 4.15). The Al_2O_3 (16.11-17.89 wt %) and Na_2O (2.12-3.25 wt %) contents show positive correlation with SiO_2 (Fig. 4.15). As expected, a well defined negative relationship with SiO_2 content is shown by MgO (4.41-12.2 wt %), Fe_2O_3 (2.82-6.15 wt %) and CaO (9.05-13.83 wt %). The K_2O , P_2O_5 and MnO contents (1.45 to 1.08 wt %, 0.23-0.77 wt % and 0.11-0.42 wt %, respectively) do not exhibit any significant relationship with SiO_2 concentration. The positive correlation between CaO and TiO_2 and their negative relation with SiO_2 most probably indicate fractionation of sphene. The positive relation between Na_2O and Al_2O_3 indicates the crystallization of sodic plagioclase. The fractionation of clinopyroxene and/ or calcic amphibole is also indicated by the positive relationship of CaO with Fe_2O_3 and MgO and negative correlation of SiO_2 with them. The insignificant correlation between CaO and P_2O_5 precludes the possibility for any apatite fractionation. These geochemical characteristics are also supported by the modal mineralogical compositions of these rocks (Section 3.3.2).

4.4.2. Minor and trace element geochemistry

The concentrations of selected trace elements are plotted against silica (Fig. 4.16). Yttrium ranges from 27 ppm to 40 ppm and shows a well defined positive relationship with SiO_2 . On the other hand, Nb (22-34 ppm), Zr (224-405 ppm) and Ba (40-138 ppm) display negative relationships with SiO_2 . The concentrations of both Rb (7-43 ppm) and Sr (255-641 ppm) do not exhibit any meaningful correlation with SiO_2 . The lack of any meaningful correlation of Ce and La with P_2O_5 (Fig. 4.17) coupled with a strongly negative relationship between Th and P_2O_5 (Fig. 4.17) provides a clue about the non-fractionation of monazite.

4.4.3. Tectonic Setting

These dykes are calc-alkaline in character as evidenced by their high CaO content and reasonably low values of $\text{FeO}^{\text{I}}/\text{MgO}$ ratio of the studied samples (Fig. 4.18). Plotting the trace element data on the studied samples on various discriminant diagrams i.e. Ti vs Zr (Fig. 4.19), Zr/Y vs Zr, $\text{Nb}^*2\text{-Zr}/4\text{-Y}$, $\text{Ti}/100\text{-Zr-Y}^*3$ and $\text{Hf}/3\text{-Th-Ta}$ (Figs. 4.20-4.23), however, reveals a within-plate tectonic setting for the Utla dykes.

Table 4.2. Whole-rock chemical analyses of representative dyke samples

Sample	U-1	U-2	U-8	U-11	U-14	U-20	U-21	U-25
SiO ₂	48.32	49.76	52.12	50.61	48.56	49.78	51.98	54.78
TiO ₂	4.8	2.68	3.88	5.51	4.56	5.52	3.95	3.76
Al ₂ O ₃	16.23	16.2	17.89	16.34	16.23	16.11	16.73	17.78
Fe ₂ O ₃	5.28	6.15	4.66	2.82	5.06	5.47	6.07	3.47
MnO	0.42	0.12	0.12	0.12	0.11	0.11	0.11	0.11
MgO	8.72	7.71	4.41	7.57	12.2	6.51	5.72	5.24
CaO	13.38	12.99	8.78	12.69	11.66	11.65	10.28	9.05
Na ₂ O	3.14	3.2	2.62	2.57	2.12	3.25	3.07	3.22
K ₂ O	0.84	0.88	0.9	0.45	0.47	1.08	0.96	0.56
P ₂ O ₅	0.59	0.23	0.57	0.77	0.41	0.77	0.48	0.48
L.O.I	0.03	0.03	0.02	0.01	0.05	0.02	0.03	0.04
Total	101.5	99.93	95.84	99.31	101.32	100.18	99.27	98.38
Minor and trace elements (ppm)								
Sc	10	11	15	10	9	8	9	8
V	186	179	227	199	136	167	158	145
Cr	141	139	136	67	526	46	26	15
Co	498	174	201	214	180	191	148	142
Ni	1476	1338	1458	1125	1116	655	448	303
Cu	1144	1013	1058	759	460	593	670	643
Zn	93	97	81	89	96	91	111	119
Ga	43	44	41	41	38	42	41	40
As	9	5	3	1	6	0	2	2
Br	3	5	4	4	4	5	5	6
Rb	16	26	7	10	14	18	43	29
Sr	505	531	568	641	411	548	255	282
Y	32	31	27	28	27	33	38	40
Zr	278	274	250	287	296	405	227	224
Nb	33	32	22	27	34	32	22	24
Mo	4	3	3	4	4	6	3	3
Ag	20	25	32	32	29	36	32	36
Cd	9	12	14	16	15	16	10	16
Sn	20	21	19	18	19	23	18	17
Sb	7	7	17	6	5	5	5	5
Ba	138	119	77	87	55	102	48	40
La	16	15	13	14	13	14	10	9
Ce	73	58	65	57	54	67	42	39
Nd	16	18	14	19	30	14	9	7
Hf	38	46	43	41	38	38	45	40
Ta	35	46	32	47	-41	31	42	124
Bi	24	23	25	24	26	21	25	24
Th	34	33	33	32	35	33	35	36

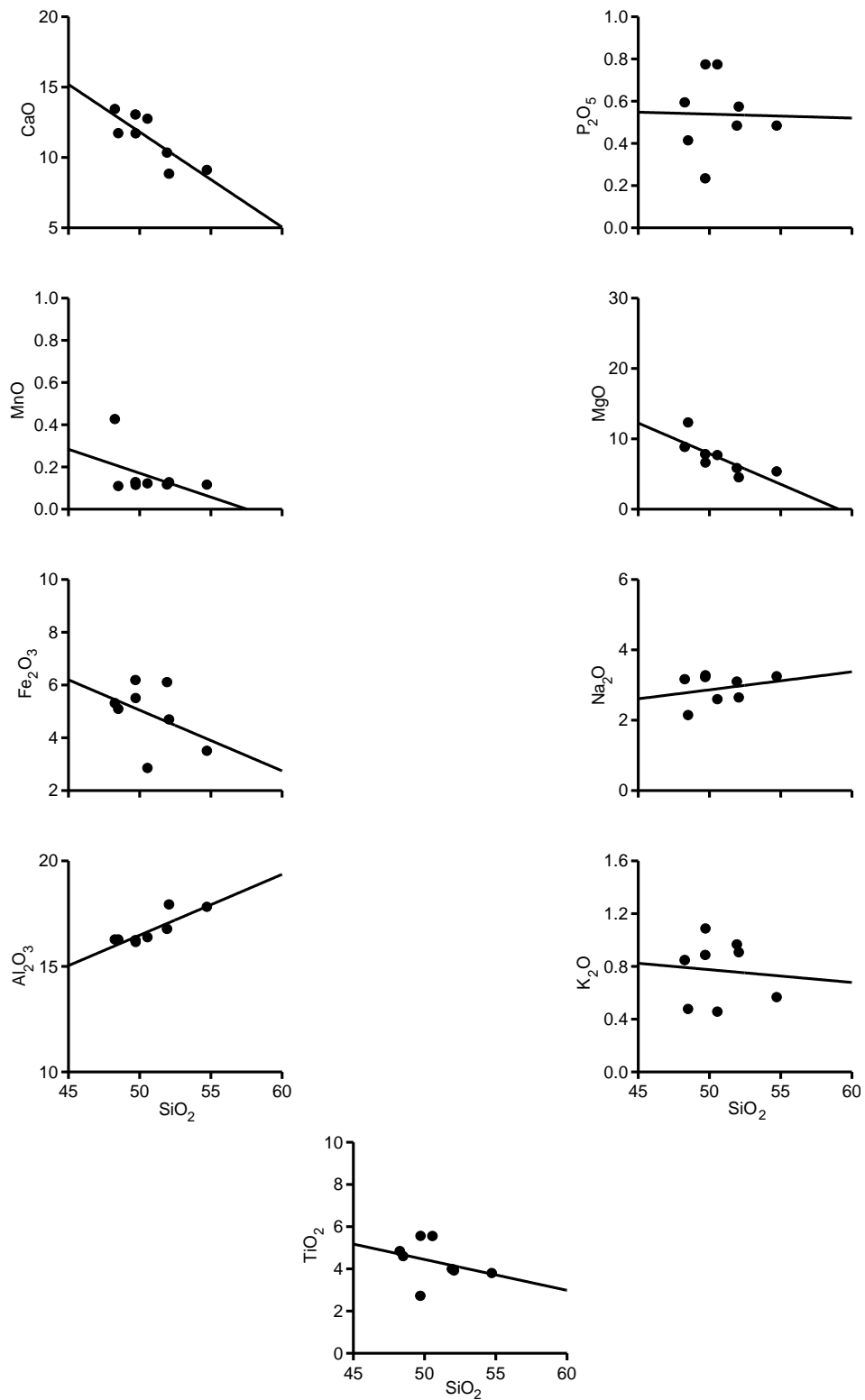


Fig. 4.15. Major element oxides versus SiO_2 variation diagrams of the Utla dykes.

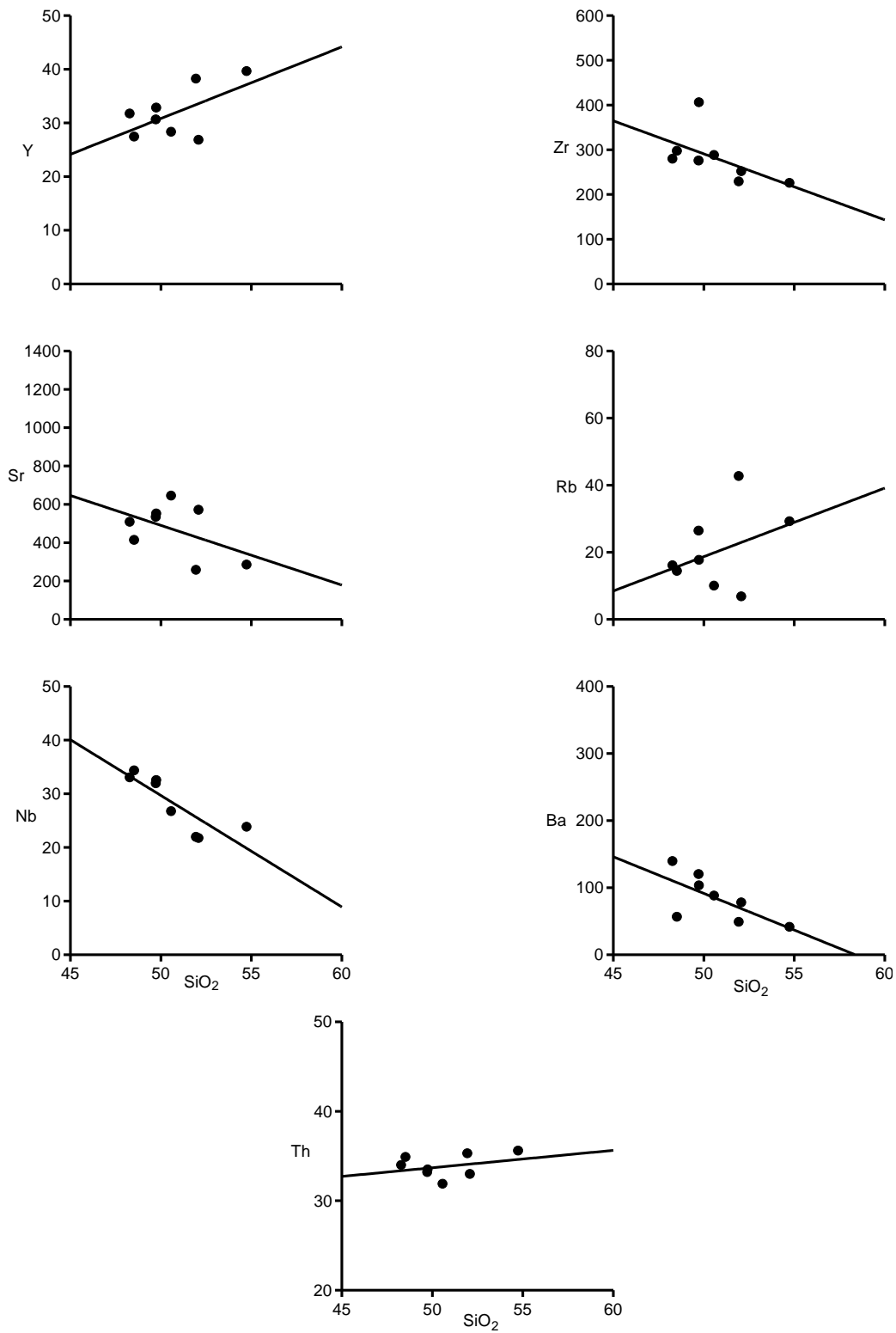


Fig. 4.16. Trace elements versus silica variation diagrams of the Utla dykes.

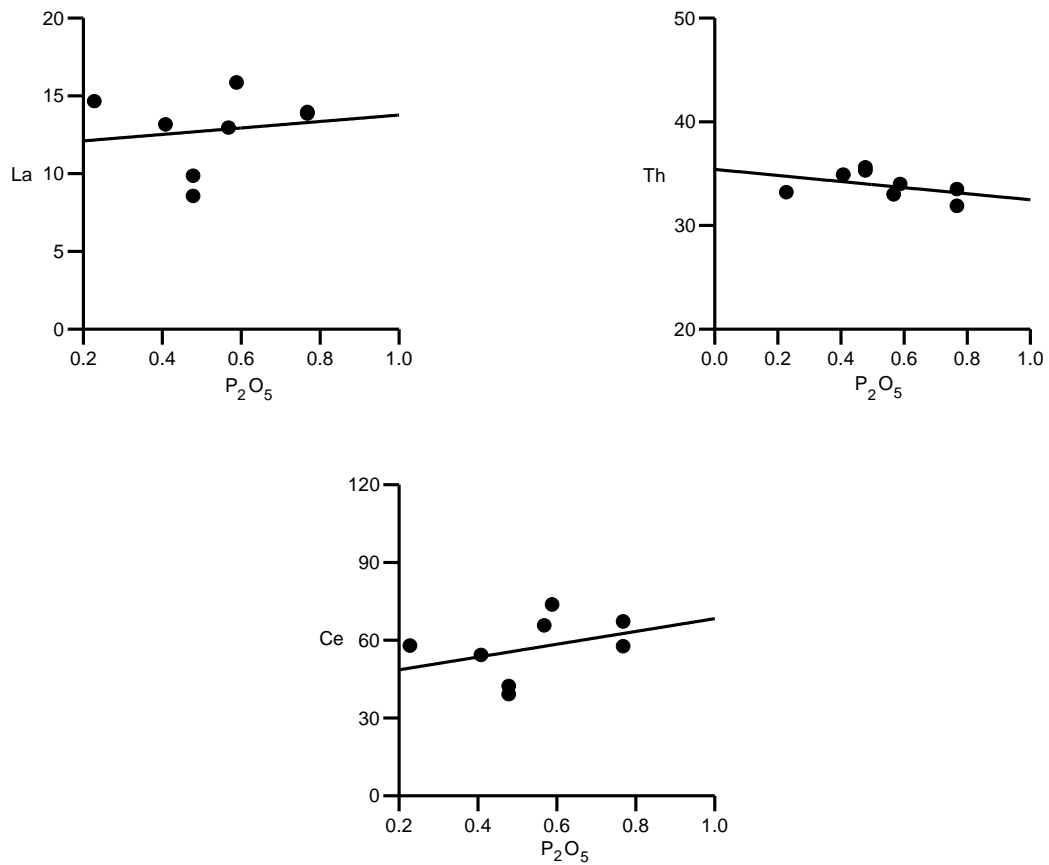


Fig. 4.17. Selected trace elements versus P_2O_5 variation diagrams of the Utlá dykes.

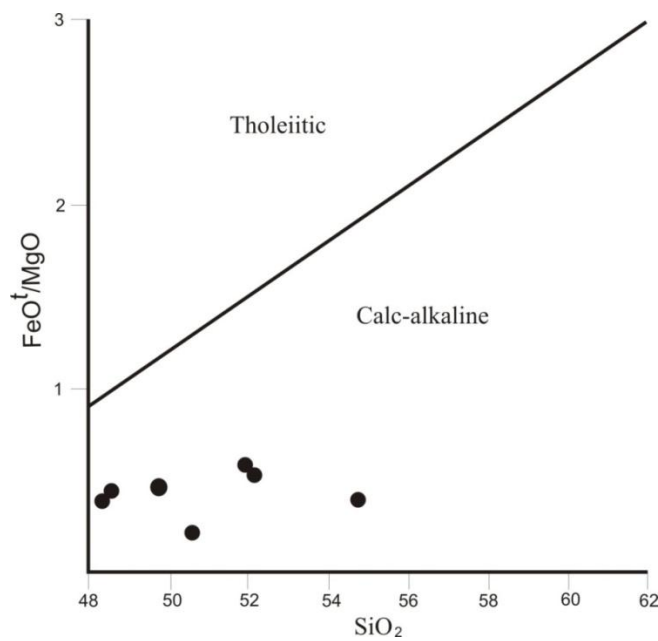


Fig. 4.18. FeO^t/MgO versus SiO_2 plot of the Utlá dykes (after Miyashiro, 1973).

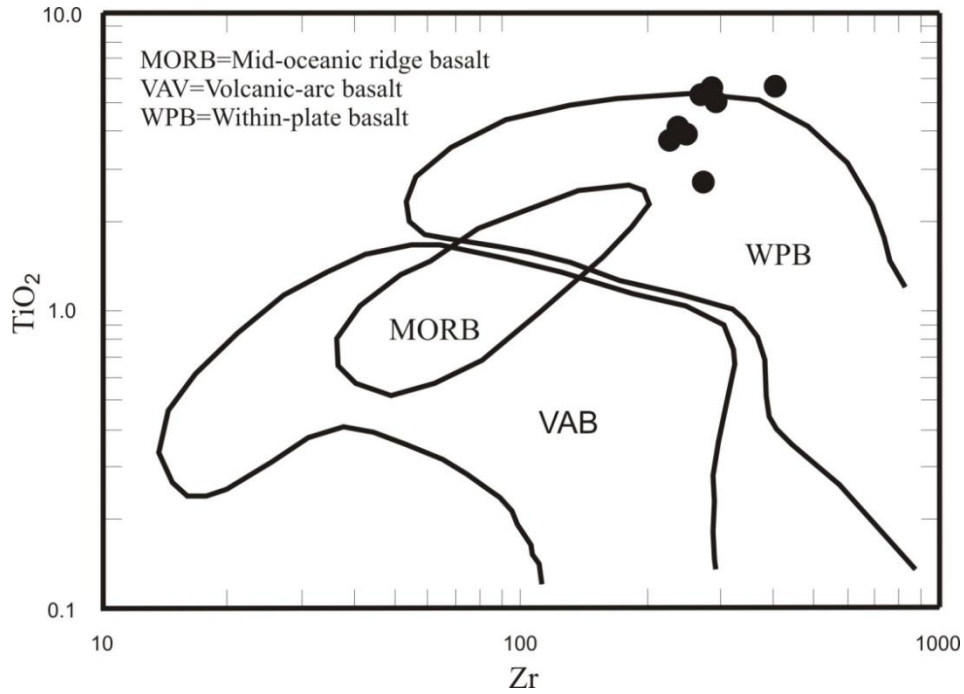


Fig. 4.19. TiO₂-Zr discriminant diagram for the Utla dykes (after Pearce et al., 1981).

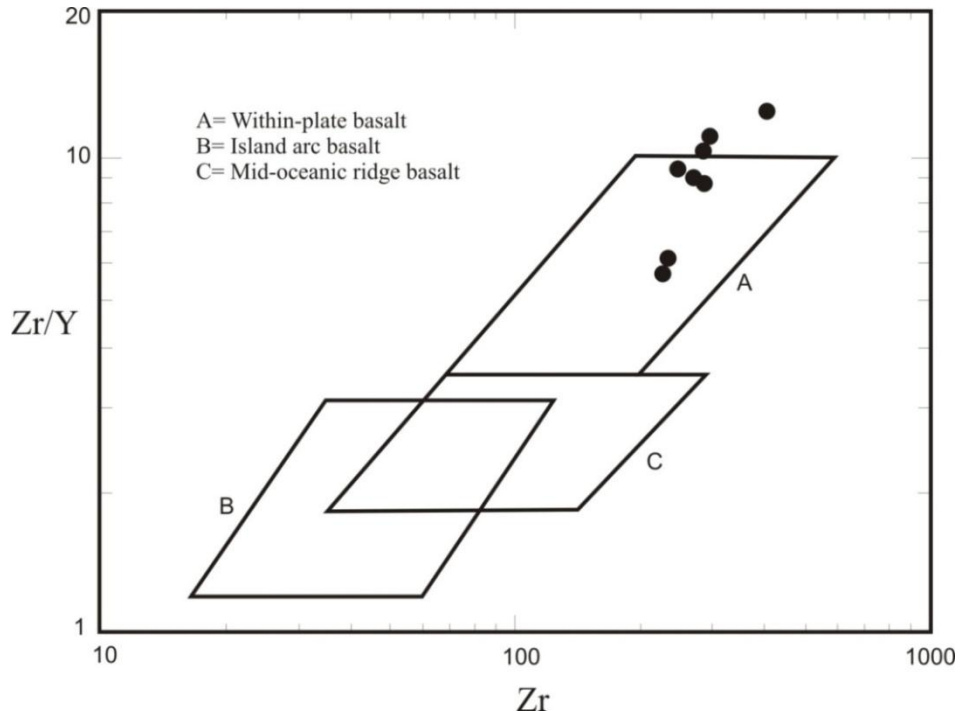


Fig. 4.20. Zr/Y-Zr discriminant diagram of the Utla dykes (after Pearce and Norry, 1979).

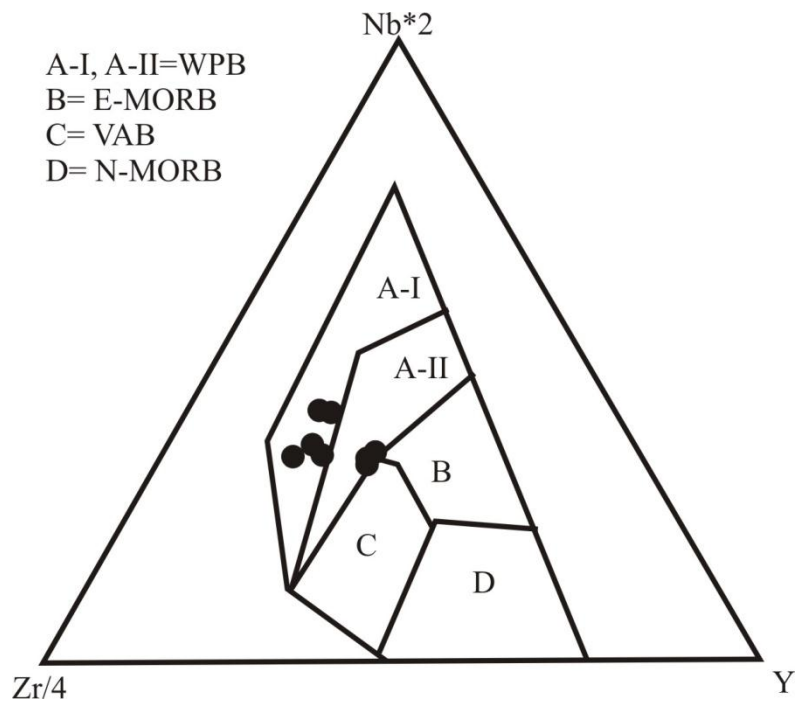


Fig. 4.21. Nb*2-Zr/4-Y discriminant diagram of the Uta dykes (after Meschede, 1986). WPB=Within-plate basalts, E-MORB=Enriched mid-oceanic ridge basalts, VAB= Volcanic arc basalts, N-MORB= normal mid-ocean ridge basalts.

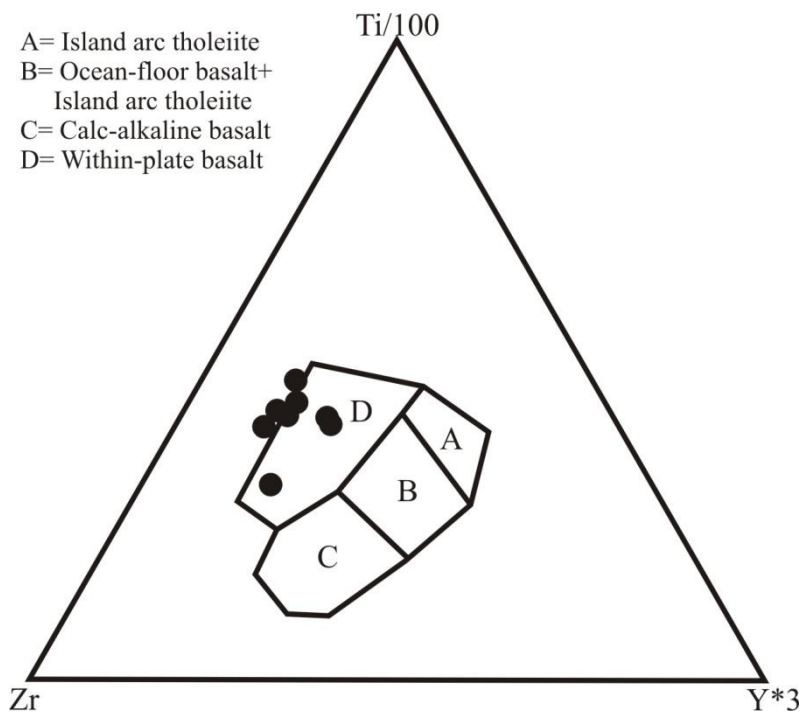


Fig. 4.22. Ti/100-Zr-Y*3 discriminant diagram (after Pearce and Cann, 1973).

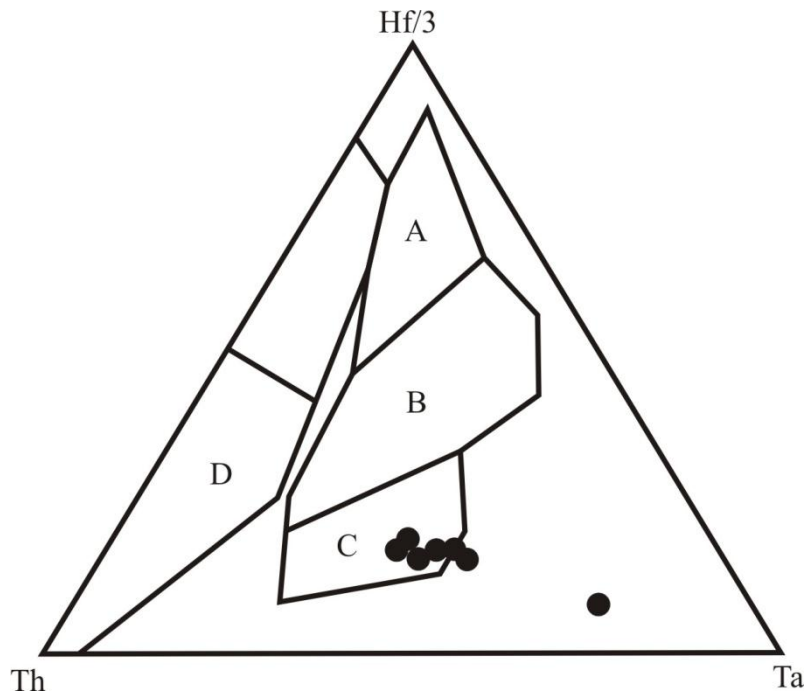


Fig. 4.23. Hf/3-Th-Ta discriminant diagram of the Utla dykes (after Wood, 1980). A= Normal mid-oceanic ridge basalts (N-MORB), B= Enriched mid-oceanic ridge basalts (E-MORB), C= Alkaline within-plate basalts (WPB), D= Destructive plate margin basalts.

MECHANICAL PROPERTIES

5.1. General Statement

Designing, construction, operation and maintenance of engineering works are largely affected by various geological factors. These factors include physical and mechanical properties of rocks. Some of the rocks are chiefly used in a number of engineering projects because of their stability in a variety of conditions e.g. exposures to moistures/temperature, mechanical load etc. Granites are one of the common rock types used in various engineering operations throughout the world. These rocks show a variety of engineering properties that may affect their use as construction material. Several authors have worked on determining the engineering properties of granites (Dwivedi et al., 2008; Sousa et al., 2005; Akesson et al., 2003; Tugrul and Zarif, 1999).

The properties of rocks are influenced by their mineralogical composition, texture and resistance to weathering. Texture is defined in the petrologic sense as the size, shape and mutual spatial arrangement of mineral grains (Mc Phie et al., 1993; Bucher and Frey, 1994) and is a product of rock's origin and tectonic history (Akesson et al., 2003). Lindqvist et al. (2007) have shown that the intrinsic properties of rocks, including mineralogy and texture, can be used to assess their engineering properties. Several authors have worked to establish relationship between the petrographic characteristics and engineering properties of rocks (Shakoor and Bonelli, 1991; Howarth and Rowlands, 1987; Akesson et al., 2003; Sajid et al., 2009).

Granitic rocks are exposed at various localities in the north-western Pakistan. Din et al. (1993) and Din and Rafiq (1997) worked on the strength properties of some of the rocks from different areas including granites from Malakand and Ambela, NW, Pakistan. Similarly, Arif et al. (1999) worked on the mechanical properties of Mansehra granite and concluded that the investigated rocks have very low values of compressive strength as compared to granitic rocks from elsewhere in northern Pakistan probably because of their older age, coarser grain size and weathered character.

As pointed out earlier, a vast body of extensively exposed and readily accessible granitoids occurs around the Utla area of Gadoon, northwestern Pakistan. The mechanical properties of the Utla granitoids are currently lacking and hence need to be investigated. The aim of this chapter is to present an account of the various physical and mechanical

properties of the Utlā granitoids and to correlate them with their petrographic characteristics.

5.2. Methodology

Three representative bulk samples from different textural varieties of Utlā granite were collected. These bulk samples were cored with the help of core drilling machine in the rocks cutting laboratory of Department of Geology, University of Peshawar. Seven core samples were drilled from each bulk sample. One thin section from each core sample was prepared for detailed petrographic observation. The cylindrical samples were cut according to the ASTM specifications for the determination of mechanical properties including unconfined compressive strength (UCS) and unconfined tensile strength (UTS). These strength tests were carried out in the Material Testing Laboratory, Department of Civil Engineering, KPK University of Engineering and Technology, Peshawar. Some of the physical properties including water absorption, specific gravity and porosity were also determined for each sample in the geochemistry laboratory of the National Center of Excellence in Geology, University of Peshawar. The details of these determinations and their correlation with petrographic observations through statistical analysis are presented here.

5.3. Petrographic descriptions

The studied rocks were classified into three textural varieties (Fig. 5.1). The location of the studied samples and their petrographic details are as follows:

- i. **Mega-crystic granite (CG)** (N34⁰ 20' 28.7", E72⁰ 45' 41.5"): Large subhedral to euhedral phenocrysts of plagioclase and alkali feldspar occur in medium grained groundmass that consists of quartz, alkali feldspar, biotite, muscovite and tourmaline with trace amounts of apatite, andalusite and monazite. Most of the phenocrysts are partially to completely sericitized. The groundmass constituents are fresh and exhibit features of recrystallization. The modal mineralogy of these rocks is presented in the table 5.1.



Fig. 5.1. Core samples of the different textural varieties of the Utla granite

- ii. **Foliated mega-crystic granite (CGF)** (N34⁰ 20' 3.2", E72⁰ 45' 31"): Gneissose fabric is evident in these rocks in hand specimen. These rocks contain greater abundance of biotite and muscovite than the other textural varieties. Partially sericitized, subhedral phenocrysts of alkali feldspar and plagioclase are present. Fine to medium grained quartz also occur in the groundmass. The modal mineralogy of these rocks is presented in the table 5.2.
- iii. **Fine grained homogenous granite (FG)** (N34⁰ 18' 48.4", E72⁰ 46' 25.9"): These rocks consist of equidimensional, subhedral, fine grained alkali feldspar, quartz and plagioclase. Both the alkali feldspar and plagioclase show variable degrees of alteration to muscovite, sericite and clay minerals. The modal abundance of biotite is lower than the foliated and megacrystic types. The modal mineralogy of these rocks is presented in the table 5.3.

5.4. Physical and Mechanical Properties

The various physical and mechanical properties that were determined in the course of the present study include:

- i. Strength
- ii. Water absorption
- iii. Specific gravity
- iv. Porosity

Table 5.1. Modal composition of mega-crystic granite

S. No.	Qtz	Alkf	Plg	Bt	Mus	Tour	Apt	And	Mzt	OM
CG-1	24	41	16	6	8	4.4	--	0.2	--	0.4
CG-2	23	40	19	6	6.25	5.35	0.1	--	--	0.3
CG-3	27	43	13	6	5.7	5	--	0.1	0.2	--
CG-4	25	42	15.5	5.4	6.3	5.1	0.1	--	0.1	0.5
CG-5	26.5	39	15.8	6	8	4.5	--	--	--	0.2
CG-6	27	42	14	4	7	5.7	--	0.2	--	0.1
CG-7	25.75	40	11.5	6.5	10.75	4.7	0.4	--	--	0.4

Table 5.2. Modal composition of foliated mega-crystic granite

S. No.	Qtz	Alkf	Plg	Bt	Mus	Sph	Tour	Apt	Mzt	OM
CGF-1	27.5	20	20	15	16	0.8	--	0.2	--	0.5
CGF-2	29	20	20	17	13	--	0.5	0.1	0.1	0.3
CGF-3	30	20	20	13	16	0.6	--	--	0.1	0.3
CGF-4	28	24	19	15	13	0.5	0.3	--	--	0.2
CGF-5	28	24	18	15	14	0.6	--	--	--	0.4
CGF-6	30	20	20	16	13	0.2	--	0.2	--	0.6
CGF-7	31	19	18	16	15	0.2	--	--	--	0.8

Table 5.3. Modal composition of fine grained homogeneous granite

S. No.	Qtz	Alkf	Plg	Bt	Mus	Tour	Apt	And	Mzt	OM
FG-1	32.5	36.34	13.4	5.45	9.01	2.7	--	0.2	--	0.4
FG-2	26.5	38.68	17.5	5.23	8.99	2.6	0.5	--	--	--
FG-3	25.7	41.2	14.5	4.8	10.6	2.3	--	0.6	--	0.3
FG-4	28	40.3	13.2	5.3	9.5	2.9	--	--	0.2	0.6
FG-5	31	43.2	10.6	4.2	7.6	2.6	--	0.8	--	--
FG-6	26.6	40.2	15	5.5	10.15	2.15	0.1	0.3	--	--
FG-7	27.25	36.6	16.5	5.75	9.7	2.5	--	0.9	--	0.8

Note: **Qtz**= Quartz, **Alkf**=Alkalifeldspar including orthoclase and microcline, **Plg**= Plagioclase, **Bt**= Biotite, **Mus**= Muscovite, **Tour**= Tourmaline, **Sph**= Sphene, **Apt**= Apatite, **And**= Andalusite, **Mzt**= Monazite, **OM**= Opaque Minerals

5.4.1. Strength Tests

The strength tests include Unconfined Compressive Strength (UCS) and Unconfined Tensile Strength (UTS). The UCS test was performed on cylindrical core samples using a universal testing machine (UTM) according to the ASTM (1971) specifications. Brazilian test or Splitting tensile test was performed for the determination of UTS (ASTM, 1986). The direct determination of tensile strength has proved difficult because it is not easy to grip the specimen without introducing bending stress (Bell, 2007). Details regarding the preparation of samples and determination of strength values are as outlined previously (Sajid et al., 2009). Tables 5.4 and 5.5 enlist the details and results of the UCS and UTS testing of the studied core samples.

Table 5.4. Details and results of the UCS testing of the studied samples

S. No.	Length(m)	Diameter(m)	Area (m ²)	Load(Ton)	Load (N)	UCS (Pa)	UCS (MPa)
CG -1	0.087	0.044	0.0015	6.25	61291.56	40256537.27	40.257
CG -2	0.089	0.044	0.0015	4.54	44522.19	29242348.67	29.242
CG -3	0.087	0.044	0.0015	7.5	73549.88	48307844.72	48.308
CG -4	0.081	0.044	0.0015	6.33	62076.09	40771820.94	40.772
CG -5	0.086	0.044	0.0015	7.38	72373.08	47534919.2	47.535
CG -6	0.086	0.044	0.0015	8.13	79728.06	52365703.67	52.366
CG -7	0.087	0.044	0.0015	9.83	96399.37	63315481.81	63.315
CGF-1	0.102	0.044	0.0015	4.44	43541.53	28598244.07	28.598
CGF-2	0.097	0.044	0.0015	5.63	55211.44	36263088.77	36.263
CGF-3	0.094	0.044	0.0015	5.75	56388.24	37036014.28	37.036
CGF-4	0.093	0.044	0.0015	2.68	26281.82	17262003.18	17.262
CGF-5	0.092	0.044	0.0015	3.58	35107.81	23058944.55	23.059
CGF-6	0.093	0.044	0.0015	6.22	60997.36	40063305.89	40.063
CGF-7	0.094	0.044	0.0015	6.6	64723.89	42510903.35	42.511
FG -1	0.092	0.044	0.0015	7.15	70117.55	46053478.63	46.053
FG -2	0.091	0.044	0.0015	6.36	62370.29	40965052.32	40.965
FG -3	0.095	0.044	0.0015	5.94	58251.5	38259813.02	38.260
FG -4	0.092	0.044	0.0015	6.74	66096.82	43412649.79	43.413
FG -5	0.096	0.044	0.0015	6.93	67960.08	44636448.52	44.636
FG -6	0.089	0.044	0.0015	6.42	62958.69	41351515.08	41.352
FG -7	0.080	0.044	0.0015	6.59	64625.82	42446492.89	42.446

Table 5.5. Details and results of the UTS testing of the studied samples

S. No.	Length(m)	Diameter(m)	Load (Ton)	Load (N)	UTS (Pa)	UTS(MPa)
CG - 1	0.024	0.044	0.866	8492.559	5222209.464	5.222
CG - 2	0.024	0.044	0.786	7708.027	4697843.237	4.698
CG - 3	0.019	0.044	0.758	7433.441	5518918.312	5.519
CG - 4	0.022	0.044	0.828	8119.906	5226379.928	5.226
CG - 5	0.018	0.044	0.676	6629.295	5332498.248	5.332
CG - 6	0.021	0.044	0.924	9061.345	6288513.093	6.289
CG - 7	0.021	0.044	0.952	9335.931	6387128.862	6.387
CGF-1	0.024	0.044	0.450	4412.993	2638459.051	2.638
CGF-2	0.025	0.044	0.747	7325.568	4239630.995	4.237
CGF-3	0.025	0.044	0.842	8257.199	4763558.142	4.764
CGF-4	0.022	0.044	0.178	1745.584	1162341.902	1.162
CGF-5	0.022	0.044	0.410	4020.727	2575334.418	2.575
CGF-6	0.022	0.044	0.732	7178.468	4786579.119	4.787
CGF-7	0.023	0.044	0.854	8374.879	5250298.422	5.250
FG -1	0.024	0.044	0.502	4922.938	2958021.592	2.958
FG -2	0.022	0.044	0.326	3196.968	2084633.781	2.085
FG -3	0.018	0.044	0.266	2608.569	2083228.456	2.083
FG -4	0.018	0.044	0.336	3295.034	2634355.754	2.631
FG -5	0.018	0.044	0.354	3471.554	2712505.055	2.713
FG -6	0.021	0.044	0.372	3648.074	2534171.063	2.534
FG -7	0.023	0.044	0.428	4197.246	2586451.817	2.586

5.4.2. Water Absorption

Water absorption is a useful property in evaluating the durability of rocks utilized as building material (Shakoor and Bonelli, 1991). It refers to the quantity of water that can be readily absorbed by a rock. It was determined for the studied granitic rocks using saturation and calliper method. The results of water absorption test are presented in table 5.6. The plutonic rocks having absorption value less than 1% by weight can be used as dimension stone because of their high resistance to weathering (Blyth and de Freitas, 1974). In contrast to the fine grained variety, the measured water absorption capacities of both the massive and foliated varieties of the coarse grained Utlá granite are within the range of values permissible for use as dimension stone and engineering material.

5.4.3. Specific Gravity

Specific gravity for the studied rock samples was also determined and the results are presented in table 5.6. The rocks having specific gravity ≥ 2.55 are considered to be suitable for heavy construction work (Blyth and de Freitas, 1974). The observed specific

gravity of all the studied samples suggests their suitability for use in heavy construction projects.

5.4.4. Porosity

It is a measure of the total void volume in a rock. The factors that affect porosity of rocks include grain size, grain shape and mineralogical composition particularly the presence of clay minerals (Bell, 1978). The increasing percentage of porosity leads to a corresponding decrease in the rock strength. The porosity of the samples under investigation was determined by the saturation method (Harrison, 1993) and calculated with the help of the following formula. The relevant details and results obtained are presented in table 5.6:

$$P = \frac{(\text{Wt. in air}) - (\text{Dry wt.})}{(\text{Wt. in air}) - (\text{Wt. in water})} \times 100$$

Table 5.6. Details and results of water absorption, specific gravity and porosity of the studied samples

S. No.	Dry Wt. (g)	Wt. in water (g)	Wt. in air (g)	Water Absorption	Specific Gravity	Porosity
CG - 1	31.233	19.607	31.515	0.903	2.686	2.368
CG - 2	32.524	20.435	32.818	0.904	2.690	2.374
CG - 3	31.795	19.900	32.065	0.849	2.673	2.219
CG - 4	34.971	22.128	35.270	0.855	2.723	2.275
CG - 5	31.109	19.452	31.376	0.858	2.669	2.239
CG - 6	28.305	17.781	28.520	0.760	2.690	2.002
CG - 7	33.707	21.347	33.958	0.745	2.727	1.990
CGF-1	32.471	20.437	32.760	0.890	2.698	2.345
CGF-2	38.614	24.367	38.933	0.826	2.710	2.190
CGF-3	31.333	19.700	31.582	0.795	2.693	2.096
CGF-4	35.597	22.464	36.005	1.146	2.711	3.013
CGF-5	33.283	20.961	33.589	0.919	2.701	2.423
CGF-6	31.545	19.855	31.787	0.767	2.698	2.028
CGF-7	34.126	21.466	34.378	0.738	2.696	1.952
FG -1	31.451	19.500	31.925	1.507	2.632	3.815
FG -2	20.709	12.812	21.035	1.574	2.622	3.964
FG -3	18.078	11.198	18.372	1.626	2.628	4.098
FG -4	25.831	16.002	26.229	1.541	2.628	3.892
FG -5	21.935	13.609	22.267	1.514	2.635	3.835
FG -6	21.789	13.509	22.128	1.556	2.632	3.933
FG -7	26.484	16.435	26.893	1.544	2.635	3.911

5.5. Relationship among Petrographic, Physical and Mechanical Properties

The petrographic, physical and mechanical properties of the different textural varieties of Utlá granite are plotted against each other to investigate the possible relationship among them.

In order to see the relationship between modal mineralogical composition and strength, UCS and UTS values of the studied samples are plotted against their respective quartz to feldspar ratios (Figs. 5.2 and 5.3). The resulting graphs show direct relationship between these two parameters. A more or less similar relationship is also noted by Tugrul and Zarif (1999) and Gunsallus and Kulhawy (1984). In contrast, Shakoor and Bonelli (1991), Fahy and Guccione (1979) and Bell (1978) believe the type of grain contact to be more important than the total amount of quartz and that there is no significant relationship between quartz content and strength of rocks.

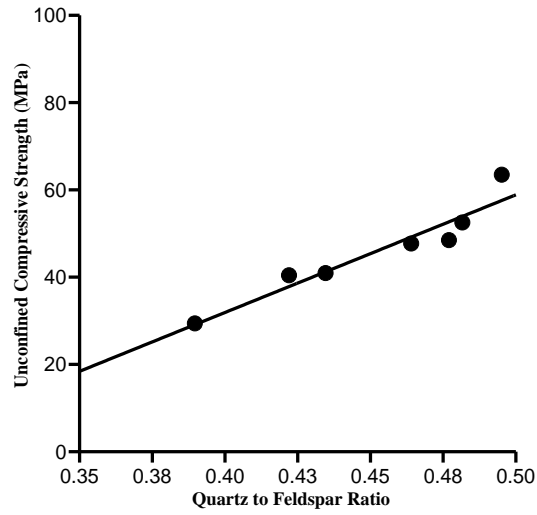
The quartz content has an influence on the total porosity of a rock because anhedral quartz grains fill spaces between the other grains (Tugrul and Zarif, 1999). Quartz to feldspar ratios of the studied samples are plotted against their respective porosity values. The resulting plots demonstrate negative correlation between the two variables (Fig. 5.4). Tugrul and Zarif (1999) have noted a more or less similar relationship for the granitic rocks from Turkey.

Increase in the volume of voids in a rock markedly decreases its strength. A small change in pore volume can produce an appreciable mechanical effect (ISRM, 1981). That is why the UCS values of the studied samples are plotted against their respective porosity and water absorption values. The resulting plots display inverse relationships between the plotted parameters (Figs. 5.5 and 5.6).

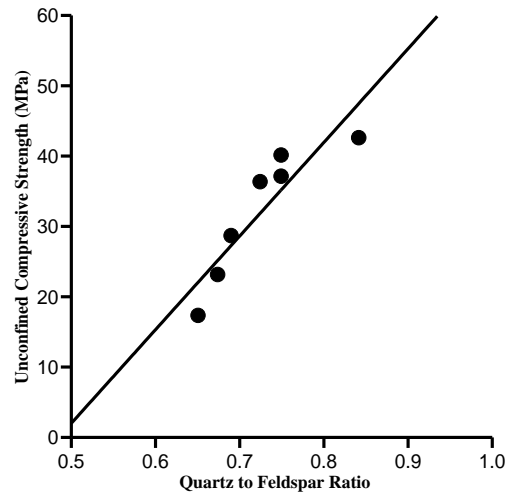
The UCS versus UTS plot yields a strong positive relationship (Fig. 5.7). Tugrul and Gurpinar (1997), Shakoor and Bonelli (1991) and D'Andrea et al. (1965) also utilized the USC-UTS plot for different rock types and found a similar relationship.

The UCS values of the studied samples are plotted against their respective mica content. No significant relation is interpreted from these plots (Fig. 5.8).

a)



b)



c)

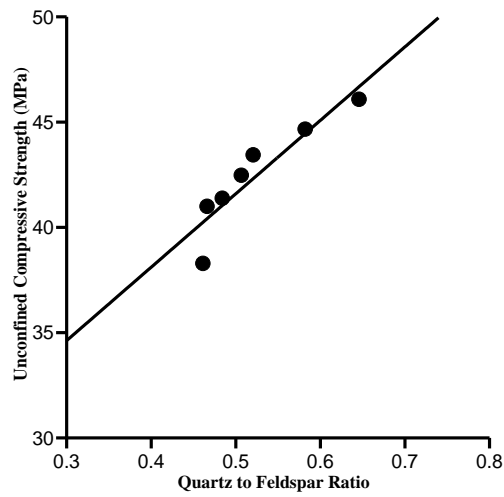
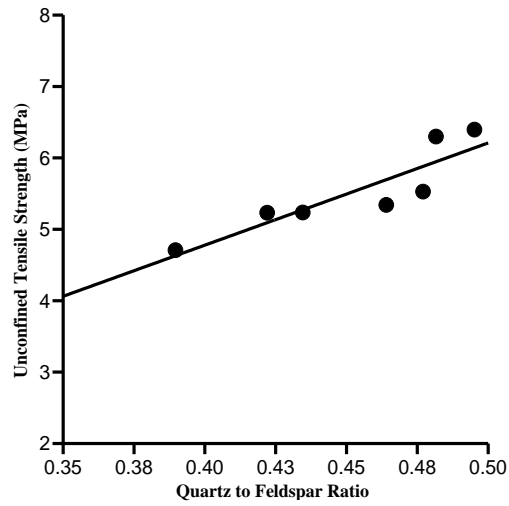
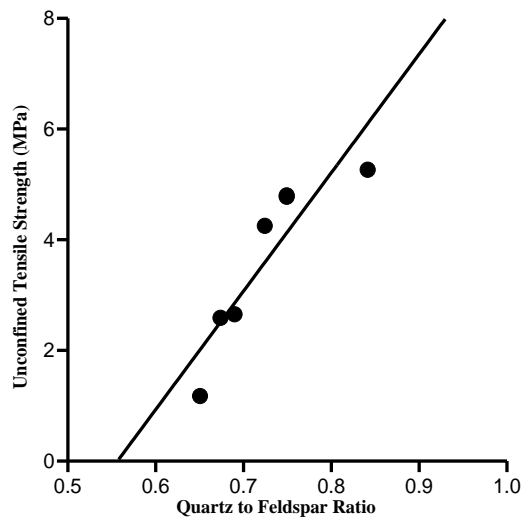


Fig. 5.2. Relationship between UCS and quartz to feldspar ratio: (a) Megacrystic granite, (b) Foliated granite and (c) Fine-grained granite

a)



b)



c)

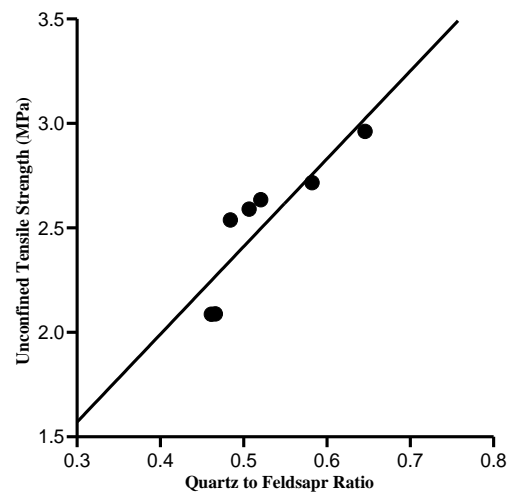
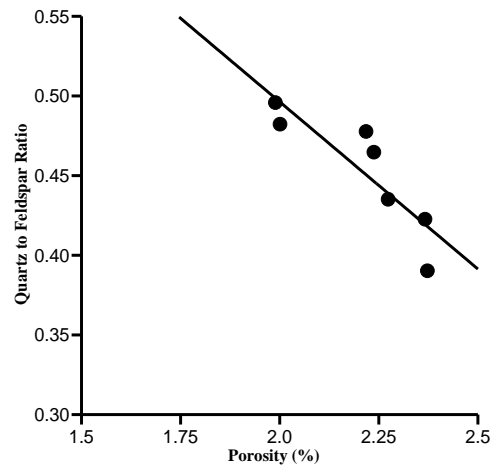
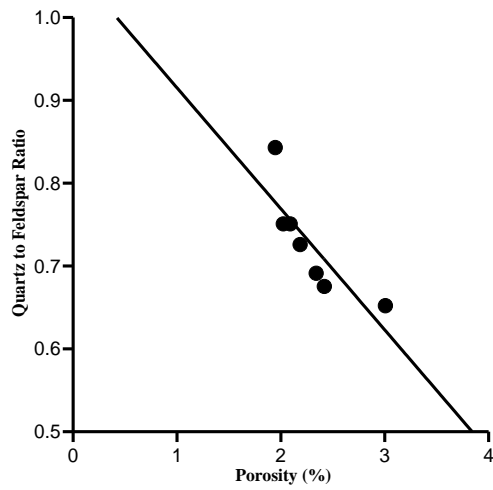


Fig. 5.3. Relationship between UTS and quartz to feldspar ratio: (a) Megacrystic granite, (b) Foliated granite and (c) Fine-grained granite

a)



b)



c)

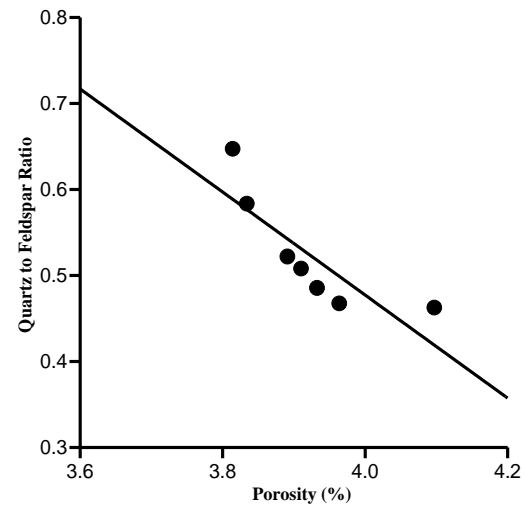
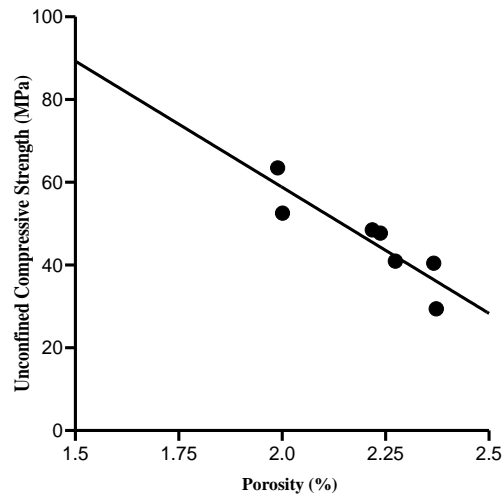
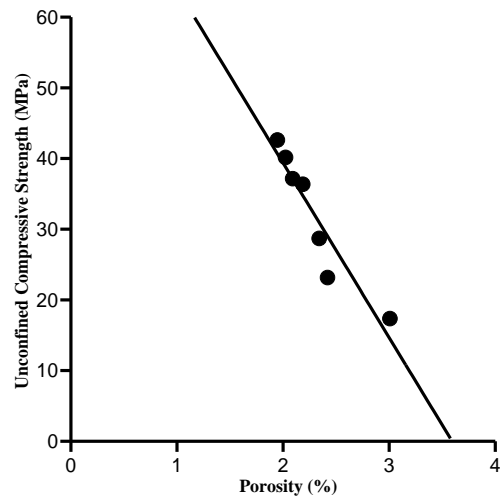


Fig. 5.4. Relationship between porosity and quartz to feldspar ratio: (a) Megacrystic granite, (b) Foliated granite and (c) Fine-grained granite

a)



b)



c)

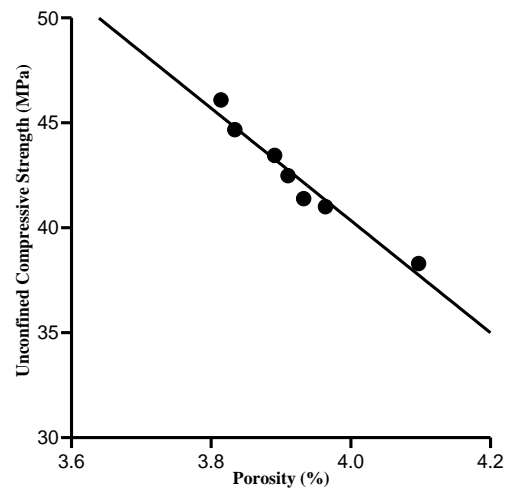
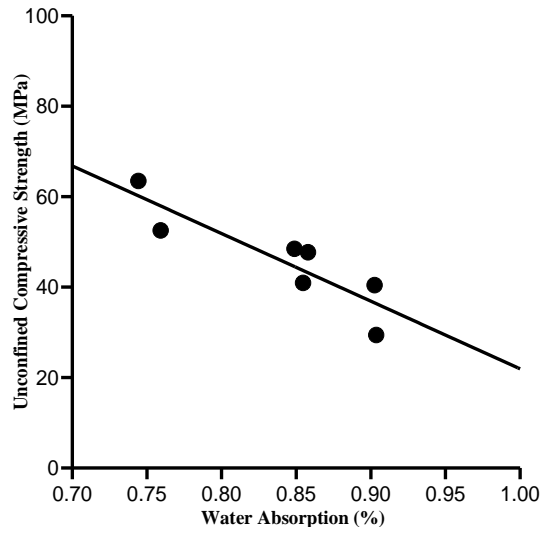
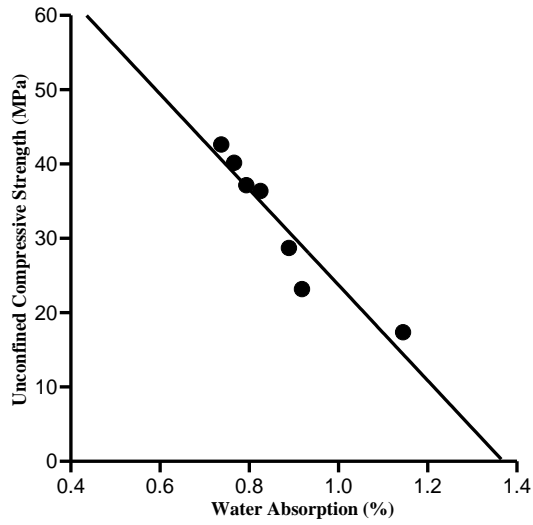


Fig. 5.5. Relationship between UCS and porosity: (a) Megacrystic granite, (b) Foliated granite and (c) Fine-grained granite

a)



b)



c)

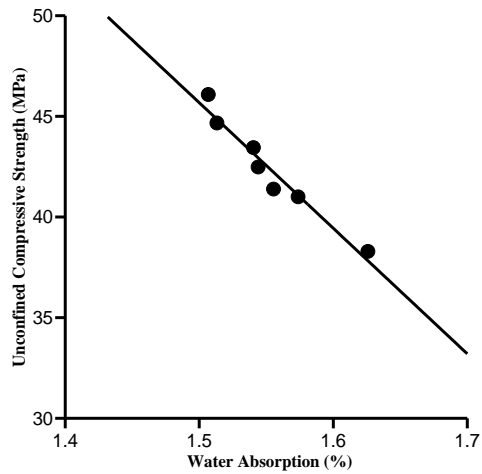
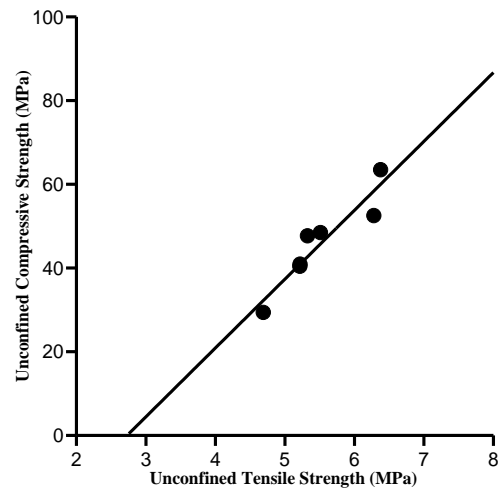
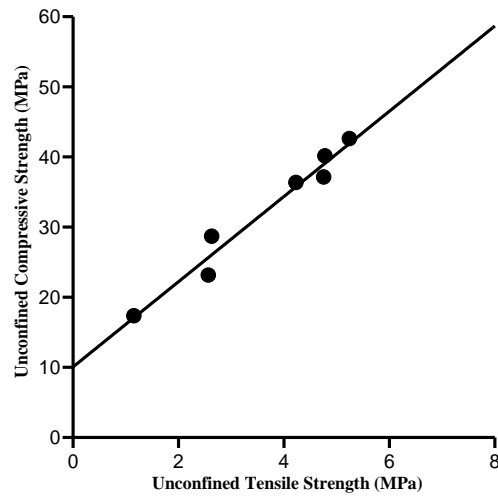


Fig. 5.6. Relationship between UCS and water absorption: (a) Megacrystic granite, (b) Foliated granite and (c) Fine-grained granite

a)



b)



c)

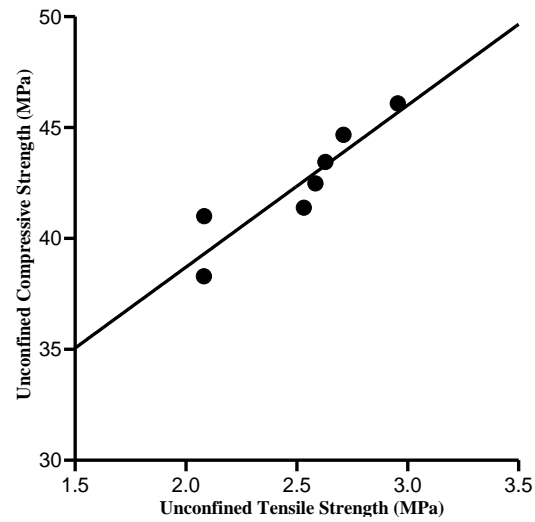
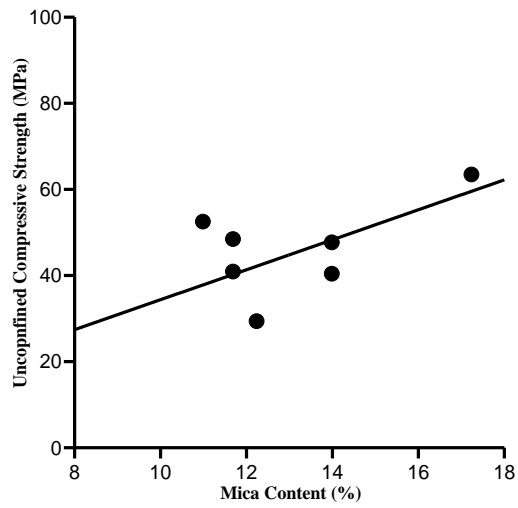
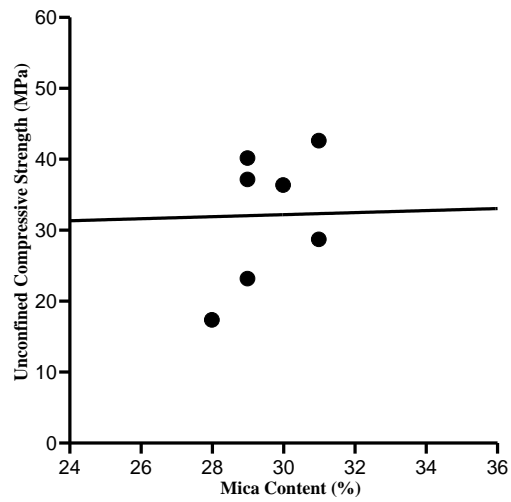


Fig. 5.7. Relationship between UCS and UTS: (a) Megacrystic granite, (b) Foliated granite and (c) Fine-grained granite

a)



b)



c)

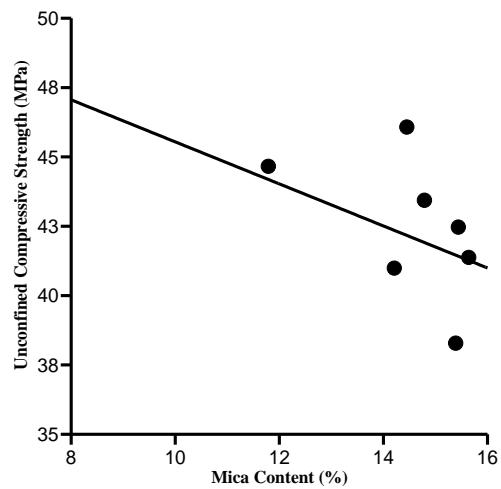


Fig. 5.8. Relationship between UCS and Mica Content: (a) Megacrystic granite, (b) Foliated granite and (c) Fine-grained granite

DISCUSSION

6.1. General Statement

The petrographic, geochemical and physico-mechanical studies of the igneous rocks from the Utla area, Gadoon are the main objectives of the present study. The results from these studies are used for the petrogenetic and tectonic modeling of these rocks. Details about the different methods employed and results obtained from these studies are presented in the previous chapters. These results are briefly discussed in the following paragraphs:

6.2. Petrographic and Geochemical Characteristics

Petrographically, the igneous rocks of Utla can be grouped into granites and basic dykes. The Utla granites are mega-porphyrific containing phenocrysts of altered plagioclase, perthitic alkali feldspar and quartz. Quartz and alkali feldspar also constitute the groundmass with minor to accessory amounts of tourmaline, muscovite and biotite and accessory to trace amounts of apatite, andalusite, garnet, zircon, monazite, epidote and sphene. The tourmaline grains display irregular zoning and variable degree of alteration and is the most common and abundant mafic mineral present in these granitic rocks. As mentioned in the previous chapters, most of the earlier workers believe that the Utla granites represent the eastward extension of the Ambela granitic complex, however, some of the recent workers have mapped and hence genetically grouped these rocks with the granitic rocks of Swat and Mansehra (DiPietro et al., 1998; Hussain et al., 2004; Sajid and Arif, 2010).

Like those from Utla, the granitic rocks from both the Swat and Mansehra areas contain tourmaline (Le Fort et al., 1980). On the other hand, none of the available petrographic details suggests any occurrence of tourmaline in the Ambela rocks. These observations suggest that the Utla granites most probably represent a southwestward continuation of the Mansehra granites rather than any eastward extension of the Ambela complex. The occurrence of andalusite in Utla granites and its total absence from the Ambela granites lends further support to this conclusion.

Trace to accessory amounts of sphene, mostly forming thin rims or borders around grains of an opaque ore mineral, also occur in the Utla granites. Such an opaque ore-sphene corona texture is also observed and appears to be a more or less common petrographic characteristic of the Ambela rocks.

Accessory to traces amounts of apatite occur as discrete grains in the Utla granites. Chappell and White (2001) have noted that apatite occurs in the form of larger discrete crystals in S-types

granites and in high-temperature I-type granites. In contrast, it occurs as inclusions in biotite and hornblende in low-temperature I-type granites. The occurrence of larger crystals of apatite in S-type granites is not fully understood. However, it seems to be an indirect result of the higher solubility of P_2O_5 in the more per-aluminous melts (London, 1992) so that apatite crystals are precipitated from them on cooling. Garnet and cordierite may also occur in the S-type granites (Chappell and White, 2001).

The presence of apatite as discrete grains, accessory amount of andalusite and garnet and the total absence of hornblende suggest S-type origin for the Utla granites. The occurrence of zoned epidote grains with presumably Fe^{3+} richer core and Al-rich margin indicates low (-medium) grade metamorphism of the studied rocks.

The results of geochemical analysis reveal that the Utla granites are calc-alkaline and per-aluminous. The presence of Al-rich phases, e.g. andalusite and high ASI values of the studied samples also support this argument. These diagnostic mineralogical and chemical features may be observed where the host rocks contain higher amounts of Al than alkalis and Ca. Relative to that for I-type granites, the melt source rocks for the S-type granites are oversaturated in Al most probably due to the preferential loss of Na and Ca during weathering (Chappell, 1999).

In strongly per-aluminous granitic melts, Rb, Sr and Ba provide information regarding source rocks and place critical constraints on the conditions prevailed during the melting process (Miller, 1985; Harris and Inger, 1992). The geochemical plots for the studied samples (Fig. 4.8) on the Rb/Sr versus Rb/Ba and Al_2O_3/TiO_2 versus CaO/Na_2O diagrams of Sylvester (1998) suggest a plagioclase-poor, clay-rich source for the Utla granites.

As discussed in the earlier chapters, dykes of mostly basic composition cut across the pre-Permian rocks exposed in the area between the MMT and Khairabad thrust (Fig. 2.2). Likewise, the Utla granites are traversed with dykes whose petrographic and geochemical characteristics are described in the previous chapters. These descriptions reveal two subgroups of dykes. Dykes from one of the subgroups essentially consist of plagioclase and clinopyroxene and display ophitic to sub-ophitic texture and thus appear to be dolerite. The clinopyroxene gives a pinkish/violet color in plane light, and hence may contain a significant amount of Ti. Besides, brownish hornblende also occurs as discrete grains in some of these dolerite dykes. Dykes from the other group largely consist of plagioclase and amphibole. A subordinate amount of clinopyroxene occurs as relics. The occurrence of appreciable amounts of epidote and zoisite together with green amphibole and chlorite mostly after clinopyroxene indicates metamorphism of these rocks

under greenschist to epidote amphibolite facies conditions. The metamorphosed character of the studied samples of basic dykes cutting the Utla granites contributes a further support to the idea that the latter have also experienced a low to medium-grade metamorphism. As is the case with the host granite, sphene occurs both as discrete grains and thin rims or zones around opaque ore grains forming corona texture in both the types of dykes.

The occurrence of sphene and indications for the titaniferous character of both the clinopyroxene and amphibole support the alkaline character of studied dykes. Discriminant diagrams based on different trace and rare earth elements suggest within-plate magmatic settings for these dykes (Figs. 4.19-4.23). More or less similar petrographic features and geochemical characteristics were noted and a broadly similar subdivision was proposed for the dykes exposed in the Malka area (Majid et al., 1991). These workers have proposed a rift-related extensional tectonic setting for the Malka dykes.

6.3. Comparison with Ambela Granitic Complex and Mansehra Granite

As highlighted earlier, most of the earlier workers regard the Utla granites to represent the eastward extension of the Ambela granitic complex (AGC) (Rafiq and Jan, 1988; Jan and Karim, 1990). The AGC comprises of three rock groups i.e. Group-I includes granites and alkali granites representing the earliest magmatic episode, Group-II includes syenites, feldspathoidal syenites and related rocks representing the second magmatic episode and Group-III comprises of dolerite dykes which invade the group I and II rocks (Rafiq and Jan, 1988). A detailed geochemical account of these rocks is presented by Rafiq and Jan (1989). A study of the published geochemical data reveals that both the group-I and group-II rocks of the AGC are per-aluminous to meta-aluminous in character displaying an alkaline affinity. Furthermore, the trace element characteristics indicate a within-plate magmatic setting for the granitic rocks of the AGC (Figs. 4.13 and 4.14) (Rafiq and Jan, 1989). In contrast to these conclusions, the present studies on the Utla granites portray a markedly different picture in terms of their geochemical affinity and tectonic setting. Although being per-aluminous to meta-aluminous, much like the Ambela ones, the Utla granites exhibit a strong calc-alkaline rather than alkaline affinity (Figs. 4.3; 4.5; 4.6). Accordingly, the geochemical characteristics of the Utla granitoids are transitional between those representing volcanic-arc and syn-collisional settings (Figs. 4.12-4.14). As mentioned earlier, the alkaline rock suites including alkali granites, syenites and feldspathoidal syenites constitute the

major component of group-I and group-II rocks of the AGC. In contrast, the present study reveals that rocks of alkaline character do not occur in the Utla area.

A detailed investigation of the whole-rock geochemical data suggests a within-plate setting for the Utla dykes (Figs. 4.19-4.23). Hence these dykes might be related genetically to the group-III rocks of the AGC and the Malka dykes (Majid et al., 1991).

The Mansehra granitic pluton lies to the east of the studied Utla granite (Fig. 1.1). There is no obvious spatial discontinuity between the Mansehra and Utla granites (Hussain et al., 2004). Le Fort et al. (1980) presented a detailed geochemical and geochronological account of the Mansehra rocks, which reveals that granitic rocks of the Mansehra pluton have calc-alkaline affinity (Fig. 4.5). The Mansehra granites are characterized as collisional granites while Utla granites show transitional character between collisional and within-plate granites on the basis of Rb-Ba-Sr discriminant diagram (Fig. 6.1).

The Rb/Ba vs Rb/Sr plot of Sylvester (1998) has been employed to determine the nature of the source rock for the melt parental to the Utla granite. This exercise reveals a clay-rich, plagioclase-poor source for the granitic rocks of both the Utla and Mansehra areas (Fig. 4.8). Hence it seems reasonable to conclude that the Utla granites are more like the Mansehra granite than those representing the AGC.

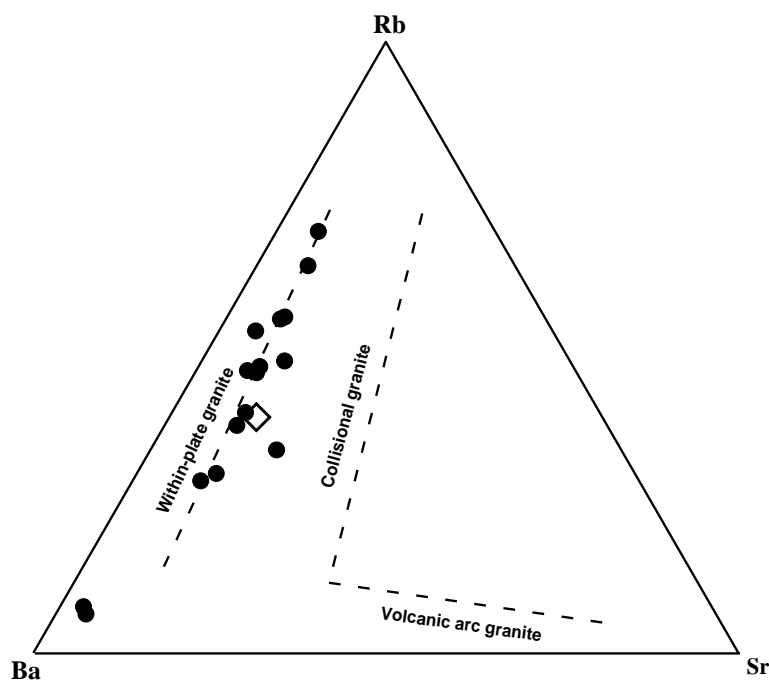


Fig. 6.1. Rb-Ba-Sr discriminant diagram (El Bouseily and El Sockary, 1975). The symbols are as in Fig. 4.6.

The ORG-normalized and chondrite-normalized spidergrams for the Utla granites have been compared with those of the AGC granites (Rafiq and Jan, 1989) and pink porphyritic Singo granite (Nagudi et al., 2003) (Fig. 6.2). The Singo granite is regarded as a typical example of granites representing syn-collisional to post-collisional tectonic settings. For the purpose of comparison with the Utla granitoids, the corresponding data from both the Ambela and Singo granites are shown as shaded areas in figure 6.2. The Ambela samples display (i) a strong negative Th anomaly, (ii) lack any Hf spike and (iii) show enrichment in K and Y. On the other hand, the relative abundances of most of the elements, except Hf, in the Utla granitoids display a more or less similar pattern as the Singo granite. The enrichment of the studied Utla samples in Hf most probably represents a higher degree of Hf for Zr substitution in zircon. It also indicates fractionation of zircon from the original melt as the Hf/ Zr ratio increases with increasing degree of magmatic differentiation (Deer et al., 1992).

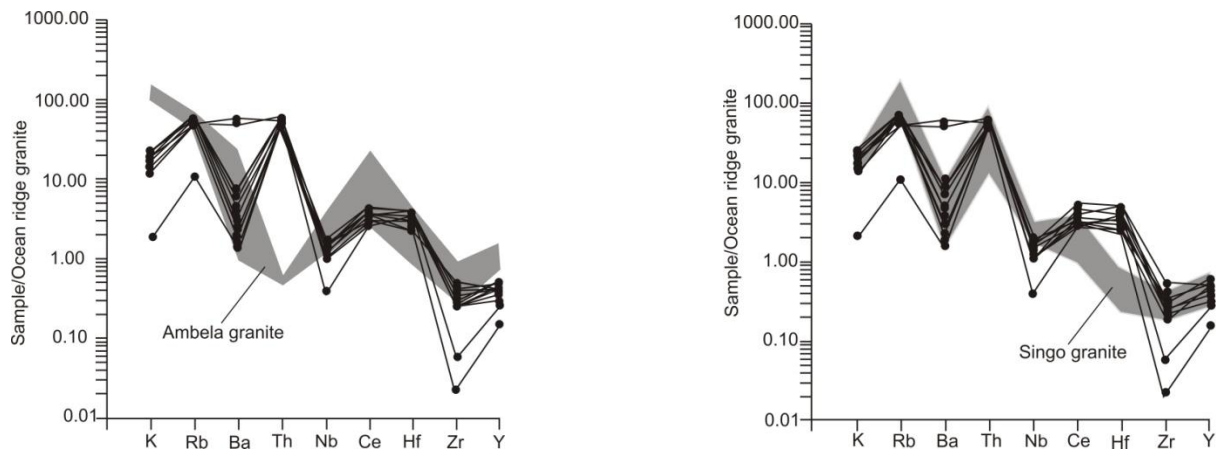
6.4. Mechanical Properties

As a part of the present study, some of the physical and mechanical properties of different textural varieties of the Utla granites were determined to assess their suitability for use as construction material. As described in chapter five, the strength values of the Utla granites vary drastically. The UCS of most of the samples falls in the range of those rocks which are designated as moderately strong (Table 6.1); only two of the mega-crystic granite samples (CG-6 and CG-7), with UCS values of more than 50 MPa, are regarded as strong (Table 6.1).

An attempt is made here to establish the possible relationship among the petrographic characteristics, physical properties and strength of these rocks. The strength values of the investigated rock samples are plotted against their respective physical properties and petrographic characteristics (Figs. 5.2-5.8). A detailed comparison and thorough examination lead to suggest that the following petrographic features are the most important in determining and controlling the strength of the studied rocks:

1. Modal mineralogical composition
2. Grains size and shape and scope of their variation
3. Preferred alignment and segregation of mineral grains
4. Volume of voids

a)



b)

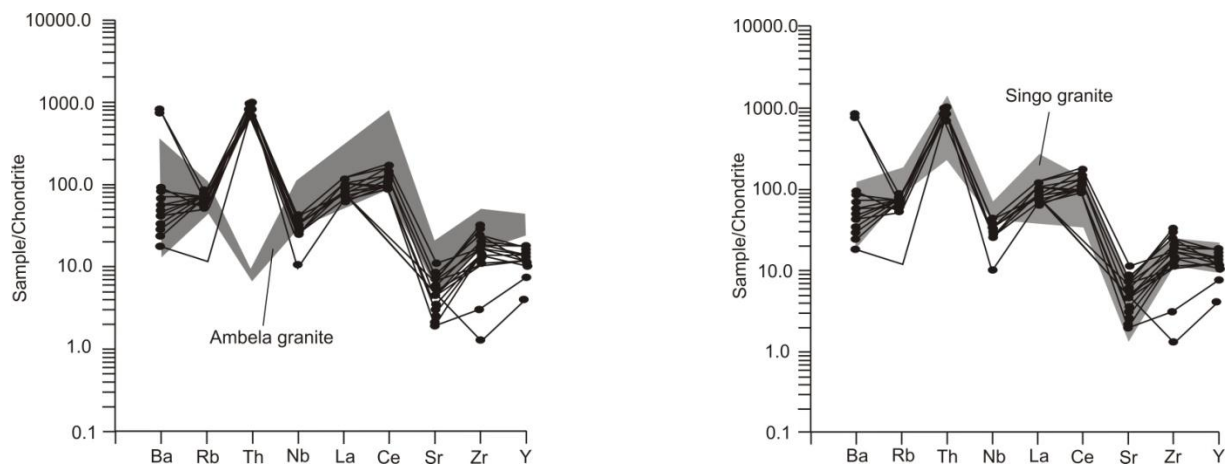


Fig. 6.2. Spidergrams showing comparison of Utla granites with Ambela granite (Rafiq and Jan, 1989) and Singo granite (Nagudi et al., 2003): a) ocean ridge granite (ORG)-normalized plot (normalization factor after Pearce et al., 1984), b) chondrite-normalized plot (normalization factor after Taylor and McLennan, 1985). The geochemical patterns of both the Ambela and Singo granites are shown as shaded areas.

Several earlier workers including Willard and Williams (1969), Howarth and Rowlands (1987), Shakoor and Bonelli (1991), Tugrul and Zarif (1999), Akesson et al. (2003), Bell (2007), Lindqvist et al. (2007) and Sajid et al. (2009) have also drawn more or less similar conclusions.

The investigated physical and mechanical properties of different textural varieties of the Utla granite are statistically analyzed to determine their mean values and standard deviation (Table 6.2). The fine-grained rocks are generally found to be stronger than their coarse grained counterparts (Bell, 2007). Comparison of results from the present investigation, however, leads to an entirely different conclusion. That is, the strength values of the coarse-grained mega-crystic

Utla granites (CG) are higher than those of the fine grained (FG) ones (Table 6.2). Although seemingly anomalous, the conclusion is in conformity with the higher porosity and water absorption values of the fine grained variety since, as noted in the previous chapter, increasing porosity and water absorption capacity adversely affect the rock strength.

The rocks containing large amount of physically strong minerals are evidently strong, however, the textural relation of these minerals with the associated minerals may also affect the strength. Despite the overall greater concentration of quartz (average = 29 %), the coarse-grained foliated variety (CGF) of Utla granites tolerates with the lowest strength values relative to the other two studied varieties. The diminution in strength of CGF granites is because of the overall greater concentration and orientation of flaky minerals, including biotite and muscovite (averaging ~29 %) (Table 6.2). In addition to being relatively weak, the preferred alignment of micaceous minerals imparts foliation to their host rocks. This is because the foliation planes can act as large discontinuities where cracks can initiate and propagate easily (Lindqvist et al., 2007).

Table 6.1. Grades of unconfined compressive strength.

Geological Society (Anon, 1977)		IAEG* (Anon, 1979)		ISRM** (Anon, 1981)	
Description	UCS (MPa)	Description	UCS (MPa)	Description	UCS (MPa)
Very weak	<1.25	Weak	<15	Very low	<6
Weak	1.25-5.00	Moderately weak	15-50	Low	6-10
Moderately weak	5.00-15.50	Strong	50-120	Moderate	20-60
Moderately strong	12.50-50	Very strong	120-130	High	60-200
Strong	50-100	Extremely Strong	Over 230	Very high	Over 200
Very strong	100-200				
Extremely Strong	Over 200				

*International Association of Engineering Geologists

**International Society for Rock Mechanics

Similarly, as mentioned earlier, the strength of the fine-grained variety is lower than the megacrystic type despite the greater concentration of quartz in the former (averaging ~28 %) than the latter (averaging ~25 %). The relatively low strength values of the fine-grained, quartz-richer

samples are most probably because of the greater uniformity in their grain size compared to the coarse-grained (mega-crystic) type. This is in accordance with the Lindqvist et al.'s (2007) interpretation that “it is not only the grain size but also the grain size distribution that is important, with the effect that a large size range gives higher strength and better resistance to fragmentation and wear compared to a more equigranular or idiomorphic rock”.

It follows from the above discussion that the mega-crystic variety of the Ulla granites has the highest strength values most probably because of (i) greater variation in their grain size (ii) lower abundance and non-alignment of micaceous minerals (iii) lower values of water absorption and porosity. Although the extent of grain size variation in the foliated variety is more or less similar to that of the mega-crystic type, yet its strength values are lower than the latter probably because of the greater abundance and marked preferred orientation of its micaceous minerals.

Table 6.2. Average values of UCS, UTS, porosity, water absorption, specific gravity, quartz to feldspar ratio and mica content of the studied samples

S. No.	UCS	UTS	Porosity	WA	SG	Q/F	Mica
CG	45.97± 10.71	5.52 ± 0.61	2.21 ± 0.15	0.84 ± 0.06	2.69 ± 0.02	0.45 ± 0.04	13.1 ± 2.1
CGF	32.11 ± 9.38	3.63 ± 1.52	2.29 ± 0.36	0.87 ± 0.14	2.7 ± 0.006	0.72 ± 0.06	29.5 ± 1.13
FG	42.45 ± 2.57	2.51 ± 0.32	3.92 ± 0.09	1.55 ± 0.04	2.63 ± 0.004	0.52 ± 0.06	14.5 ± 1.32

CONCLUSIONS AND RECOMMENDATIONS

7.1. Conclusions

The various details regarding field and petrographic observations, geochemical analyses and mechanical properties of rocks from the Utla area are presented in the previous chapters. These discussions lead to the following conclusions:

1. The igneous rocks of the Utla area are broadly divided into two categories:
 - a. Granites: These granites are predominantly mega-porphyritic; however, fine grained massive and foliated varieties are also present along shear zones. Besides, fine-grained granitic dykes also cut across these rocks at places.
 - b. Dykes: These are basic in composition and further distinguished on the basis of their textural and mineralogical characteristics into (i) dolerite dykes and (ii) altered/metamorphosed dykes.
2. The geochemical analyses of the Utla granites point to their per-aluminous and calc-alkaline character.
3. S-type origin is anticipated for the Utla granites. Furthermore, plagioclase-poor, clay-rich sedimentary rocks appear to have acted as source for the melt whose crystallization led to the formation of the Utla granites.
4. An environment transitional between volcanic arc and syn-collisional tectonic settings is suggested for Utla granites on the basis of different geochemistry-based diagrams that are commonly used for discriminating among various petro-tectonic scenarios.
5. Plots of geochemical data on discriminant diagrams suggest a within-plate tectonic setting for the Utla dykes. The petrographic and geochemical characteristics of these rocks are broadly similar to those of the Malka dykes that are exposed in close proximity and both these might be related genetically to the group-III rocks of the AGC.
6. The following petrogenetically important features of the Utla granites are also shared by the Mansehra granites:
 - a. Mega-porphyritic texture
 - b. Occurrence of andalusite and tourmaline
 - c. Per-aluminous (high ASI) and calc-alkaline character
 - d. Volcanic arc to syn-collisional tectonic setting
 - e. Absence of alkaline rocks

- f. Rock of broadly similar composition (i.e. pelite) appears to have acted as source for the melt parental to both the Utla and Mansehra granites
7. A number of petrographic features, including mineralogical composition, grain size and shape distribution, modal abundance and orientation of flaky minerals and volume of empty spaces, appear to have collectively contributed to determining the actual strength of the Utla granites.

7.2. Recommendations for Future Studies

- The present study leads to conclusion that granitic rocks from the Utla area resemble more the Mansehra granite than granitic rocks from the AGC. The geochronological studies for both the Mansehra granites and AGC were performed by earlier workers, however, such details for the Utla rocks are lacking and hence need to be investigated so that their relationship with either of the two can be properly established.
- Garnet is an uncommon yet petrologically significant accessory mineral in granitic rocks. As discussed in chapter three, trace amounts of seemingly magmatic garnet occur in the Utla granite. A detailed mineral chemical investigation is required to substantiate this probability and help determine the pressure-temperature conditions that prevailed during crystallization.
- Some of the petrographic features, discussed in earlier chapters, indicate that the Utla granites have experienced a low (-medium) grade progressive metamorphism. A detailed investigation of intra- and inter-granular variation in the chemical composition of some of the mineral phases, especially epidote and garnet, would help in finding out the sense and conditions of metamorphism.
- The optical properties of clinopyroxene and amphibole from the Utla basic dykes point to their titaniferous character. Determination of their chemical composition would not only help in looking further into this possibility but would also aid in better understanding of the genesis and magmatic affiliation of their host dykes.
- The geo-technical investigation of the Utla granites is limited to only a few of their mechanical properties. However, to portray a broader picture of applied nature, other physico-mechanical properties including triaxial compressive strength, shear strength, permeability, seismic velocity and modulus of elasticity also need to be explored.

REFERENCES

- Ahmed, I., 1986. Geology of Jowar area, Karakar pass, Swat district, NWFP Pakistan. M.Phil thesis, University of Peshawar, 144p.
- Akesson, U., Stigh, J., Lindqvist, J. E. and Goransson, M., 2003. The influence of foliation on the fragility of granitic rocks, image analysis and quantitative microscopy. *Engineering Geology*, 68, 275–288.
- Anon, 1977. The description of rock masses for engineering purposes. Engineering group working party report, *Quarterly Journal Engineering Geology*, 10, 43-52.
- Anon, 1979. Classification of rocks and soil for engineering geological mapping, part-1 rock and soil materials. *Bulletin of International Association Engineering Geology*, 19, 364-371.
- Anon, 1981. Basic geotechnical description of rock masses. International society of rock mechanics commission on the classification of rocks and rock masses. *International Journal Rock Mechanics and Mining sciences and geo-mechanical Abstracts*, 18, 85-110.
- Arif, M., Mulk, A., Tariq, M. M. and Majid, S. H., 1999. Petrography and mechanical properties of the Mansehra granite, Hazara, Pakistan. *Geological Bulletin, University of Peshawar*, 32, 41-49.
- ASTM, 1971. D-2938, Standard test method for unconfined compressive strength of intact rock core specimens. American Society for Testing Material, Philadelphia, Pennsylvania, U.S.A..
- ASTM, 1986. D-3976, Standard test method for splitting tensile strength of intact rock core specimens. American Society for Testing Material, Philadelphia, Pennsylvania, U.S.A.
- Baig, M. S., 1990. Structure and geochronology of pre-Himalayan and Himalayan orogenic events in northwest Himalaya, Pakistan, with special reference to Besham area. Ph. D. dissertation. Oregon State University, Corvallis, 300p.
- Bell, F. G., 1978. The physical and mechanical properties of the Fell sandstones, Northumberland, England. *Engineering Geology*, 12, 1–29.
- Bell, F. G., 2007. *Engineering Geology*, 2nd edition. Butterworth-Heinemann: an imprint of Elsevier, United Kingdom.
- Blyth, F. G. H. and de Freitas, M. H., 1974. *Geology of engineers*. ELBS and Edward Arnold, London, 514p.
- Bucher, K. and Frey, M., 1994. *Petrogenesis of Metamorphic Rocks*. Springer, Berlin.
- Butt, K. A., 1983. Petrology and geochemical evolution of Lahor pegmatoid/granite complex, northern Pakistan, and genesis of associated Pb-Zn-Mo and U mineralization. In: *Granite of Himalayas, Karakoram and Hindukush* (F. A. Shams ed.), Institute of Geology, Punjab University, Lahore, 309-326.
- Butt, K. A., Arif, A. Z., Ahmed, J., Ahmed, A. and Qadir, A., 1989. Chemistry and petrography of the Sillai Patti carbonatite complex, North Pakistan. *Geological Bulletin, University of Peshawar*, 22, 197-215.
- Calkins, J. A., Offield, T. W., Abdullah, S. K. M. and Ali, S. T., 1975. Geology of southern Himalaya in Hazara, Pakistan and adjacent areas. U. S. Geological Survey Professional paper, 716-C, 29p.
- Chappell, B. W. and White, A. J. R., 1992. I- and S-type granites in the Lachlan Fold Belt. *Transactions of the Royal Society of Edinburgh: Earth Sciences*, 83, 1–26.

- Chappell, B. W., 1999. Aluminium saturation in I- and S-type granites and the characterization of fractionated haplogranites. *Lithos*, 46, 535-551.
- Chappell, B. W. and White, A. J. R., 2001. Two contrasting granite types: 25 years later. *Australian journal of earth sciences*, 48, 489-499.
- Coward, M. P., Jan, M. Q., Rex, D., Tarney, J., Thirlwall, M. and Windley, B. F., 1982. Geo-tectonic framework of the Himalaya of N. Pakistan. *Journal of Geological Society of London*, 139, 299-308.
- Coward, M. P., Windley, B. F., Broughton, R.D., Luff, I. W., Petterson, M. G., Pudesy, C. J., Rex, D. C. and Asif, K. M., 1986. Collision tectonics in the NW Himalaya. In: Coward, M. P., Ries, A. (Eds.), *Collision tectonics: Geological Society of London Special Publication*, 19, 203-219.
- Coward, M. P., Buffer, R. W. H., Chambers, A. F., Graham, R. H., Izatt, C. N., Khan, M. A., Knipe, R. J., Prior, D. J., Treloar, P. J. and Williams, M. P., 1988. Folding and imbrication of the Indian crust during Himalayan collision. *Philosophical Transaction of the Royal Society London*, A326, 89-116.
- D'Andrea, D. V., Fischer, R. L. and Fogelson, D. E., 1965. Prediction of compressive strength of rock from other properties. *US Bureau of Mines Rep. Investigation*, No. 6702.
- Dahiquist, J. A., Galindo, C., Pankhurst, R. J., Rapela, C. W., Alasino, P. H., Saavedra, J. and Fanning, C. M., 2007. Magmatic evolution of the Penon Rosado granite; Petrogenesis of garnet bearing granitoids. *Lithos*, 95, 177-207.
- Deer, W. A. Howie, R.A. and Zussman, J., 1992. *An Introduction to the Rock-Forming Minerals*, 2nd Edition. Longman scientific and technical, England.
- Dhuime, B., Bosch, D., Bodinier, J. L., Garrido, C. J., Bruguier, O., Hussain, S. S. and Dawood, H., 2007. Multistage evolution of the Jijal ultramafic- mafic complex (Kohistan, N Pakistan): Implications for building the roots of island arcs. *Earth and Planetary Science Letters*, 261, 179-200.
- Din, F., Rafiq, M. and Mohammad, N., 1993. Strength properties of various building stones of N.W.F.P. Pakistan. *Geological Bulletin, University of Peshawar*, 26, 119-126.
- Din, F. and Rafiq, M., 1997. Correlation between compressive strength and tensile strength/index strength of some rocks of North-West Frontier Province (Limestone and Granite). *Geological Bulletin, University of Peshawar*, 30, 183-190.
- DiPietro, J. A., 1990. Stratigraphy, structure and metamorphism near Saidu Sharif, Lower Swat, Pakistan. PhD Thesis, Oregon state University, Corvallis.
- DiPietro, J. A., Pogue, K. R., Lawrence, R. D., Baig, M. S., Hussain, A. and Ahmed, I., 1993. Stratigraphy south of the Main Mantle Thrust, Lower Swat, Pakistan. *Himalayan Tectonics, Special publication*, 74, 207-220.
- DiPietro, J. A., Pogue, K. A., Hussain, A. and Ahmed, I., 1998. Geologic map of Indus syntaxis and surrounding area, northwest Himalaya, Pakistan. *Geological society of America, Special paper*, 328, plate-1.
- DiPietro, J. A., Hussain, A., Ahmad, I. and Khan, M. A., 2000. The Main Mantle Thrust in Pakistan: its character and extent. *Geological Society, London, Special publication*, 170, 375-393.

- du Bray, E. A., 1988. Garnet composition and their use as indicators of per-aluminous granitoid petrogenesis, Southeastern Arabian shield. *Contributions to mineralogy and petrology*, 100, 204-212.
- Dwivedi, R. D., Goel, R. K., Prasad, V. V. R. and Amalendu Sinha, 2008. Thermo-mechanical properties of Indian and other granites. *International Journal of Rock Mechanics & Mining Sciences*, 45, 303–315.
- El Bouseily, A. M. and El Sokkary, A. A., 1975. The relation between Rb, Ba and Sr in granitic rocks. *Chemical Geology*, 16, 207-219.
- Fahy, M. P. and Guccione, M. J., 1979. Estimating strength of sandstones using petrographic thin-section data. *International Association of Engineering Geology Bulletin*, 16(4), 467–485.
- Gunsallus, K. L. and Kulhawy, F. H., 1984. A comparative evaluation of rock strength measures. *International Journal of Rock Mechanics and Mining Sciences, Geomechanical Abstracts*, 21, 233–248.
- Harris, N. B. W. and Inger, S., 1992. Trace element modeling of pelite-derived granites. *Contributions to Mineralogy and Petrology*, 110, 46–56.
- Harrison, D. J., 1993. *Industrial minerals laboratory manual*, Technical report, Mineralogy and Petrology series. British Geological Survey, Nottingham.
- Holtz, F. and Johannes, W., 1991. Genesis of peraluminous granites: I. Experimental investigation of melt compositions at 3 and 5 kb and various H₂O activities. *Journal of Petrology*, 32, 935–958.
- Howarth, D. F. and Rowlands, J. C., 1987. Quantitative assessment of rock texture and correlation with drillability and strength properties. *Rock Mechanics and Rock Engineering*, 20, 57–85.
- Huang, W. T., 1957. Origin of sillimanite rocks by alumina metasomatism, Wichita mountains, Oklahoma. *Bulletin of Geological Society of America*, 68, 1748p.
- Hussain, A., Dipietro, J. A., Pogue, K. A. and Ahmed, I., 2004. Geologic map of 43-B degree sheet of NWFP Pakistan. Geologic map series, Geological survey of Pakistan, Map No. 11.
- Inger, S. and Harris, N., 1993. Geochemical constraints on leucogranite magmatism in the Langtang Valley, Nepal Himalaya. *Journal of Petrology*, 34, 345–368.
- Irfan, T.Y., 1996. Mineralogy, fabric properties and classification of weathered granites in Hong Kong. *Quaternary Journal of Engineering Geology*, 29, 535.
- Irvine, T. N. and Baragar, W. R. A., 1971. A guide to chemical classification of common volcanic igneous rocks. *Canadian Journal of Earth Sciences*, 8, 523-548.
- ISRM (International Society for Rock Mechanics), 1981. *Rock Characterization, Testing and Monitoring*. In Brown, E.T. (Ed.), *ISRM Suggested Methods*. Pergamon, Oxford.
- Jagoutz, O., Müntener, O., Schmidt, M. W. and Burg, J. P., 2010. The roles of flux- and decompression melting and their respective fractionation lines for continental crust formation: Evidence from the Kohistan arc. *Earth and Planetary Science Letters*, 261, 179–200.
- Jan, M. Q., 1988. Geochemistry of amphibolites from the southern part of Kohistan arc, N. Pakistan. *Mineralogical magazine*, 52, 147-160.

- Jan, M. Q. and Howie, R. A., 1981. The mineralogy and geochemistry of the metamorphosed basic and ultrabasic rocks of the Jijal Complex, Kohistan, NW Pakistan. *Journal of Petrology*, 22, 85–126.
- Jan, M. Q., Khan, M. A., Tahirkheli, T. and Kamal, M., 1981a. Tectonic subdivision of granitic rocks of north Pakistan. *Geological Bulletin, University of Peshawar*, 14, 159-182.
- Jan, M. Q., Khan, M. A. and Tahirkheli, T., 1981b. The Geology and Petrology of the Tarbela Alkaline Complex. *Geological Bulletin, University of Peshawar*, 14, 1-28.
- Jan, M. Q., 1988. Geochemistry of amphibolites from the southern part of Kohistan arc, North Pakistan. *Mineralogical Magazine*, 52, 147-159.
- Jan, M. Q. and Karim, A., 1990. Continental magmatism related to late Paleozoic-early Mesozoic rifting in north Pakistan and Kashmir. *Geological Bulletin, University of Peshawar*, 23, 1-25.
- Jan, M. Q. and Kazmi, A. H., 2005. Plate tectonic configuration of gemstones of Pakistan. 1st Kashmir international conference proceeding, University of AJK, Muzaffarabad.
- Kazmi, A. H., Lawrence, R. D., Dawood, H., Snee, L. W. and Hussain, S. S., 1984. Geology of Indus suture in the Mingora-Shangla area of Swat, north Pakistan. *Geological Bulletin, University of Peshawar*, 17, 127-144.
- Kebede, T., Koeberl, C. and Koller, F., 2001. Magmatic evolution of the Sijii-Wagga garnet bearing two mica granite, Wallagga area, western Ethopia. *Journal of African earth sciences*, 32, 193-221.
- Kempe, D. R. C., 1973. The Petrology of the Warsak Alkaline granites, Pakistan, and their relationship to other alkaline rocks of the region. *Geological Magazine*, 110, 385-404.
- Kempe, D. R. C. and Jan, M. Q., 1970. An Alkaline Igneous Province in North West Frontier Province, west Pakistan. *Geological Magazine*, 107, 395-398.
- Kempe, D. R. C., Jan, M. Q., 1980. The Peshawar Plain Alkaline Igneous Province, NW Pakistan. *Geological Bulletin, University of Peshawar*, 13, 71-77.
- Khan, M. A., Stern, R. J., Gribble, R. F. and Windley, B. F., 1997. Geochemical and isotopic constraints on subduction polarity, magma sources, and paleogeography of the Kohistan intra-oceanic arc, northern Pakistan Himalaya. *Journal of Geological Society, London*, 154, 935-946.
- Khan, M. I. and Hammad, M., 1978. Petrology of Utla granite, Gadoon area. Unpublished M Sc thesis, University of Peshawar.
- Khattak, N. U., Qureshi, A. A., Akram, M., Ullah, K., Azhar, M. and Khan, M. A., 2005. Unroofing histories of the Jambil and Jawar Carbonatite Complexes from NW Pakistan: Constraints from Fission- Track Dating of Apatite. *Journal of Asian Earth Sciences*, 25, 643-652.
- Khattak, N. U., Akram, M., Khan, M. A. and Khan, H. A., 2008. Emplacement of Loe Shilman carbonatite from NW Pakistan: Constraints from fission track dating. *Radiation Measurements*, 43, S313–S318.
- King, B. H., 1964. The structure and petrology of part of lower Swat, west Pakistan, with special reference to the origin of granitic gneisses. PhD thesis, University of London.

- Koh, J. S. and Yun, S. H., 2003. The geochemistry of Yuksipryeong two-mica leucogranite, Yeongnam massif, Korea. *Journal of petrological society of Korea*, 12(3), 119-134.
- Lamoen, B. E., 1980. Ti zoning in corona hornblende of iron ore bearing gabbros. Shsimaki, Finland. *Neus Jahrab. Mineral. MountShefte*, 88-96.
- Lawrence, R. D., Kazmi, A. H. and Snee, L. W., 1989. Geological settings of emerald deposits of Swat, north Pakistan. In: Kazmi, A. H., Snee, L. W., eds., *Emeralds of Pakistan*.
- Le Bas, M. J., Mian, I. and Rex, D. C., 1987. Age and nature of carbonatites emplacement in north Pakistan. *Geol. Rund.*, 76 (2), 317–323.
- Le Fort, P., Debon, F. and Sonet, J., 1980. The “lessor Himalayan” cordierite granite belt, typology and age of the pluton of Mansehra, Pakistan. *Geological Bulletin, University of Peshawar*, 13, 51-62.
- Le Fort, P., Debon, F. and Sonet, J., 1983. The lower Paleozoic “lesser Himalayan” granite belt: Emphasis on Simchar pluton of central Nepal. In: *Granite of Himalayas, Karakoram and Hindukush* (F. A. Shams ed.), Institute of Geology, Punjab University, Lahore, 235-256.
- Le Maitre, R. W., 2002. *Igneous rocks: a classification and glossary of terms*, 2nd edition. Cambridge University Press.
- Lindqvist, J.E., Akesson, U. and Malaga, K., 2007. Microstructure and functional properties of rock materials. *Materials Characterization*, 58, 1183–1188.
- London, D., 1992. Phosphorous in S-type magmas: the P₂O₅ content of feldspar from per-aluminous granites, pegmatites and rhyolites. *American mineralogist*, 77, 126-145.
- Majid, M., Danishwar, S. and Hamidullah, S., 1991. Petrographic and Chemical Variations in the Rift-Related Basic Dykes of The Malka Area (Lower Swat), NWFP, Pakistan. *Geological Bulletin, University of Peshawar*, 24, 1-23.
- Martin, N. R., Siddique, S. F. A. and King, B. H., 1962. A geological reconnaissance of the region between lower Swat and Indus river of Pakistan. *Geological Bulletin, Punjab University*, 2, 1-13.
- Meschede, M., 1986. A method of discriminating between two different types of mid-oceanic basalts and continental tholeiites with the Nb-Zr-Y diagram. *Chemical Geology*, 56, 207–218.
- Maniar, P. D. and Piccoli, P. M., 1989. Tectonic discrimination of granitoids. *Geological society of America bulletin*, 101, 635-643.
- Mc Phie, J., Doyle, M. and Allen, R., 1993. *Volcanic textures*. Centre for Ore Deposits and Exploration Studies. University of Tasmania, 198p.
- Miller, C. F., 1985. Are strongly peraluminous magmas derived from pelitic sedimentary sources? *Journal of Geology*, 93, 673–689.
- Miyashiro, A., 1973. *Metamorphism and metamorphic belts*. George Allen and Unwin, London.
- Nagudi, B., Koeberl, C. and Kurat, G., 2003. Petrography and Geochemistry of Singo granite, Uganda, and implications for its origin. *Journal of African Earth Sciences*, 36, 73-87.

- Patino Douce, A. E. and Johnston, A. D., 1991. Phase equilibria and melt productivity in the polytic system: implication for the origin of per-aluminous granitoids and aluminous granulites. *Contributions to mineralogy and petrology*, 107, 202-218.
- Patino Douce, A. E. and Beard, J.S., 1995. Dehydration-melting of biotite gneiss and quartz amphibolite from 3 to 15 kbar. *Journal of Petrology*, 36, 707–738.
- Pearce, J. A. and Cann, J. R., 1973. Tectonic settings of basic volcanic rocks investigated using trace element analysis. *Earth and Planetary Sciences letters*, 19, 290-300.
- Pearce, J. A. and Gale, G. H., 1979. Identification of ore deposition environment from trace element geochemistry of associated igneous host rocks. In: volcanic processes in ore genesis. Geological Society of London, Special Publication, 7, 14-24.
- Pearce, J. A. and Norry, M. J., 1979. Petrogenetic implications of Ti, Zr, Y and Nb variation in volcanic rocks. *Contributions to Mineralogy and Petrology*, 69, 33-47.
- Pearce, J. A., Alabaster, T., Shelton, A. W. and Searle, M. P., 1981. The Oman ophiolite as a cretaceous arc-basin complex: evidence and implications. *Philosophical Transaction of the Royal Society London*, A300, 299-317.
- Pearce, J. A., Harris, N. B. W. and Tindle, A. G., 1984. Trace element discrimination diagrams for the tectonic interpretation of granitic rocks. *Journal of Petrology*, 25, 956–983.
- Pogue, K. R. and Hussain, A., 1986. New light on stratigraphy of Nowshera area and the discovery of early to middle Ordovician trace fossils in NWFP Pakistan. *Geological survey of Pakistan information release*, 135, 15p.
- Pogue, K. R., Wardlaw, B. R., Harris, A. G. and Hussain, A., 1992a. Paleozoic and Mesozoic stratigraphy of Peshawar basin, Pakistan; Correlations and implications. *Geological society of America bulletin*, 104, 915-927.
- Pogue, K. R., DiPietro, J. A., Khan, S. R., Hughes, S. S., Dilles, J. H. and Lawrence, R. D., 1992b. Late paleozoic rifting in northern Pakistan. *Tectonic*, vol. 11 (4), 871-883.
- Rafiq, M. and Jan, M. Q., 1988. Petrography of Ambela granitic complex, NW Pakistan. *Geological Bulletin, University of Peshawar*, 21, 27-48.
- Rafiq, M. and Jan, M. Q., 1989. Geochemistry and petrogenesis of Ambela granitic complex, NW Pakistan. *Geological Bulletin, University of Peshawar*, 22, 159-179.
- Ringuette, L., Martignole, J. and Windley, B. F., 1999. Magmatic crystallization, isobaric cooling and decompression of the garnet-bearing assemblages of the Jijal Sequence (Kohistan Terrane, western Himalayas). *Geology*, 27, 139–142.
- Sajid, M., Arif, M. and Muhammad, N., 2009. Petrographic characteristics and mechanical properties of rocks from Khagram-Razagram area, Lower Dir, NWFP, Pakistan. *Journal of Himalayan Earth Sciences, University of Peshawar*, 42, 25-36.
- Sajid, M. and Arif, M., 2010. Field features and petrography of igneous rocks from Utlā (Gadoon), NW Pakistan: Preliminary investigation. *Journal of Himalayan Earth Sciences, University of Peshawar*, 43, 75-76.
- Searle, M. P., Khan, M. A., Fraser, J. E. and Gough, S. J., 1999. The tectonic evolution of the Kohistan-Karakoram collision belt along Karakoram highway transect, north Pakistan. *Tectonics*, 18(6), 929-949.

- Shah, S. M. I., Siddique, R. A. and Talent, J. A., 1980. Geology of eastern Khyber agency, NWFP Pakistan. Geological survey of Pakistan records, 44, 31p.
- Shakoor, A. and Bonelli, R. E., 1991. Relationship between petrographic characteristics, engineering index properties, and mechanical properties of selected sandstones. Bulletin of International Association of Engineering Geologist, XXVIII, 1, 55-71.
- Shaltegger, U., Zeilinger, G., Frank, M. and Burg, J. P., 2002. Multiple mantle sources during island arc magmatism: U-Pb and Hf isotopic evidence from the Kohistan arc complex, Pakistan. Terra Nova, 14, 461-468.
- Shams, F. A., 1969. Geology of the Mansehra-Amb state area, north-western Pakistan. Geological Bulletin, Punjab University, Lahore, 1-32.k
- Shams, F. A., 1983a. Granites of NW Himalayas in Pakistan. In: Granite of Himalayas, Karakoram and Hindukush (F. A. Shams ed.), Institute of Geology, Punjab University, Lahore, 75-122.
- Shams, F. A., 1983b. Plate tectonic model for the Himalayas and Uranium mineralization. In: Granite of Himalayas, Karakoram and Hindukush (F. A. Shams ed.), Institute of Geology, Punjab University, Lahore, 299-308.
- Shannon, R. D., Rossi, R. C., 1964. Definition of Topotaxy. Nature, 202, 1000 – 1001.
- Siddique, S. F. A., Chaudhry, M. N. and Shakoor, A., 1968. Geology and petrology of feldspathoidal Syenites and the associated rocks of Koga area, Chamla valley, Swat, west Pakistan. Geological Bulletin, Punjab University, 7, 1-29.
- Skjerlie, K.P. and Johnston, A.D., 1996. Vapour-absent melting from 10 to 20 kbar of crustal rocks that contain multiple hydrous phases: implications for anatexis in the deep to very deep continental crust and active continental margins. Journal of Petrology, 37, 661-691.
- Sousa, L. M., del Rio, L. M. S., Calleja, L., de Argandona, V. G. R. and Rey, A. R., 2005. Influence of microfractures and porosity on the physico-mechanical properties and weathering of ornamental granites. Engineering Geology, 77, 153-168.
- Stauffer, K. W., 1968. Silurian-Devonian reef complex near Nowshera, west Pakistan. Geological society of America bulletin, 79, 1331-1350.
- Sylvester, P. J., 1998. Post-collisional strongly per-aluminous granites. Lithos, 45, 29-44.
- Tahirkheli, R. A. K. and Jan, M. Q., 1979. A preliminary geological map of Kohistan and adjoining areas, N. Pakistan. Geological Bulletin, University of Peshawar, (Special issue), 11.
- Taylor, S. R. and McLennan, S. M., 1985. The continental crust: Its composition and evolution. Blackwell, Oxford, 312pp.
- Treloar, P. J. and Rex, D. C., 1990. Cooling and uplift history of the crystalline thrust stack of the Indian plate internal zones west of Nanga Parbat, Pakistan Himalaya. Tectonophysics, 180, 323-349.
- Treloar, P. J., Broughten, R. D., Coward, M. P., Williams, M. P. and Windley, B. F., 1989. Deformation, metamorphism and imbrication of the Indian plate south of MMT, north Pakistan. Journal of Metamorphic Geology, 7, 111-127.
- Tugrul, A. and Gurpinar, O., 1997. The effect of chemical weathering on the engineering properties of Eocene basalts in north eastern Turkey. Environmental and engineering geosciences, 3, 225-234.

- Tugrul, A. and Zarif, I.H., 1999. Correlation of mineralogical and textural characteristics with engineering properties of selected granitic rocks from Turkey. *Engineering Geology*, 51, 303–317.
- Willard, R. J. and McWilliams, J. R., 1969. Microstructural techniques in the study of physical properties of rocks. *International Journal of Rock Mechanics and Mining Sciences*, 6, 112.
- Wood, D. A., 1980. The application of a Th-Hf-Ta diagram to the problems of tectonomagmatic classification and establishing the nature of crustal contamination of basaltic lavas of the British Tertiary volcanic province. *Earth and Planetary Sciences*. 50, 151–162.
- Yeats, R. S. and Hussain, A., 1987. Time of structural events in Himalayan foothills of northwestern Pakistan. *Geological society of America bulletin*, 99, 161-176.